Fakultät für Medizin

Institut/Klinik/Lehrstuhl für:

Institut für Medizinische Mikrobiologie, Immunologie und Hygiene

Immunological characterization of Cytomegalovirus-specific T cells and generation of HLA-C7-*Strep*Tamers for adoptive T cell therapy

Fabian Emanuel Schlott

Vollständiger Abdruck der von der Fakultät für Medizin der Technischen Universität München zur Erlangung des akademischen Grades eines

Doktors der Naturwissenschaften

genehmigten Dissertation.

Vorsitzende(r):	Prof. Dr. Percy A. Knolle
Prüfer der Dissertation:	1. Prof. Dr. Dirk Busch 2. Prof. Dr. Johannes Müller

Die Dissertation wurde am 28.11.2016 bei der Fakultät für Medizin der Technischen Universität München eingereicht und durch die Fakultät für Medizin am 14.6.2017 angenommen

Index

Abbreviations

A	
Ab	Antibody
ACT	Adoptive T cell therapy
AIDS	Acquired immune deficiency syndrome
APC	Allophycocyanin
B	
BV	Brilliant violet
BSA	Bovine serum albumin
bp	Base pair
C	
CCR7	C-C chemokine receptor type 7
CD	Cluster of differentiation
cDC	Classical dendritic cells
cG	Glycoprotein complex
CNI	Calcineurin-inhibitors
CMV	Cytomegalovirus
CsA	Cyclosporine A
D	
D	Donor
DC	Dendritic cell
DE	Delayed early
dH_2O	Distilled water
DMSO	Dimethylsulfoxid
DNA	Deoxyribonucleic acid
E	
EBV	Epstein-Barr virus
ECD	Energy coupled dye
EDTA	Ethylenediaminetetraacetic acid
ELISA	Enzyme-linked immunosorbent assay
EMA	Ethidium monoazide bromide
ESRD	End-stage renal disease
F	
Fab	Fragment antigen binding
FACS	Fluorescence-activated cell sorting
FCS	Fetal calf serum
FDA	U.S. Food and Drug Administration
FITC	Fluorescein isothiocyanate
FMO	Fluorescence minus one
FPLC	Fast protein liquid chromatography
G	
g	Standard acceleration due to gravity
GM-CSF	Granulocyte-macrophage colony-stimulating factor
GMP	good manufacturing practice
GvHD	Graft versus host disease

H

HHV	Human herpesviruses
HSCT	Hematopoietic stem cell transplantation
Hep	Heparin
HLA	Human leukocyte antigen
HSV	Herpes simplex virus
hβ2m	Human β2-microglobulin

I

ICS	Intracellular cytokine staining
IE	Immediate early
IgG	Immunoglobulin G
IgM	Immunoglobulin M
IFN	Interferon
IL	Interleukin
IS	Immunosuppression
ITAM	Immuno-receptor tyrosine-based activating motif
ITIM	Immune-receptor tyrosine-based inhibitory motif

K

kDa	Kilo Dalton
KLRG1	Killer cell lectin-like receptor subfamily G member 1

L

L	Late
LB	Lysogenic broth
Li	Lithium
LIR-1	leukocyte immunoglobulin-like receptor 1

M

MAGE-A12	Melanoma-associated antigen 12
MAIT	Mucosal-Associated Invariant T Cells
Max	Maximum
MFI	Mean fluorescence intensity
MHC	Major histocompatibility complex
Min	Minimum
MMF	Mycophenolate mofetil
mTORi	mechanistic Target of Rapamycin inhibitors

N

nm	Nanometer
No	Number

O

OD	Optical density
ORF	Open reading frame

P

PACT	Prophylactic Central Memory Transfer
PAMP	Pathogen-associated molecular patterns
PBS	Phosphate buffered saline
PCR	Polymerase chain reaction
pDC	plasmacytoid DC
PE	Phycoerythrin
PE-Cy7	Phycoerythrin-Cy7

PerCP	Peridinin chlorophyll
PFA	Paraformaldehyde
PMA	Phorbol 12-myristate 13-acetate
pMHC	MHC/Peptide-complex
PMSF	Phenylmethanesulfonyl fluoride
pp50	Phosphoprotein 50
pp65	Phosphoprotein 65
POD	Postoperative day
PRR	Pattern recognition receptors
PTLD	Post-transplant lymphoproliferative disorder
Q	
QF	QuantiFERON
R	
R	Recipient
rATG	Rabbit anti-thymocyte globulin
rpm	Rounds per minute
RPMI	Roswell Park Memorial Institute medium
S	
SCID	Severe combined immunodeficiency
SDS	Sodium dodecyl sulfate
SOT	Solid organ transplantation
SPP	Single patient pack
S. aureus	Staphylococcus aureus
T	
TAC	Tacrolimus
T_{CM}	Central memory T cells
T_{EM}	Effector memory T cells
T_{EMRA}	Terminally differentiated effector memory T cells
T_{FH}	Follicular B helper T cells
$T_{naïve}$	Naïve T cells
T_{RM}	Tissue-resident memory T cells
T_{SCM}	T memory stem cell
TLR	Toll-like receptor
TMB	3,3’,5,5’-tetramethylbenzidine
TNF	Tumor necrosis factors
U	
UL	Unique long
US	Unique short
V	
V	Volt
VZV	Varicella zoster virus
Y	
y	Years

1. Introduction

1.1 Human Cytomegalovirus (CMV)

Human Cytomegalovirus (CMV), also known as Human Herpes Virus 5 (HHV-5), is a member of the *Herpesviridae* family. Thus far, more than 200 different herpesviruses were defined and beside CMV, eight viruses are known to infect humans: herpes simplex virus 1 (HSV-1), herpes simplex virus 2 (HSV-2), varicella-zoster virus (VZV), Epstein-Barr virus (EBV), human herpesviruses 6A, 6B, and 7 (HHV-6A, HHV-6B, and HHV-7), and Kaposi's sarcoma–associated herpesvirus (HHV-8). These viruses share similar characteristics and cause a lifelong infection due to cellular latency (Pellett & Roizman, 2013). According to biological properties, the family of *Herpesviridae* is divided into three different subfamilies: *Alpha-*, *Beta-,* and *Gammaherpesvirinae* (Davison, 2010). The three subfamilies differ in cell tropism, host specificity, and replication characteristics (Pellett & Roizman, 2013). CMV is allocated in the family of *Betaherpesvirinae* (Davison, 2010; Roizman et al., 1981). Genome sequencing analyses support the classification into the three different subfamilies and reveal coevoluntionary aspects of *Alpha*- and *Betaherpesvirinae* with the human host (McGeoch et al., 2000). Furthermore, several CMV strain variants were identified by genome sequencing, including more than 50 wild-type strain variants and the laboratory stains *Toledo*, *AD169*, and *Towne* (Chee et al., 1990; Dolan et al., 2004; Dunn et al., 2003; Murphy et al., 2003; A. Walker et al., 2001).

1.2 Morphology of CMV

Like all other herpesviruses, CMV consist of an icosahedral capsid of up to 162 capsomeres containing a double stranded DNA. The capsid is surrounded by a proteinaceous matrix, the tegument, which is in turn shrouded by a host-cell-derived viral envelope. Furthermore, the envelope is modified by approximately 23 viral glycoproteins, which are essential for cell attachment and entry (Britt, 2007; Cheung et al., 2006). A schematic overview is shown in Figure 1.1. In comparison to all other herpesviruses, CMV has the largest genome with approximately 236 kbp encoding for more than 167 genes (Davison et al., 2003) and has a size of 200 to 300 nm in diameter (Moscarski et al., 2013). The CMV virion consist of more than 70 proteins (Varnum et al., 2004) with approximately 20 proteins accounted to the tegument (Moscarski et al., 2013). The most frequent protein within the tegument is the phosphoprotein

65 (pp65), also known as unique long 83 (UL83) protein (Varnum et al., 2004). Next to pp65, other tegument proteins, such as virion transactivator pp71 and virion maturation protein pp150 can be found in addition to some cellular and viral RNA (Moscarski et al., 2013; Varnum et al., 2004). The tegument proteins are responsible for assembly of virion particles, disassembly after entry, and modulation of host cell responses to infection (Moscarski et al., 2013). Within the host cell derived lipid bilayer (envelope), the major glycoproteins gB (UL55), gH (UL75) , gL (UL115), gM (UL100), gN (UL73), and gO (UL74) are expressed, which are involved in host cell attachment and membrane penetration (Varnum et al., 2004). Three glycoprotein complexes (gc) gcI, gcII, and gcIII are described. gB is highly conserved within human herpes viruses and by forming a trimer constitutes gcI (Backovic & Jardetzky, 2009; Isaacson & Compton, 2009). gB is a class III fusion protein and is essential for attachment and fusion of the virus with the host cell (Backovic & Jardetzky, 2009; Isaacson & Compton, 2009; Moscarski et al., 2013). The glycoprotein complex II (gcII) is formed by gM and gN and plays an essential role in viral maturation, as experimental deletion of this complex leads to a replication-incompetent virus (Krzyzaniak et al., 2009; Mach et al., 2000; Mach et al., 2005). The gH:gL complex displays the central subunit of gcIII and are able to form trimeric structures with gO, mediating cell attachment and enhancing gB-mediated fusion (Huber & Compton, 1998; Moscarski et al., 2013). Furthermore, the glycoproteins gH:gL can interact with the gene products UL131a-128 and form the pentameric complex gH:gL:pUL128:pUL131:pUL131a (Ryckman et al., 2008; D. Wang & Shenk, 2005b). The trimeric and pentameric complexes are thought to additionally influence cell tropism of CMV (Gerna et al., 2005; Patrone et al., 2007; Ryckman et al., 2006; Ryckman et al., 2008; Vanarsdall et al., 2008; D. Wang & Shenk, 2005a, 2005b).

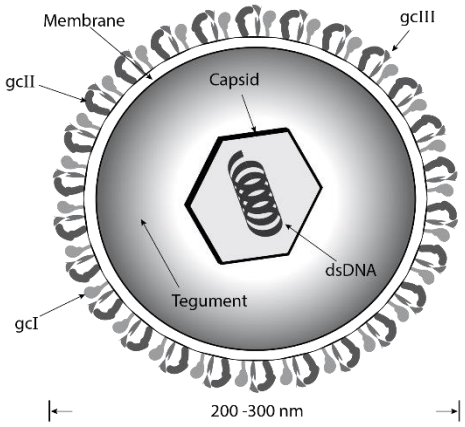

Figure 1.1: Schematic overview of CMV
The double stranded DNA (dsDNA) is surrounded by the icosahedral capsid, followed by the tegument layer and a host cell derived envelope, supplemented by three major viral glycoproteins: gcI (gB), gcII (gM:gN), and gcIII (gH:gL:gO/ gH:gL:pUL128:pUL131:pUL131a). CMV has a size of approximately 200 to 300 nm in diameter.

1.3 Viral replication

CMV can infect and replicate in a large variety of human cells including fibroblast, epithelial, endothelial, smooth muscle, neuronal, and myeloid (e.g. dendritic cells, macrophages) cells (Crough & Khanna, 2009; Moscarski et al., 2013; Ryckman et al., 2006; Sinzger et al., 1995). Entry of the virus may occur by pH-independent fusion with the plasma membrane of the host cell (e.g. fibroblast) or by pH-dependent endocytosis (e.g. myeloid cells) (Compton et al., 1992; Sinzger, 2008; Sinzger et al., 1995). CMV replication is divided into three phases of viral protein expression: immediate early (IE), delayed early (DE) and late (L) (Stinski, 1978). 48 to 72 h after attachment and fusion of the virus with the host cell, productive viral particles are discharged. The translocation of the capsid to the nucleus initiates IE gene transcription (0 - 2 hours after entry) by upstream enhancer binding and tegument protein pp71 translocation (Kalejta, 2008; Moscarski et al., 2013; Stasiak & Mocarski, 1992). IE gene expression is induced within minutes after infection and is linked to p53 activity, as IE gene expression can only be activated in G1 phase (Moscarski et al., 2013). Expression of functional IE genes induces transcription of DE genes (<24 hours after entry) which are essential for CMV DNA synthesis. Likewise, expression of L genes (>24 hours after entry) depends on DE genes and is essential for virion formation and maturation (Crough & Khanna, 2009; Moscarski et al., 2013). In comparison to other herpesviruses, CMV replication is rather slow and discharging of virions peaks on day 5 after entry. Shedding of mature viruses lasts for several days until infected cells die (Moscarski et al., 2013).

1.4 Pathogenesis

As mentioned above, CMV causes a lifelong latent infection leading to a high seroprevalence of the world's population and is dependent on geographic and socioeconomic factors. Hence, the rate of CMV-infected individuals in developing countries reaches 90% whereas seroprevalence in industrial nations is approximately 50% (Alford & Pass, 1981; Bate et al., 2010; Hecker et al., 2004).

Primary CMV-infection of immunocompetent individuals is mostly asymptomatic and is controlled by the immune system (Moscarski et al., 2013). After an initial immune response, CMV becomes latent, resting mainly in hematopoietic and myeloid cells, e.g. $CD34^+$ stem cells, DCs or macrophage precursors, where sporadic viral replications can occur (Moscarski et al., 2013; M. Reeves & Sinclair, 2008; M. B. Reeves et al., 2005; Taylor-Wiedeman et al., 1991). Furthermore, these cells are central for viral transmission in blood products or transplants (Cannon et al., 2011; Moscarski et al., 2013). On the contrary, infection of immunocompromised individuals, including acquired immune deficiency syndrome (AIDS) patients or transplant recipients, can lead to excessive, uncontrolled viral replication followed by severe clinical symptoms (Crough & Khanna, 2009; Emery, 2012; Fishman, 2007; Kotton, 2010; Moscarski et al., 2013). Main sites for clinical manifestations are the gastrointestinal tract, the retina, the liver, and the lung. Clinical symptoms comprise CMV-syndrome (fever in combination with bone marrow suppression, neutropenia or thrombocytopenia), pneumonia, hepatitis, and colitis with potentially fatal outcomes (M. Boeckh & Geballe, 2011; Kotton, 2010; Ljungman, 2002; Per Ljungman et al., 2002; P. Ljungman et al., 2002). A recent study analyzing the risk of CMV-disease after kidney transplantation showed that mainly the gastrointestinal tract is affected in this patient population (Helantera et al., 2014). Based on the CMV-IgG serostatus of donor (D) and recipient (R), a high (D+/R-), intermediate (D+/R+ and D-/R+), and low (D-/R-) risk constellation has been defined in the setting of solid organ transplantation (Kotton, 2013; Kotton et al., 2013). On the contrary, allogeneic hematopoietic stem cell transplant (HSCT) recipients with D-/R+ constellations have the highest risk for CMV-reactivation (Ariza-Heredia et al., 2014; Michael Boeckh & Nichols, 2004; Zhou et al., 2009). Notably, primary CMV-infection is defined as the detection of CMV DNA/ proteins or seroconversion in a previously CMV-seronegative individual and CMV-reactivation is defined by the recurrence from latency leading to measurable viral load (Per Ljungman et al., 2002).

Next to primary pathology by CMV, several indirect effects caused by CMV-replication were reported including secondary bacterial/ fungal infections (Arthurs et al., 2008; Fortun et al., 2010; Linares et al., 2011), viral infections (Freeman, 2009), immunosenescence (Koch et al., 2007), and chronic or acute rejection (Dzabic et al., 2011; Monforte et al., 2009; Paraskeva et al., 2011; Reischig et al., 2009).

Furthermore, congenital infections of neonates play a crucial role in CMV pathology. In up to 40%, primary CMV-infection of a CMV-seronegative woman leads to CMV-transmission to the unborn child (Gaytant et al., 2002; Kenneson & Cannon, 2007; Naing et al., 2016). Hence, this leads in approximately 12% of the cases to a symptomatic infection of newborns, which can cause hearing loss, microcephaly, poor feeding, seizures, and periventricular calcification (Boppana et al., 1992; Goderis et al., 2014).

1.5 CMV-specific innate immune responses

Innate immune cells, such as dendritic cells (DC), macrophages, and Natural Killer cells (NK cells), play a central role in host-derived immunity against invading pathogens and represent the first line of defense. Innate immune cells express pattern recognition receptors (PRRs), such as Toll-like receptors (TLR), enabling the recognition of pathogen-associated molecular patterns (PAMPs). Recognition of foreign molecules and subsequent activation of innate immune cells induces an antiviral response mainly by the secretion of type I Interferons (IFN), cytotoxic effects by NK cells, and production of pro-inflammatory cytokines and chemokines inducing maturation, recruitment, and memory generation of adaptive immune cells (Akira et al., 2006; Hanley & Bollard, 2014). Furthermore, DCs and macrophages are professional antigen presenting cells (APC), able to present peptides loaded on major histocompatibility complex (MHC) I and II, which are encoded by the human leukocyte antigen (HLA) (Janeway, 2005).

1.5.1 NK cells

The important role of NK cells in viral control has been demonstrated already in the 1980s. Shellham et al. used beige mice with defects in NK cell-mediated cytotoxicity to show that these mice were highly susceptible to murine CMV-infections. Interestingly, they could restore CMV-specific immunity by transferring NK cells form normal healthy mice (Shellam et al., 1981). Furthermore, it was shown in humans that a NK cell-deficient patient was highly susceptible to herpes virus infections, including CMV (Biron et al., 1989).

NK cells exert their effector functions by the secretion of granzymes and perforin. Furthermore, NK cells produce a large variety of cytokines, such as IFNγ and TNFα, modulating other innate and adaptive immune responses (Lanier, 2005). NK cells are able to constitutively express IFNγ-transcripts causing immediate cytokine synthesis upon activation and by this are able to perform their immunological task within minutes (Stetson et al., 2003). In contrast to T cells, NK cells are not dependent on activation by other immune cells and are therefore tightly regulated by several activating and inhibitory receptors (Lanier, 2005). Activating NK cell receptors lack classical signaling domains but include DAP10 adaptor and the immuno-receptor tyrosine-based activating motif (ITAM), including CD3ζ, FcεRIγ, and DAP12 (Lanier, 2009). The large variety of activating receptors include among others the Fc receptor CD16, the activating members of the Killer Cell Immunoglobulin-like Receptor (KIR) family, NKG2D, and natural cytotoxicity receptors. Ligands for theses receptors are mainly self-ligands, such as IgG antibodies and stress-induced NKG2D ligands, and non-self ligands, such as gpm157 expressed by murine CMV (Lanier, 2008). On the other side, inhibitory NK cell receptors although bind to several self-molecules. The best known ligand is MHC class I which is bound by human inhibitory KIRs (Parham, 2005). Furthermore, HLA-E, a non-classical MHC class I molecule that presents leader peptides of MHC class I, is recognized by the heterodimeric receptor CD94-NKG2A leading to NK cell inhibition. In addition, non MHC class I molecules can induce inhibitory signals, such as cadherins sensed by Killer cell lectin-like receptor subfamily G member 1 (KLRG1) (V. Kumar & McNerney, 2005). These receptors include, similarly to ITAMs, an immune-receptor tyrosine-based inhibitory motif (ITIM) (Long, 2008). In order to prevent potentially harmful immune responses, NK activation is dependent on inhibitory receptor ligand interactions and intact ITIM signaling (Lanier, 2005).

1.5.2 Other innate immune cells

The role of innate immune cells, except NK cells, in CMV-specific immunity is still not fully elucidated. Nevertheless, it is known that DNA viruses, such as CMV, carry CpG-rich DNA motifs which are almost absent in vertebrates and lead to a stimulation of Toll-like receptor (TLR) 9 (Hochrein et al., 2004; Krug et al., 2004). Murine CMV-infection studies demonstrated a drastic increase of IFNα and β secretion by plasmacytoid DC (pDC) already 6 hours after infection, thereby promoting NK cell-mediated cytotoxicity (Grundy et al., 1982; Shellam et al., 1981). Furthermore, it was shown that gB and gH can activate TLR2 on fibroblasts leading

to the secretion of inflammatory cytokines with unknown effect on the virus (Boehme et al., 2006).

1.6 CMV-specific adaptive immune responses

1.6.1 Humoral immunity

The humoral immunity is based on antibody-secreting B cells which are activated by $CD4^+$ T_H2 cells. B cells play an important role controlling CMV-associated disease severity. Guinea pigs treated with CMV-specific antibodies, controlled elsewise lethal viral titers but could not prevent CMV-infection (Bratcher et al., 1995). Furthermore, several studies using hyper immunoglobulin treatment for a potential congenital infection, revealed a moderated disease pattern (Buxmann et al., 2012; Nigro et al., 2005; Nigro et al., 2012; Visentin et al., 2012). In addition, B cells were shown to mediate protection of maternal and congenital primary CMV-infection after vaccination with gB and adjuvant MF59 (Pass et al., 2009). Antibodies directed against several CMV-associated proteins can be found including neutralizing antibodies directed against envelope glycoprotein gB and glycoprotein complexes, such as gH:gL:pUL128:pUL131:pUL131a (Genini et al., 2011; Li et al., 1995; Lilleri et al., 2012).

1.6.2 T cells

CMV-infection triggers a brought spectrum of high-frequency virus-specific T cells. The protective capacities of CMV-specific T cells are irrevocably as immunocompromised individuals and patients undergoing immune reconstitution after bone marrow transplantation have increased rates of CMV-reactivations. This statement is also strengthened by animal experiments as IE-specific T cells protected from a usually lethal dose of murine CMV challenge (Reddehase et al., 1987). Furthermore, it was shown that T cells can control viral replication in B cell deficient mice (Polic et al., 1998).

Two main subsets of T cells are known: $CD8^+$ T cells recognizing peptide-loaded MHC class I (HLA-A, B, C) by the T cell receptor (TCR) and $CD4^+$ T cells recognizing peptide-loaded MHC class II (HLA-DM, DQ, DR) by the TCR.

1.6.2.1 $CD8^+$ T cells

Already in the early 1980s, the cytotoxic effects of CMV-specific $CD8^+$ T cells, isolated from healthy donors, against CMV-infected cells were demonstrated (Borysiewicz et al., 1983). In

the meanwhile, large efforts have been made in order to evaluate specific T cell targets, phenotype and cytokine secretion profiles. CMV expresses more than 165 open reading frames (ORF) and several CMV epitopes were identified that induce a $CD8^+$ T cell response. These epitopes encompass several structural and nonstructural antigens, such as gB, gH, IE-1, IE-2, pp50, pp65, pp71, pp150, and UL28/29 (Boppana & Britt, 1996; Elkington et al., 2003; Gamadia et al., 2003; Moscarski et al., 2013; Willis et al., 2013). The best characterized epitopes are pp65 and IE-1 which were used in numerous functional studies and epitope mapping analysis (Borysiewicz et al., 1983; Elkington et al., 2003; Reddehase et al., 1987; Willis et al., 2013; Wills et al., 2002). Therefore, several single epitopes and corresponding HLA-restrictions were identified and several MHC class I-restricted multimers were generated, such as HLA-A0101/$pp65_{363\text{-}373}$, HLA-A201/$pp65_{495\text{-}503}$, HLA-B*0702/$pp65_{417\text{-}426}$, and HLA-B0801/$IE\text{-}1_{199\text{-}207}$ (Diamond et al., 1997; Kern et al., 1999; Longmate et al., 2001; Wills et al., 2002).

The phenotype of the different $CD8^+$ T cell memory populations is based on the expression of CD45RA/CD45RO in combination with CCR7 and CD95 (Figure 1.2). After the recognition of a suitable MHC/Peptide-complex (pMHC) presented by an APC and a secondary signal provided by $CD4^+$ T_H1 cells, a naïve antigen-specific $CD8^+$ T cell (T_{naive}; $CD45RA^+CD45RO^-CCR7^+CD95^-$) gets activated (Janeway, 2005). Afterwards, the T_{naive} cell differentiates and starts to proliferate. The earliest memory T cell is the T memory stem cell (T_{SCM}; $CD45RA^+CD45RO^-CCR7^+CD95^+$) which has an naive-like phenotype but upregulates CD95 after antigen encounter (Gattinoni et al., 2011). T_{SCM} cells have high self-renewal capacities and are highly polyfunctional (Gattinoni & Restifo, 2013; Mahnke et al., 2013). These cells differentiate into central memory T cells (T_{CM}; $CD45RA^-CD45RO^+CCR7^+CD95^+$). T_{CM} cells are intensively investigated showing a long life span, mediate protection and are able to produce large amounts of IL-2 and other cytokines (Appay et al., 2008; Mahnke et al., 2013). These observations were supported by Gräf et al. who used a serial adoptive T cell transfer mouse model. They could demonstrate that this subset has stem cell-like capacities, is long-lived and is able to mediate protection on a single cell level after an usually lethal dose of *Listeria monocytogenes* (Graef et al., 2014). Afterwards, T_{CM} cells differentiate into effector memory T cells (T_{EM}; $CD45RA^-CD45RO^+CCR7^-CD95^+$) which are able to produce large amounts of cytotoxic cytokines, such as IFNγ, perforin, and granzymes B (Appay et al., 2008; van Leeuwen et al., 2006). Finally, T_{EM} cells re-express CD45RA (T_{EMRA}; $CD45RA^+CD45RO^-CCR7^-CD95^+$) which resembles a short-lived effector phenotype ($CD57^+CD27^-CD28^-$) (Mahnke et al., 2013). The

differentiation cascade of CD8⁺ T cells is unidirectional and the polyfunctionality of cells decreases with progressing maturation (Appay et al., 2008; Buchholz et al., 2013; Gattinoni & Restifo, 2013; Mahnke et al., 2013).

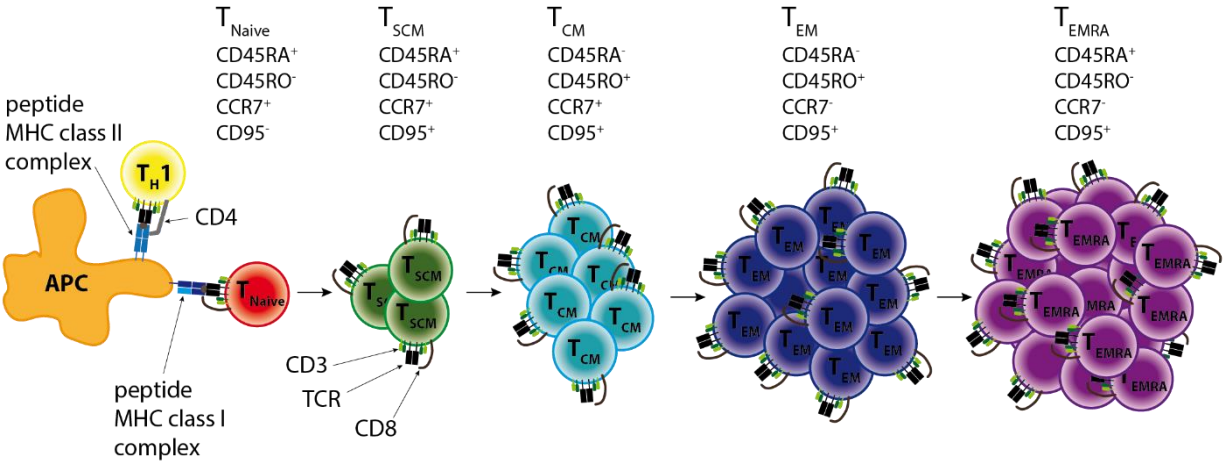

Figure 1.2: Memory subpopulations of CD8⁺ T cells.
CD8⁺ T cells are divided into different memory subpopulations according to the expression of CD45RA, CD45RO, CCR7, and CD95. Before activation, proliferation and differentiation, naïve T cells (T_{naive}; $CD45RA^+CD45RO^-CCR7^+CD95^-$) have to recognize a peptide in combination with MHC class I presented by APCs followed by an activating signal from $CD4^+$ T_H1 cells. Afterwards, T_{naive} cells differentiate into stem cell memory T cells (T_{SCM}; $CD45RA^+CD45RO^-CCR7^+CD95^+$), central memory T cells (T_{CM}; $CD45RA^-CD45RO^+CCR7^+CD95^+$), effector memory T cells (T_{EM}; $CD45RA^-CD45RO^+CCR7^-CD95^+$), and finally re-express CD45RA (T_{EMRA}; $CD45RA^+CD45RO^-CCR7^-CD95^+$).

Interestingly, large frequencies of CMV-specific T cells have a T_{EM} or T_{EMRA} phenotype which is associated with viral control, as these T cell subsets are able to migrate into the tissue (Appay et al., 2002a; Khan et al., 2002a; Wills et al., 1999; Wills et al., 2002). It has been shown, that reconstitution of T_{EMRA} cells correlates with increased control of CMV-reactivations after allogeneic HSCT (Luo et al., 2010; Moins-Teisserenc et al., 2008). Furthermore, CMV-specific T_{EMRA} cells can already be found at young age and expand to very large frequencies with age (Willis et al., 2013). This phenomenon is called “memory inflation” and CMV-specific T cells can comprise more than 20% of all CD8⁺ T cells (Khan et al., 2002b).

In addition to phenotypic characteristics, the functional profile of CMV-specific T cells is essential for viral control and the parameters are intensively debated. In the setting of HSCT, several studies monitored CMV-specific single IFNγ-secretion or IFNγ/IL-2-secretion after *ex vivo* stimulation and described reduced CMV-reactivations in patients with highly functional cells (Barron et al., 2009; Eid et al., 2009; Gratama et al., 2008). Therefore, several companies develop now commercially available tests based on the detection of IFNγ after stimulation, such as the QuantiFERON® CMV assay (Qiagen) or the T-Track® CMV (Lophius Biosciences)

(Giulieri & Manuel, 2011). Measurements, using the QuantiFERON CMV assay revealed an increased viral clearance in patients with effective immunity in comparison to patients without T cell immunity (Lisboa et al., 2012). On the other hand, the production of more than one cytokine by antigen-specific T cells (polyfunctionality) was reported to be essential for the prediction of CMV-reactivations (Krol et al., 2011; Scheinberg et al., 2009).

1.6.2.2 $CD4^+$ T cells

$CD4^+$ T cell are a major population of the adaptive immune system. The important role of CMV-specific $CD4^+$ T cells was shown at the end of the 1980s as depletion of $CD4^+$ T cells in a murine CMV model caused persistent viral replication (Jonjic et al., 1989). Furthermore, CMV-specific $CD4^+$ T cells were shown to expand before $CD8^+$ T cells in a kidney transplant setting and protracted viremia occurred in patients with delayed CMV-specific $CD4^+$ T cell responses (Gamadia et al., 2003).

$CD4^+$ T cells recognize exogenous peptides loaded on MHC class II that are presented by APCs. $CD4^+$ T cells comprise several subsets, such as T_H1 cells (activation of $CD8^+$ T cells) and T_H2 cells (activation of B cells), regulatory T cells, T_H17 cells, and follicular B helper T cells (T_{FH}) (Janeway, 2005). The role of $CD4^+$ T cells in the setting of CMV was interpreted primarily as help for sufficient $CD8^+$ T cell activation but is was shown that a large number of CMV epitopes induce cytotoxic CD4-specific immune responses (Gamadia et al., 2003). The majority of identified peptides are derived from structural proteins, such as gB, gH, pp65, and pp150, but also nonstructural epitopes, such as IE-1, induced $CD4^+$ T cell responses (Gamadia et al., 2003; Kern et al., 2002; Li Pira et al., 2004).

The phenotype and the different function of $CD4^+$ T cell subsets are similarly defined as for $CD8^+$ T cells. It consist of T_{naive} cells ($CD45RA^+CD45RO^-CCR7^+CD95^-$), T_{SCM} ($CD45RA^+CD45RO^-CCR7^+CD95^+$), T_{CM} ($CD45RA^-CD45RO^+CCR7^+CD95^+$), and T_{EM} ($CD45RA^-CD45RO^+CCR7^-CD95^+$). T_{EMRA} cells can classically only be found in the $CD8^+$ T cell compartment (Mahnke et al., 2013). The phenotypical characterization of $CD4^+$ CMV-specific T cells is difficult due to the availability of only few MHC class II multimers, and the effect that short-term culture for intracellular cytokine staining (ICS) also influences the expression of CD45RA/CD45RO and CCR7. Nevertheless, it was shown that CMV-specific $CD4^+$ T cells are enriched in the effector memory compartment (Bitmansour et al., 2002; Rentenaar et al., 2000; Willis et al., 2013). Interestingly, the existence of a $CD28^-CD27^-CD45RO^-$ CD45RA re-expressing CMV-specific $CD4^+$

T cell subpopulation, similarly to $CD8^+$ T_{EMRA} cells, was reported after stimulation and cell culture experiments (Weekes et al., 2004; Willis et al., 2013).

Similar to $CD8^+$ T cells, CMV-specific $CD4^+$ T cells initiate IFNγ-secretion upon stimulation with CMV-restricted peptides and express partially large amounts of perforin indicating a cytotoxic effect by $CD4^+$ T cells (Appay et al., 2002b). Furthermore, the polyfunctional profile is related to the quality of T cells (Boaz et al., 2002; Emu et al., 2005; Munoz-Cobo et al., 2012). In an observational trial the ability of CMV-specific $CD4^+$ T cells to secret IFNγ and IL-2 was associated with clearance of high-level viremia in liver transplanted patients, whereas patients with low frequencies of polyfunctional $CD4^+$ T cells had higher viral titers (Nebbia et al., 2008).

1.7 Immune modulation and evasion by CMV

During coevolution of CMV with the human host (McGeoch et al., 2000), CMV has established several mechanisms leading to immune modulation and evasion of immunogenic surveillance that are essential for maintaining latency (Freeman, 2009). Several genomic unique short (US) regions encode proteins that influence antigen presentation on MHC class I molecules. For example US6 prevents peptide transport, US3 can cause retention of MHC complexes in the ER, and expression of US2 and US11 leads to degradation of MHC molecules (Ahn et al., 1996; Wiertz et al., 1996a; Wiertz et al., 1996b). Furthermore, CMV can interfere with T cell proliferation, increases programmed cell death receptor 1 (PD-1) expression on activated T cells and, therefore, facilitates apoptosis of activated cells. Further, CMV is able to block innate immune responses by inhibition of macrophage migration and MHC class II downregulation (Fletcher et al., 1998; Frascaroli et al., 2009; Schrier et al., 1986; Sester et al., 2008; Soderberg-Naucler, 2006). Interestingly, analyzes of the US2 and US11 gene products revealed a locus-specific inhibition of MHC class I molecules causing downregulation in different degrees (Gewurz et al., 2001; Schust et al., 1998). In line with that, Ameres et al. could show that fibroblasts, infected with a fully competent CMV virus strain (AD169), were efficiently recognized by HLA-C*0702/IE-$1_{309-317}$-specific T cells and induced intensive IFNγ-secretion. In contrast to this observation, HLA-A*0201/$pp65_{495-503}$-specific T cells and other T cells with different HLA-restrictions were hampered by HLA-downregulation and were not capable to recognize and produce cytokines after coincubation with CMV-infected fibroblasts (Ameres et al., 2014; Ameres et al., 2013).

In addition to T cell escape, CMV encodes a large variety of genes modulating NK cell-mediated activation and killing of infected cells. One of these is the CMV UL18 gene product (gpUL18) which has high homology to the MHC class I molecule. Formation of a trimeric complex in combination with β_2-microglobulin leads to a high affinity ligand for the leukocyte immunoglobulin-like receptor 1 (LIR-1) expressed on NK cells and thereby inhibits MHC class I downregulation-induced NK cell-mediated cytotoxicity (Browne et al., 1990; Reyburn et al., 1997; Wagner et al., 2008; Willcox et al., 2003; Yang & Bjorkman, 2008). Furthermore, the CMV UL40 signal peptide (SP^{UL40}) leads to an increased expression of HLA-E on the cell surface and represents another important protein for NK cell evasion (Prod'homme et al., 2012).

1.8 CMV and transplantation

As previously addressed, CMV is the most common viral infection of patients after solid organ transplantation (SOT) or allogeneic HSCT and remains a major source of morbidity and mortality (Crough & Khanna, 2009; Emery, 2012; Fishman, 2007; Kotton, 2010; Moscarski et al., 2013). An overview about kidney transplantation (1.8.1) and HSCT (1.8.2) is given below.

1.8.1 Kidney transplantation

In case of end-stage renal disease (ESRD), patients can be treated by dialysis (hemodialysis or peritoneal dialysis) or by kidney transplantation. Kidney transplantation is advantageous since transplantation is more cost effective, improves quality of life, and overall survival is drastically increased in comparison to dialysis (KIDGO, 2009; Wolfe et al., 1999). Since the first successful kidney transplantation in 1954, the number of performed kidney transplantations within the United States has increased over the last decades. In 2013, 17.600 kidney transplantation were preformed within the United States (US-Renal-Data-System, 2016b). Main reasons for ESRD are diabetes and hypertension, but socioeconomic factors play also a role, as the prevalence of ESRD is higher in African Americans and other less privileged minorities in comparison to white Americans (US-Renal-Data-System, 2016a). The 5-year and 10-year kidney graft survival rate is approximately 77% and 56% (Gondos et al., 2013). In order to prevent graft rejection, patients have to accept a lifelong immunosuppressive medication, usually consisting of Calcineurin inhibitors (CNI), such as Tacrolimus and Cyclosporine A (CsA), antimetabolites, such as Mycophenolate Mofetil (MMF), and steroids (e.g. prednisolone). Less commonly mechanistic Target of Rapamycin inhibitors (mTORi), such as Sirolimus und Everolimus are used (KIDGO, 2009). Even though, immunosuppressive therapies have

decreased the incidence of acute graft rejection, long-term graft survival is still limited, depending in part on the HLA-match (Legendre et al., 2014; Susal & Opelz, 2013). Freitas reported, that patients with more than 5 mismatches have a 10% reduced 5-year graft survival in comparison to patients without any mismatch (Freitas, 2011). Furthermore, patients with known risk factors, such as advanced HLA-mismatch, panel reactive antibodies, and secondary transplantation receive an induction therapy in order to reduce the incidence of acute graft rejection (KIDGO, 2009). As an induction therapy reagent, lymphocyte-depleting agents such as anti-thymocyte globulin (ATG), or IL-2 receptor antagonists, like Basiliximab, are widely used and can be administered before, during, or immediately after transplantation (KIDGO, 2009). Several studies analyzing the benefit of these induction reagents, demonstrated a decreased risk of rejection and an increase in graft survival in comparison to placebo (Charpentier et al., 2003; Morton et al., 2009; Szczech et al., 1997; Szczech et al., 1998; Thibaudin et al., 1998). Due to these immunosuppressive regiments, kidney transplant recipients have an increased risk for secondary infections, such as urinary tract infections, tuberculosis, and viral infections (e.g.: CMV, EBV, or BK virus) (KIDGO, 2009).

1.8.2 Allogeneic HSCT

Allogeneic HSCT is a potentially curative treatment for malignant and non-malignant diseases of the hematopoietic system which are not treatable by conventionally therapies. The number of transplantations has increased over the last years (Passweg et al., 2014). The aim of HSCT is the replacement of the patient's hematopoietic system by HSCs of a suitable donor, in order to cure hematopoietic malignancies, like leukemia or lymphoma, other hematopoietic disorders, such as sickle-cell anemia, and immunodeficiency (e.g. severe combined immunodeficiency syndrome (SCID)) (Moss & Rickinson, 2005). In order to reduce graft rejection and graft versus host disease (GvHD) a complete HLA match is favored. In line with that, several studies described an increased risk of graft loss in case of HLA-mismatched and major ABO-mismatched transplants (Crocchiolo et al., 2009; Remberger et al., 2007). In order to reduce these major complications, patients need a conditioning treatment, manly consistent of total body irradiation and chemotherapy. As this treatment is myeloablative, the complete recipient's hematopoietic system needs to be restored by donor stem cells. Approximately 6 – 12 month after HSCT, immunosuppressive therapy can then often be completely stopped, whereas solid organ transplantation recipients need a lifelong

immunosuppressive regimen. Engraftment leads to the maturation of pro-thymocytes in the recipients' thymus terminating in central tolerance (Douek et al., 2000; Dumont-Girard et al., 1998; Roux et al., 2000). However, until full reconstitution of adaptive immunity, HSCT recipients are highly susceptible to opportunistic pathogens, like fungi, CMV, EBV, and Adenovirus.

1.9 Prevention and treatment of CMV-reactivations

In the late 1980s, CMV-reactivations and CMV-associated graft dysfunction and malaise were reported in up to 75% of transplanted patients, especially in month 1-4 after transplantation (Rubin, 1990). This changed with the development of antiviral agents and establishment of prophylactic regiments. Today approximately 20 to 40% of transplanted patients suffer from CMV-reactivations, depending on the type of transplant (Kotton, 2010).

1.9.1 Antiviral therapy

Four antiviral drugs are approved by the U.S. Food and Drug Administration (FDA) for prophylaxis or treatment of CMV-replications, namely Ganciclovir, Valganciclovir, Foscarnet, and Cidofovir (Moscarski et al., 2013). The nucleoside analog Ganciclovir ($C_9H_{13}N_5O_4$, M_r = 255.2 g/ mol) was discovered first. It accumulates in CMV-infected cells and is phosphorylated to Ganciclovir monophosphate or triphosphate by a CMV-encoded kinase (UL97) (Coen & Richman, 2013). Both are incorporated into the viral DNA and thereby prevent DNA-synthesis (Reid et al., 1988). Furthermore, Valganciclovir ($C_{14}H_{22}N_6O_5$, M_r = 354.4 g/ mol) is widely used in prophylactic treatment. Valganciclovir is an L-valine ester prodrug of Ganciclovir and gets hydrolyzed after absorption to Ganciclovir. Valganciclovir has an increased bioavailability in comparison to Ganciclovir and therefore can be administered orally (Coen & Richman, 2013). The debate about the appropriate duration of prophylactic treatment is still ongoing. Often a 90 days Valganciclovir prophylaxis is used, but a 200 days Valganciclovir prophylaxis has been recently reported to be superior for patients after kidney transplantation (Andrews et al., 2011; Humar et al., 2010; Kotton, 2010; Lowance et al., 1999). Like every other potent drug, these reagents can have serious side-effects. Ganciclovir is known to cause bone marrow suppression, especially neutropenia, and Valganciclovir can induce kidney damage (Coen & Richman, 2013; Jacobsen & Sifontis, 2010). In addition, these drugs can cause late onset CMV manifestations, by viral replications after discontinuation of prophylaxis or can induce resistance of the virus by UL97 mutants (Gohring et al., 2015; Murray & Subramaniam, 2004;

Schoeppler et al., 2013). Cidofovir, an analogue for deoxycytidine triphosphate needs also UL97-mediated phosphorylation to inhibit the viral DNA polymerase. Due to the low oral bioavailability, Cidofovir needs to be administered intravenously (Coen & Richman, 2013). In contrast, Foscarnet is the only approved antiviral that inhibits CMV polymerase directly by preventing pyrophosphate release. Foscarnet also has to be administered intravenously and is nephrotoxic (Coen & Richman, 2013; Eriksson et al., 1982). Furthermore, a recent study showed that prophylactic treatment was associated with increased tubular atrophy and reduced graft survival (Reischig et al., 2012).

1.9.2 Preemptive therapy

An alternative to the administration of antiviral prophylaxis is preemptive therapy in the SOT setting. After transplantation the patient is intensively screened for viral replication by PCR instead of receiving prophylactic treatment. In case of viral DNA detection above threshold (e.g. 500 copies/ml blood) the patient receives oral Valganciclovir or intravenous Ganciclovir. The selection of prophylaxis or preemptive therapy is dependent on the risk status of the patients. Guidelines recommend prophylactic treatment of SOT patients at high risk (D+/R-) for primary CMV-infection (KIDGO, 2009). In contrast, several studies analyzed the differences of prophylactic and preemptive therapy in standard risk patients (D+/R+, D-/R+) without significant benefit of either therapy (KIDGO, 2009; Mengelle et al., 2015). However, it is still uncertain if early CMV-reactivations are associated with graft damage and reduced graft survival (Dzabic et al., 2011; Reischig et al., 2009).

1.9.3 Adoptive T cell therapy (ACT)

An alternative to prophylactic or preemptive treatment with antivirals is the use of adoptively transferred T cells. Adoptive T cell therapy (ACT) defines the transfer of T cells in order to cure or compensate immunological defects. In theory, ACT can be used to remedy infectious diseases, autoimmunity, and cancer. As T cells play a major role for the surveillance of CMV-reactivations, the transfer of CMV-specific T cells is highly suitable. HSCT patients are at an enormous risk for CMV-associated disease and ACT is mainly used in this patient group (Moss & Rickinson, 2005). Starting in the early 1990s, the first reports of ACT using CMV-specific T cells after HSCT showed reconstitution and functional activity of the transferred T cells (Riddell et al., 1992; Walter et al., 1995). In order to obtain sufficient numbers of CMV-specific T cells different methods are available. Initially, CMV-specific T cell clones from the stem cell donor

were generated *in vitro* by stimulation of CMV-peptide or -lysate loaded fibroblast or APCs (Einsele et al., 2002; Micklethwaite et al., 2007; Peggs & Mackinnon, 2004; Riddell et al., 1992; Walter et al., 1995). Furthermore, CMV-specific T cells from the stem cell donor can be stimulated *in vitro* by Adenovirus-transfected B cells expressing a pp65 antigen (Leen et al., 2006). Recently, several studies selected CMV-specific T cells based on the TCR specificity using MHC-multimers in combination with magnetic beads (Cobbold et al., 2005; Uhlin et al., 2012). Even though lower numbers of CMV-specific T cells were obtained, the clinical efficacy was high, potentially reflecting the higher potency of *ex vivo* isolated T cells (Cobbold et al., 2005; Uhlin et al., 2012). An improvement of these methods is the purification of minimally manipulated $CD8^+$ CMV-specific T cells by reversible MHC-*Strep*Tamers (Schmitt et al., 2011). The MHC-*Strep*Tamer complex can be monomerized by addition of d-Biotin, resulting in non-modified T cell products with respective regulatory advantages (Knabel et al., 2002). This circumvents the *in vitro* generation of CMV-specific T cells under good manufacturing practice (GMP) conditions which is extremely time consuming and expensive. In addition, ACT could benefit from the usage of early differentiated pathogen-specific T cells, enabling low dose cell transfers with potentially reduced GvHD induction and prolonged cell survival (Busch et al., 2016; Stemberger et al., 2014). The limitation of MHC-*Strep*Tamer selection lies in the availability of HLA-compatible pathogen-specific MHC-*Strep*Tamers. Finally, new developments, such as the Fab-*Strep*Tamer technology enabled recently the prophylactic transfer of *ex vivo* isolated, early differentiated poly-specific memory T cells (Stemberger et al., 2012).

1.10 The CMV-restricted IE-$1_{309\text{-}317}$ peptide presented on HLA-C*0702

As briefly mentioned, CMV-specific T cells restricted to HLA-C*0702 are less susceptible to viral immune evasion strategies (Ameres et al., 2014; Ameres et al., 2013). Furthermore, Ameres et al. showed that $CD8^+$ T cell responses directed against the HLA-C*0702-restriceted CMV IE-$1_{309\text{-}317}$ epitope dominated the response to IE-1 in HLA-C-positive healthy donors (Ameres et al., 2013). Interestingly, a previous study described the CMV IE-$1_{309\text{-}317}$ peptide as HLA-B*0702-restricted (Kern et al., 1999). This study disregarded the high linkage disequilibrium of 0.96 for HLA-B*0702 and HLA-C*0702, leading to a strict co-expression of both HLA-types in the Caucasian population and causing the misinterpretation of the epitope's HLA-restriction (Ameres et al., 2013; Schmidt et al., 2009). As HLA-B*0702 is one of the most

common HLA-types within the Caucasian population with an allelic frequency of almost 15%, approximately 30% of the Caucasians carry the HLA-subtypes HLA-B*0702 and HLA-C*0702 (Schmidt et al., 2009). Notably, genomic sequencing data of archaic humans indicate an introgression of the HLA-C*0702-genotype in modern humans from the Neanderthals with potentially evolutionary advantages with regard to balance NK cell modulation (Abi-Rached et al., 2011). Indeed, HLA-C*0702 is a ligand for the inhibitory KIR2DL2/3 receptor expressed on NK cells (Parham, 2005). KIR2DL2/3 is a member of the C1-group receptors which all carry the inhibitory motive KIR2DL. C1-group ligands, like HLA-C*0702, represent the evolutionary oldest ligands being already present in orangutans and chimpanzees (Adams et al., 1999; Guethlein et al., 2002; Parham, 2005). From the virus' evolutionary perspective, CMV-induced immune evasion against HLA-C*0702-restricted T cell epitopes must be in consequence markedly less prominent than against HLA-A or –B-restricted CMV peptides in order to circumvent extensive NK cell mediated cytotoxicity (Ameres et al., 2013).

1.11 Aim of this work

CMV is still a major complication in immunocompromised patients, such SOT recipients and HSCT patients (Kotton, 2013). One option for the treatment of CMV-reactivations after HSCT is the adoptive transfer of CMV-specific T cells. As this method depends on MHC-multimers/*Strep*Tamers with given HLA-specificity, the identification of the CMV epitope IE-$1_{309\text{-}317}$ as HLA-C*0702-specific revealed an interesting new target for ACT (Ameres et al., 2013).

The first aim of this thesis was therefore the generation of an HLA-C7 *Strep*Tamer refolded with the IE-$1_{309\text{-}317}$ peptide. In addition, the phenotypical and functional characteristics of this novel T cell population needed to be examined in order to analyze the potentially protective capacities of HLA-C*0702/IE-1-specific T cells. Furthermore, the new reagent was also tested for full reversibility in order to be used for ACT. As the clinical grade production of the HLA-C*0702/IE-1 *Strep*Tamer was not part of this thesis, the MHC *Strep*Tamers were used for the *ex vivo* monitoring of kidney transplanted patients. This enabled the characterization of the behavior of this previously unknown T cell population in a clinical context.

In addition to ACT after HSCT, the reasons for CMV-reactivation and primary CMV-infection after SOT are still not fully elucidated. Furthermore, the optimal duration of antiviral prophylaxis repressing CMV-reactivation and infection in combination with minimal toxicity is

still debated. Therefore, the second aim of this thesis was the evaluation of factors predisposing of CMV-reactivation and primary infection with the aim to evaluate prognostic factors enabling the discontinuation of antiviral prophylaxis and to surveil patients by preemptive therapy. Therefore, a non-interventional clinical trial was initiated including 35 patients after kidney transplantation. Several antibody panels for flow cytometry were designed, in order to intensively monitor the included patients, if particular leucocyte subpopulations and specifically T cell subpopulations are a useful parameter for the prediction of future CMV-reactivation.

2. Materials and Methods

2.1 Materials

2.1.1 Reagents

Table 2.1: Reagents:

Agarose	Sigma-Aldrich, Taufkirchen, Germany
Ampicillin	Sigma-Aldrich, Taufkirchen, Germany
Anhydrotetracycline	IBA, Göttingen, Germany
Anti-PE MicroBeads	Miltenyi Biotec GmbH, Bergisch Gladbach, Germany
BD FACS lysing solution (10X)	BD Bioscience, San José, CA, USA
BD Trucount™ Controls	BD Bioscience, San José, CA, USA
Bicoll, Ficoll separating solution (density 1.077 g/mL)	Biochrom, Berlin, Germany
Bovine serum albumin (BSA)	Sigma-Aldrich, Taufkirchen, Germany
Brefeldin A (5 mg/mL in DMSO)	Sigma-Aldrich, Taufkirchen, Germany
Cytofix/Cytoperm reagent	BD Bioscience, San José, CA, USA
D-biotin	IBA, Göttingen, Germany
Dimethylsulfoxid (DMSO)	Sigma-Aldrich, Taufkirchen, Germany
DNA Gel Loading Dye (6X)	Thermo Fisher Scientific Inc., Waltham, MA, USA
DNAse I	Sigma-Aldrich, Taufkirchen, Germany
DTT (Dithiothreitol)	Sigma-Aldrich, Taufkirchen, Germany
Dulbecco's phosphate buffered saline (PBS)	Biochrom, Berlin, Germany
Ethanol 70% - 99.8% (v/v)	MRI Pharmacy, München, Germany
Ethidium bromide	Sigma-Aldrich, Taufkirchen, Germany
Ethidium monoazide bromide (EMA)	Life Technologies, Carlsbad, CA, USA
Ethylenediaminetetraacetic acid (EDTA)	Sigma-Aldrich, Taufkirchen, Germany
FACS Clean	BD Bioscience, San José, CA, USA
FACS Flow	BD Bioscience, San José, CA, USA
FACS Rinse	BD Bioscience, San José, CA, USA
Fetal calf serum (FCS)	Biochrom, Berlin, Germany
Formamide	Sigma-Aldrich, Taufkirchen, Germany
Glucose (40%)	Sigma-Aldrich, Taufkirchen, Germany
Glycerol	Sigma-Aldrich, Taufkirchen, Germany
Guanidine hydrochloride	Sigma-Aldrich, Taufkirchen, Germany
Human BD Tritest™ CD3 FITC/CD8 PE/CD45 PerCP	BD Bioscience, San José, CA, USA
Ionomycin calcium salt from *Streptomyces conglobatus*	Sigma-Aldrich, Taufkirchen, Germany
Isopropanol	MRI Pharmacy, München, Germany
L-arginine-HCL	Sigma-Aldrich, Taufkirchen, Germany
LB-medium	Sigma-Aldrich, Taufkirchen, Germany

Leupeptin	Sigma-Aldrich, Taufkirchen, Germany
L-Glutathione oxidized	Sigma-Aldrich, Taufkirchen, Germany
L-Glutathione reduced	Sigma-Aldrich, Taufkirchen, Germany
Lysozyme	Sigma-Aldrich, Taufkirchen, Germany
MES hydrate	Sigma-Aldrich, Taufkirchen, Germany
$MgCl_2$	Sigma-Aldrich, Taufkirchen, Germany
Sodium Azide	Sigma-Aldrich, Taufkirchen, Germany
Sodium deoxycholate	Sigma-Aldrich, Taufkirchen, Germany
Sodium EDTA	Sigma-Aldrich, Taufkirchen, Germany
Paraformaldehyde (PFA)	Sigma-Aldrich, Taufkirchen, Germany
PageRuler™ Prestained Protein Ladder, 10 to 180 kDa	Thermo Fisher Scientific Inc., Waltham, MA, USA
Pepstatin A	Sigma-Aldrich, Taufkirchen, Germany
Perm/Wash Solution	BD Bioscience, San José, CA, USA
Phenylmethanesulfonyl fluoride (PMSF)	Sigma-Aldrich, Taufkirchen, Germany
Phorbol 12-myrstate 13-acetate (PMA)	Sigma-Aldrich, Taufkirchen, Germany
RPMI 1640 (with L-Glutamine)	Gibco BRL, Karlsruhe, Germany
Sodium acetate	Sigma-Aldrich, Taufkirchen, Germany
Strep-Tactin-APC	IBA, Göttingen, Germany
Strep-Tactin-PE	IBA, Göttingen, Germany
Strep-Tactin® Magnetic Microbeads	IBA, Göttingen, Germany
Sucrose	Sigma-Aldrich, Taufkirchen, Germany
Tris-HCl	Carl Roth GmbH + Co. KG, Karlsruhe, Germany
Triton X	Sigma-Aldrich, Taufkirchen, Germany
Trizma® hydrochloride	Sigma-Aldrich, Taufkirchen, Germany
Trypan blue solution 0.4% (v/v)	Sigma-Aldrich, Taufkirchen, Germany
Urea	Thermo Fisher Scientific Inc., Waltham, MA, USA

2.1.2 Equipment

Table 2.2: Equipment:

ÄKTA Purifier 10 Protein Purification System	GE Healthcare Europe GmbH, Freiburg, Germany
Agarose gel documentation system	Bio-Rad Laboratories, Hercules, CA, USA
Agarose gel electrophoresis system (Sub-Cell® GT)	Bio-Rad Laboratories, Hercules, CA, USA
Amicon® Stirred Cells	Merck KGaA, Darmstadt, Germany
Automatic ice machine (Scotsman MF36)	Hubbard Systems, Great Blakenham, GB
Automatic pipettes (2-1000 µl)	Gilson, Inc., Middleton, USA
Balance (440-33N)	KERN & SOHN GmbH, Balingen-Frommern, Germany

Balance (XB120A)	Precisa Gravimetrics AG, Dietikon, Switzerland
BD LSRII™ flow cytometer	BD Bioscience, San José, CA, USA
Biological safety cabinet (Hera safe)	Thermo Fisher Scientific Inc., Waltham, MA, USA
Centrifuge (Eppendorf 5415 R)	Eppendorf AG, Hamburg, Germany
Centrifuge (Rotilabo®-Mini-Zentrifuge "Uni-fuge")	Carl Roth GmbH + Co. KG, Karlsruhe, Germany
Centrifuge (Rotina 420R)	Andreas Hettich GmbH & Co.KG, Tuttlingen, Germany
Centrifuge (Rotina 460R)	Andreas Hettich GmbH & Co.KG, Tuttlingen, Germany
Disperser (T10 basic Ultra-Turrax®)	IKA®-Werke GmbH & Co. KG, Staufen, Germany
DURAN® baffled flask	OMNILAB-LABORZENTRUM GmbH & Co.KG, Bremen, Germany
ELISA Reader (Infinite 200 PRO)	Tecan Group Ltd., Männedorf, Switzerland
FPLC	Amersham Biosciences, Europe GmbH, Freiburg
Freezer (-20°C)	Liebherr-International Deutschland GmbH, Biberach an der Riß, Germany
Freezer (-80°C)	Thermo Fisher Scientific Inc., Waltham, MA, USA
Freezing container (Nalgene® Mr. Frosty)	Sigma-Aldrich, Taufkirchen, Germany
Fridge	Liebherr-International Deutschland GmbH, Biberach an der Riß, Germany
Haematocytometer (Neubauer chamber)	NanoEnTek Inc., Seoul, Korea
Incubator (BBD 6220)	Heraeus Holding GmbH, Hanau, Germany
LumiNunc™ 96-well plates (white)	Nunc Labware, Sigma-Aldrich, Taufkirchen, Germany
Microscope (Zeiss)	Carl Zeiss AG, Oberkochen, Germany
Milli-Q Integral System	Millipore™, Merck KGaA, Darmstadt, Germany
Multichannel pipettes (Corning® Lambda™ Plus, 5-350 µl)	Corning Incorporated, Corning, NY, USA
Multipette® M4	Eppendorf AG, Hamburg, Germany
NanoDrop® 1000 Spectrophotometer	Thermo Fisher Scientific Inc., Waltham, MA, USA
neoLab-Rotating Mixer	neoLab, Heidelberg, Germany
pH-meter (MultiCal®)	WTW Wissenschaftlich-Technische Werkstätten GmbH, Weilheim, Germany
Pipetboy (Eppendorf Easypet® 3)	Eppendorf AG, Hamburg, Germany
Pipettes (Corning®, 2/10/20/100/200/1000 µl)	Corning Incorporated, Corning, NY, USA

Power supply (Power Pac 3000)	Bio-Rad Laboratories, Hercules, CA, USA
QuadroMACS™ Separator	Miltenyi Biotec GmbH, Bergisch Gladbach, Germany
Rotating mixer (RM 5)	Glaswarenfabrik Karl Hecht GmbH&Co KG, Sondheim v. d. Rhön, Germany
*Strep*Man Magnet for 15 ml and 50 ml tubes	IBA, Göttingen, Germany
Thermocycler T Professional Thermocycler	Biometra, Göttingen, Germany
Thermomagnetic stirrer (IKAMAG® REO)	IKA®-Werke GmbH & Co. KG, Staufen, Germany
Thermomixer (compact)	Eppendorf AG, Hamburg, Germany
Ultracentrifuge (Optima™ L-100 XP)	Beckman Coulter GmbH, Krefeld, Germany
Vi-CELL® Cell Viability Analyzer	Beckman Coulter GmbH, Krefeld, Germany
Vortex mixer (Reax top)	Heidolph Instruments GmbH & Co.KG, Schwabach, Germany
Water bath	Memmert GmbH + Co. KG, Schwabach, Germany

2.1.3 Consumables

Table 2.3: Consumables:

BD Trucount™ Tubes	BD Bioscience, San José, CA, USA
Cell strainer (40-100 µm)	BD Bioscience, San José, CA, USA
Combitips plus® (0.2-2.5 ml)	Eppendorf AG, Hamburg, Germany
Cryo vials	Alpha Laboratories Ltd, Eastleigh, GB
Culture plates (6-, 12-, 24-, 96-well)	BD Bioscience, San José, CA, USA
Dialysis tubing (MWCO 6-8000/100 mm)	Spectrum Labs, Rancho Dominguez, CA, USA
Disposable bags	Carl Roth GmbH + Co. KG, Karlsruhe, Germany
ELISA plates (96 well)	Thermo Fisher Scientific Inc., Waltham, MA, USA
Eppendorf tubes (0.5-2 ml)	Eppendorf AG, Hamburg, Germany
FACS tubes (Microtubes, 1.2 ml)	Alpha Laboratories Ltd, Eastleigh, GB
Falcon tubes (15/50 ml)	BD Bioscience, San José, CA, USA
Gloves	Rösner-Mautby Meditrade Holding GmbH, Kiefersfelden, Germany
Leucosep-Tubes	Greiner Bio-One International GmbH, Kremsmünster, Austria
LD Columns	Miltenyi Biotec GmbH, Bergisch Gladbach, Germany
One Shot® TOP10 Chemically Competent E. coli	Thermo Fisher Scientific Inc., Waltham, MA, USA
Parafilm M® (Pechiney)	Sigma-Aldrich, Taufkirchen, Germany

Pipette tips (10-1000 µl)	Nerbe plus GmbH, Winsen/Luhe, Germany
QF-CMV Test Single Patient Pack (SPP)	Qiagen, Hilden, Germany
Reservoirs (50 ml)	Corning Incorporated, Corning, NY, USA
Serological pipettes (5-50 ml)	Greiner Bio-One International GmbH, Kremsmünster, Austria
S-Monovette® (Ammonium-Heparin)	Sarstedt AG & Co., Nümbrecht, Germany
S-Monovette® (Lithium-Heparin)	Sarstedt AG & Co., Nümbrecht, Germany
Ultrafiltration Discs	Merck KGaA, Darmstadt, Germany
Ultrafree-4 filter Biomax-10 membrane	Merck KGaA, Darmstadt, Germany

2.1.4 Enzymes

Table 2.4: Enzymes:

BamH1	Sigma-Aldrich, Taufkirchen, Germany
Benzonase	Merck KGaA, Darmstadt, Germany
Nde I	Thermo Fisher Scientific Inc., Waltham, MA, USA

2.1.5 Kit systems

Table 2.5: Kit systems:

BD OptEIA™ (TMB substrate)	BD Bioscience, San José, CA, USA
BD Fixation/Permeabilization Solution Kit	BD Bioscience, San José, CA, USA
CMV-IgG-ELA Test PCS ELISA	Medac, Wedel, Germany
CMV-IgM-ELA Test PCS ELISA	Medac, Wedel, Germany
Pierce™ BCA Protein Assay Kit	Thermo Fisher Scientific Inc., Waltham, MA, USA
PureYield™ Plasmid Miniprep System	Promega GmbH, Mannhein, Germany
QIAquick Gel Extraction Kit	Qiagen, Hilden, Germany
QuantiFERON-CMV 2 Plate Kit ELISA	Qiagen, Hilden, Germany
Rapid DNA Ligation Kit	Thermo Fisher Scientific Inc., Waltham, MA, USA
StarGate® Cloning Kit	IBA, Göttingen, Germany

2.1.6 Software

Table 2.6: Software:

Adobe Illustrator CS6	Adobe Systems Software Ireland Limited, Dublin, Republic of Ireland
BD FACSDIVA™ SOFTWARE v6.0	BD Bioscience, San José, CA, USA
FlowJo 9.7.6	FlowJo LLC., Ashland, OR, USA
Graph Pad Prism 5	GraphPad Software, Inc., La Jolla, CA, USA

Magellan™ - Data Analysis Software (microplate reader)	Tecan Group Ltd., Männedorf, Switzerland
Microsoft Office Professional 2013	Microsoft Corporation, Redmond, WA, USA
QuantiFERON-CMV Analysis Software v3.03	Cellestis, Qiagen, Hilden, Germany
SigmaPlot 10.0	Systat Software, Inc., San José, CA, USA
Vector NTI® Software	Thermo Fisher Scientific Inc., Waltham, MA, USA

2.1.7 Antibodies

2.1.7.1 Antibody overview

Table 2.7: Antibodies for flow cytometry and *in vitro* stimulation:

Antibody	Clone	Dilution	Supplier
Human CD28 unlabeled	L293	0.2 µl/well	BD Bioscience
Human CD49d unlabeled	L25	0.2 µl/well	BD Bioscience
Human CD3 FITC	UCHT1	1/20	Pharmingen
Human CD3 PE	SK7	1/20	BD Bioscience
Human CD3 eF450	UCHT1	1/20	eBioscience
Human CD3 PE-Cy7	UCHT1	1/400	eBioscience
Human CD3 APC	UCHT1	1/100	Beckman Coulter
Human CD3 Alexa700	UCHT1	1/400	Pharmingen
Human CD3 APC-Alexa750	UCHT1	1/100	Life Technologies
Human CD4 V500	RPA-T4	1/20	BD Bioscience
Human CD8 FITC	SK1	1/20	BD Bioscience
Human CD8 PE	SK1	1/200	BD Bioscience
Human CD8 PerCP	SK1	1/10	BD Bioscience
Human CD8 PE-Cy7	SK1	1/20	BD Bioscience
Human CD8 APC	SK1	1/20	BD Bioscience
Human CD8 Alexa700	SK1	1/800	eBioscience
Human CD19 ECD	J3-119	1/20	Beckman Coulter
Human CD14 APC-Alexa750	RMO52	1/100	Beckman Coulter
Human CD16 APC	3G8	1/800	Caltag
Human CD27 FITC	M-T271	1/200	Pharmingen
Human CD27 Alexa700	323	1/20	Natutec
Human CD45RO PE-Cy7	N901	1/20	Beckman Coulter
Human CD45RA APC-Alexa750	UCHL1	1/20	BD Bioscience
Human CD56 PE-Cy7	2H4	1/20	Beckman Coulter
Human CD95 BV421	DX2	1/20	BioLegend
Human CD158b FITC (KIR2DL2/3)	CH-L	1/20	BD Bioscience
Human CD161 PE	191B8	1/10	Beckman Coulter
Human CD197 FITC (CCR7)	1505003	1/10	R&D

Human HLA-DR FITC	TU36	1/20	Thermo Fisher Scientific
Human GM-CSF PE	BVD2-21C11	1/40	BD Bioscience
Human IFNγ Alexa700	B27	1/200	Pharmingen
Human IL-2 APC	5344.111	1/20	BD Bioscience
Human TNFα PE-Cy7	Mab11	1/400	eBioscience

2.1.7.2 Staining panel for leucocyte subpopulations

Table 2.8: Antibodies for the detection of leucocyte subpopulations:

Single staining			
Antibody	**Clone**	**Dilution**	**Supplier**
Human CD3 eF450	UCHT1	1/20	eBioscience
Human CD3 PE-Cy7	UCHT1	1/400	eBioscience
Human CD3 APC-Alexa750	UCHT1	1/100	Life Technologies
Human CD4 V500	RPA-T4	1/20	BD Bioscience
Human CD8 FITC	SK1	1/20	BD Bioscience
Human CD8 PE	SK1	1/200	BD Bioscience
Human CD8 PerCP	SK1	1/10	BD Bioscience
Human CD8 APC	SK1	1/20	BD Bioscience
Human CD19 ECD	J3-119	1/20	Beckman Coulter
Combinatorial staining			
Human CD3 eF450	UCHT1	1/20	eBioscience
Human CD4 V500	RPA-T4	1/20	BD Bioscience
Human CD8 PerCP	SK1	1/10	BD Bioscience
Human CD19 ECD	J3-119	1/20	Beckman Coulter
Human CD14 APC-Alexa750	RMO52	1/100	Beckman Coulter
Human CD16 APC	3G8	1/800	Caltag
Human CD56 PE-Cy7	2H4	1/20	Beckman Coulter
Human CD161 PE	191B8	1/10	Beckman Coulter
Human HLA-DR FITC	TU36	1/20	Thermo Fisher

2.1.7.3 Staining panel for CMV-specific T cells by MHC-multimer staining

Table 2.9: Antibodies for the detection of CMV-specific T cells by MHC-multimer staining:

Single staining			
Antibody	**Clone**	**Dilution**	**Supplier**
Human CD3 eF450	UCHT1	1/20	eBioscience
Human CD3 PE-Cy7	UCHT1	1/400	eBioscience
Human CD3 APC-Alexa750	UCHT1	1/100	Life Technologies
Human CD4 V500	RPA-T4	1/20	BD Bioscience
Human CD8 FITC	SK1	1/20	BD Bioscience
Human CD8 PE	SK1	1/200	BD Bioscience
Human CD8 PerCP	SK1	1/10	BD Bioscience
Human CD8 APC	SK1	1/20	BD Bioscience

Human CD8 Alexa700	SK1	1/800	eBioscience
Human CD19 ECD	J3-119	1/20	Beckman Coulter
Combinatorial staining			
Human CD3 APC-Alexa750	UCHT1	1/100	Life Technologies
Human CD4 V500	RPA-T4	1/20	BD Bioscience
Human CD8 PerCP	SK1	1/10	BD Bioscience
Human CD19 ECD	J3-119	1/20	Beckman Coulter
Human CD27 Alexa700	323	1/20	Natutec
Human CD45RO PE-Cy7	N901	1/20	Beckman Coulter
Human CD95 BV421	DX2	1/20	BioLegend
Human CD197 FITC (CCR7)	#1505003	1/10	R&D
MHC-Multimer PE	-	1/10	
MHC-Multimer APC	-	1/10	

2.1.7.4 Staining panel for CMV-specific T cells by intracellular cytokine staining

Table 2.10: Antibodies for the detection of CMV-specific T cells by intracellular cytokine staining:

Single staining			
Antibody	**Clone**	**Dilution**	**Supplier**
Human CD3 eF450	UCHT1	1/20	eBioscience
Human CD3 PE-Cy7	UCHT1	1/400	eBioscience
Human CD3 APC-Alexa750	UCHT1	1/100	Life Technologies
Human CD4 V500	RPA-T4	1/20	BD Bioscience
Human CD8 FITC	SK1	1/20	BD Bioscience
Human CD8 PE	SK1	1/200	BD Bioscience
Human CD8 PerCP	SK1	1/10	BD Bioscience
Human CD8 APC	SK1	1/20	BD Bioscience
Human CD8 Alexa700	SK1	1/800	eBioscience
Human CD19 ECD	J3-119	1/20	Beckman Coulter
Combinatorial staining			
Antibody	**Clone**	**Dilution**	**Supplier**
Cell surface markers			
Human CD3 eF450	UCHT1	1/20	eBioscience
Human CD4 V500	RPA-T4	1/20	BD Bioscience
Human CD8 PerCP	SK1	1/10	BD Bioscience
Human CD19 ECD	J3-119	1/20	Beckman Coulter
Human CD27 FITC	M-T271	1/200	Pharmingen
Human CD45RA APC-Alexa750	UCHL1	1/20	BD Bioscience
Intracellular cytokines			
Human GM-CSF PE	BVD2-21C11	1/40	BD Bioscience
Human IFNγ Alexa700	B27	1/200	Pharmingen
Human IL-2 APC	5344.111	1/20	BD Bioscience
Human TNFα PE-Cy7	Mab11	1/400	eBioscience

2.1.8 Buffers and media

All buffers and solutions were prepared with Millipore Q distilled water.

Table 2.11: Buffers and solutions:

8M Urea:	25 mM	MES
	8 M	Urea
	0.5 M	Sodium EDTA
	0.1 mM	DTT
	pH 6.0	
BD FACS lysing buffer:		dH_2O
	1x	BD FACS lysing solution
Bacterial growth medium (1 l):	1 l	LB-medium
	10 ml	Glucose (40%)
	100 ng	Ampicillin
BFA working solution:	192 µl	20 µl BFA stock solution (5 mg/ml in DMSO) mixed with 180 µl PBS
	2208 µl	Cell culture medium
Cell culture medium:	1x	RPMI 1640 (with L-Glutamine)
	10%	FCS
Dissociation buffer:	1x	PBS
	1 mM	D-biotin
	0.5%	BSA
Erythrocyte Lysing Solution:	153 mM	NH_4Cl
	17 mM	Tris-HCl
	pH 7.2	
FACS buffer:	1x	PBS
	0.5%	BSA
Freezing medium:	90%	FCS
	10%	DMSO
Guanidine solution (100ml):	3 M	Guanidine-HCl
	10 mM	Sodium acetate
	10 mM	Sodium EDTA
	pH 4.2	
	RT	
Lysis buffer:	50 mM	Tris-HCl
	1%	Triton X
	0.1%	Sodium deoxycholate
	100 mM	NaCl
	0.1%	Sodium Azide
	10 mM	DTT
	pH 8.0	
PMA/Ionomycin working solution (50 µl):	0.625 µl	PMA (0.1 mg/ml in DMSO)
	5 µl	Ionomycin of 0.5 mg/ml in EtOH
		H_2O
	44.4 µl	

Refolding buffer (250 ml):		dH_2O
	100 mM	Tris-HCl
	400 mM	L-Arginine-HCl
	2 mM	Sodium EDTA
	0.5 mM	Oxidized Glutathione
	5 mM	Reduced Glutathione
	pH 8.0	
	4°C	
Washing buffer with Triton:	50 mM	Tris-HCl
	0.5%	Triton X
	100 mM	NaCl
	1 mM	Sodium EDTA
	0.1%	Sodium Azide
	1 mM	DTT
	pH 8.0	
Solution buffer:	50 nM	Tris-HCl
	25%	Sucrose
	1 mM	Sodium EDTA
	0.1%	Sodium Azide
	10 mM	DTT
	pH 8.0	

2.1.9 MHC-multimers

All MHC-multimers for the detection of CMV-specific T cells were coupled to a *Strep*-Tag III (Skerra & Schmidt, 1999) and were generated in house. All peptides were purchased from IBA (Göttingen, Germany).

Table 2.12: MHC-multimers:

HLA-type	β2m	Peptide	Segment	Sequence
A*01:01	human	pp50	245-253	VTEHDTLLY
A*01:01	human	pp65	363-373	YSEHPTFTSQY
A*02:01	human	pp65	495-503	NLVPMVATV
A*02:01	human	IE-1	316-324	VLEETSVML
A*24:02	human	pp65	341-350	QYDPVAALF
B*07:02	human	pp65	417-426	TPRVTGGGAM
B*08:01	human	IE-1	88-96	QIKVRVDMV
B*08:01	human	IE-1	199-207K	ELKRMMYM
B*27:01	human	pp65	211-219	NTRATKMQVI
B*35:01	human	pp65	123-131	IPSINVHHY
C*07:02	human	IE-1	309-317	CRVLCCYVL
C*07:02	human	MAGE-A12	170-178	VRIGHLYIL

2.1.10 CMV-peptides and mixes

Table 2.13: Single CMV-peptides for *in vitro* stimulation:

HLA-type	Peptide	Segment	Sequence	Supplier
A*01:01	pp50	245-253	VTEHDTLLY	IBA, Göttingen, Germany
A*01:01	pp65	363-373	YSEHPTFTSQY	IBA, Göttingen, Germany
A*02:01	pp65	495-503	NLVPMVATV	IBA, Göttingen, Germany
A*02:01	IE-1	316-324	VLEETSVML	IBA, Göttingen, Germany
A*24:02	pp65	341-350	QYDPVAALF	IBA, Göttingen, Germany
B*07:02	pp65	417-426	TPRVTGGGAM	IBA, Göttingen, Germany
B*08:01	IE-1	88-96	QIKVRVDMV	IBA, Göttingen, Germany
B*08:01	IE-1	199-207K	ELKRMMYM	IBA, Göttingen, Germany
B*27:01	pp65	211-219	NTRATKMQVI	IBA, Göttingen, Germany
B*35:01	pp65	123-131	IPSINVHHY	IBA, Göttingen, Germany
C*07:02	IE-1	309-317	CRVLCCYVL	IBA, Göttingen, Germany
C*07:02	MAGE-A12	170-178	VRIGHLYIL	IBA, Göttingen, Germany

Table 2.14: CMV-peptide mixes for *in vitro* stimulation:

Product	No. of peptides	Supplier
hCMV IE-1	120 peptides (peptide scan 15/11)	JPT Peptide Technologies GmbH, Berlin, Germany
hCMV pp65	138 peptides (peptide scan 15/11)	JPT Peptide Technologies GmbH, Berlin, Germany

2.1.11 Vectors

2.1.11.1 HLA-C*0702-vector sequence

The vector was order and synthesized by GeneArt Gene Synthesis (Thermo Fisher Scientific).

The vector was codon optimized for *E. coli* expression and included a *Strep*-Tag III (Figure 2.1).

CATATGGCGCTGACCGAAACCTGGGCGTGCAGCCATAGCATGCGCTATTTTGATACCGCGGTGAGCCGCCCGGGCCGCGGCGAAC
CGCGCTTTATTAGCGTGGGCTATGTGGATGATACCCAGTTTGTGCGCTTTGATAGCGATGCGGCGAGCCCGCGCGGCGAACCGCGC
GCGCCGTGGGTGGAACAGGAAGGCCCGGAATATTGGGATCGCGAAACCCAGAAATATAAACGCCAGGCGCAGGCGGATCGCGT
GAGCCTGCGCAACCTGCGCGGCTATTATAACCAGAGCGAAGATGGCAGCCATACCCTGCAGCGCATGAGCGGCTGCGATCTGGGC
CCGGATGGCCGCCTGCTGCGCGGCTATGATCAGAGCGCGTATGATGGCAAAGATTATATTGCGCTGAACGAAGATCTGCGCAGCTG
GACCGCGGCGGATACCGCGGCGCAGATTACCCAGCGCAAACTGGAAGCGGCGCGCGCGGCGGAACAGCTGCGCGCGTATCTGG
AAGGCACCTGCGTGGAATGGCTGCGCCGCTATCTGGAAAACGGCAAAGAAACCCTGCAGCGCGCGGAACCGCCGAAAACCCATG
TGACCCATCATCCGCTGAGCGATCATGAAGCGACCCTGCGCTGCTGGGCGCTGGGCTTTTATCCGGCGGAAATTACCCTGACCTGG
CAGCGCGATGGCGAAGATCAGACCCAGGATACCGAACTGGTGGAAACCCGCCCGGCGGGCGATGGCACCTTTCAGAAATGGGCG
GCGGTGGTGGTGCCGAGCGGCCAGGAACAGCGCTATACCTGCCACATGCAGCATGAAGGCCTGCAGGAACCGCTGACCCTGAGC
TGGGAACCGAGCAGCCAGCCGACCATTGGC**AGCGCGTGGAGCCATCCGCAGTTTGAAAAAGGCGGCGGCAGCGGCGGCGGCG**
GCAGCGGCGGCAGCGCGTGGAGCCATCCGCAGTTTGAAAAATAGGGATCC

Figure 2.1: Sequence of the GeneArt HLA-C*0702 vector.
Sequence of the HLA-C*0702 vector for the generation of the MHC-heavy-chain. Orange = Nde I restriction site; red = linker; bold = *Strep*-Tag III; blue = stop codon; green = BamH1 restriction site.

2.1.11.2 pASG-IBA wt1 expression vector

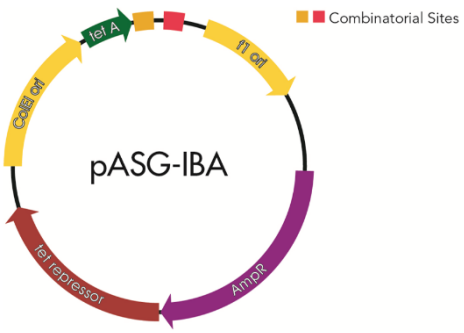

Figure 2.2: Vector map of the pASG-IBA wt1 expression vector (IBA-GmbH, 2016).
The pASG-IBA vector includes two combinatorial sites, an ampicillin-resistance and a tetracycline inducible promotor.

2.2 Methods

2.2.1 HLA-C-multimer generation

2.2.1.1 Vector design

The generation of the MHC-multimer restricted to HLA-C*0702 was started with the design of a suitable vector. Synthesis of the vector was performed by GeneArt and included a 5' Nde I restriction site, the nucleotide sequence of HLA-C*0702, the *Strep*-Tag III, a stop codon, and a BamH1 restriction site. A detailed depiction of the sequence was shown in Figure 2.1.

2.2.1.2 Vector digestion and insert extraction

The synthesized donor vector (GeneArt) was digested using a freshly prepared reaction mix:

Table 2.15: Digestion reaction mix:

Reagent	**Volume**
DNA-plasmid	10 µl
Nde I	1 µl
BamH1	1 µl
Buffer (10x)	2 µl
H_2O	6 µl

The reaction was incubated for 5 minutes at 37°C, mixed with 4 µl DNA Gel Loading Dye (6X) and loaded on a 0.8% agarose ethidium bromide gel. Fractionation of the bands was achieved with 130 V for 27 minutes. The respective gel bands were cut out and DNA-gel-extraction was performed with the QIAquick Gel Extraction Kit. DNA content was measured using a NanoDrop Spectrophotometer.

2.2.1.3 Cloning of the insert into an expression vector

In order to achieve a highly efficient production of the MHC-heavy-chain in a bacterial culture, the synthesized sequence was cloned into the pASG-IBA-wt1-expression vector (Figure 2.2) using the StarGate® Cloning Kit according to manufacturer's instructions. In brief, in a one tube reaction, the insert (2.2.1.2) was mixed with StarSolution M1-3 and the pASG-IBA-wt1 expression vector. The vector assembly was achieved during 1 hour at 37°C incubation. Afterwards, 10 µl of the reaction was mixed with one vial of competent *E. coli* (TOP10) and

incubated for 30 minutes on ice. The mixture was incubated then for 1 minute at 42°C and cooled for 5 minutes on ice. Together with 900 µl of LB-medium the cells were incubated and shaken for 45 minutes at 37°C. 200 µl of the culture was plated on Ampicillin (Amp)-containing agar plates and incubated overnight at 37°C. The next day, several colonies were picked and transferred into 15 ml-falcons containing 4 ml Amp-LB-medium. Cells were again incubated overnight at 37°C. Afterwards, plasmid-extraction was performed with the PureYield™ Plasmid Miniprep System and the vector was sequenced by GATC Biotech AG (Konstanz, Germany). For long term storage, a bacterial glycerol stock was generated by mixing 100 µl bacterial suspension with 100 µl glycerol. The resultant was stored at -80°C.

2.2.1.4 Protein expression and purification

The expression of the MHC-heavy-chain was performed using 6 x 1 liter bacterial growth medium (2.1.8) to obtain large amounts of protein. Each flask was supplemented with 20 µl of the bacterial glycerol stock (2.2.1.3.) and incubated at 37°C with 160 rpm for 8 h. At an optical density (OD_{600}) of 0.7, the expression of the plasmid was induced by adding 100 µl anhydrotetracycline for 3 hours at 37°C. Afterwards, the suspension was pooled by centrifuging the bacterial solution several times for 20 minutes at 3750 rpm at 4°C. Afterwards, the pellets were frozen over night at -80°C.

For the purification of inclusion bodies, the bacteria were thawed on ice, resuspended with 13 ml solution buffer and homogenized using a sonicator. Cells were gently mixed with 100 µl lysozyme, 250 µl DNAse I and 50 µl $MgCl_2$. After the addition of 12.5 ml lysis buffer, the solution was left to incubate for 1 hour at RT. Subsequently, the tubes were frozen at -80°C for 25 minutes and afterwards transferred to a preheated (37°C) water bath for 30 minutes. 50 µl $MgCl_2$ was added with further incubation for approximately 30 minutes at RT, and a reduced viscosity was observed. Afterwards, 350 µl Sodium EDTA was added and the suspension was centrifuged at 11.000 rpm at 4°C for 20 minutes. The supernatant was discarded, the pellet resuspended on ice in 10 ml washing buffer, supplemented with Triton X, and homogenized with a sonicator. After another centrifugation step, the supernatant was discarded, the pellet washed with 10 ml washing buffer without Triton X, homogenized using a sonicator, and centrifuged as above. The pellet was resuspended with 3 ml urea and incubated overnight at 4°C. The sample was transferred to ultracentrifugation tubes, centrifuged at 45000 rpm for 20 minutes at RT and the supernatant was collected into a 15 ml-Falcon tube. To test the purity of the freshly isolated proteins, 1 µl of protein was diluted

with 9 µl dH_2O, boiled for 3 minutes and loaded onto a 10% SDS gel. Protein concentration was determined with the Pierce™ BCA Protein Assay Kit. 2 ml aliquots from the pooled recombinant protein-in-urea-solution were stored at -80°C.

2.2.1.5 MHC-refolding

All MHC-multimers, used for the detection and the purification of antigen-specific $CD8^+$ T cells were produced by the institute, according to previously published protocols (Altman et al., 1996; Busch et al., 1998; Garboczi et al., 1992; Knabel et al., 2002). In brief, urea denatured MHC-heavy-chain (2.2.1.4) was refolded in the presence of β2-microglobulin and peptide using a refolding buffer (2.1.8). All MHC/peptide-complexes (pMHC) carried a *Strep*-Tag III and were purified by gel filtration chromatography over an ÄKTA Purifier 10 Protein Purification System (Busch et al., 1998).

2.2.1.6 Multimerization of MHC-monomers

Multimerization of MHC-monomers was performed shortly before use. For each MHC-multimer 2 µg of MHC-monomers were incubated with 5 µl *Strep*-Tactin PE or APC and 43 µl FACS buffer for 45 minutes on ice.

2.2.2 Cell culture handling

2.2.2.1 Blood collection

Blood collection from healthy donors was undertaken after obtaining written, informed consent. The study was approved by the local Institutional Review Board according to national law (Ethikkommission der Medizinischen Fakultät der Technischen Universität München).
In addition to these donors, between 2011 and 2014, we included patients who received a kidney or kidney/pancreas transplant at the University Hospital Klinikum rechts der Isar, Munich, Germany. This addendum was also approved by the local ethics committee and is in accordance with the Declaration of Helsinki and the Declaration of Istanbul. All patients enrolled gave their written informed consent.

2.2.2.2 Peripheral blood mononuclear cell (PBMC) isolation and human plasma collection

PBMC isolation was performed with heparinized (Li-Heparin or NO_4-Heparin) whole blood. For plasma collection, blood was centrifuged for 10 minutes at 700 g. Supernatant was collected,

aliquoted into cryo vials and stored long-term at -80°C. Afterwards, the remaining blood components were diluted with phosphate-buffered saline (PBS) in a 1:1 ratio and for each tube 35 ml blood/ PBS-mixture was carefully transferred on a 15 ml Ficoll layer. Separation of erythrocytes, lymphocytes and serum was accomplished by density gradient centrifugation for 25 minutes at 700 g without centrifuge breaking. The lymphocyte layer was transferred into a fresh tube and washed once with PBS and once with cell culture medium. Cells were resuspended in 2 ml cell culture medium.

2.2.2.3 Cell counting

For the determination of living cells, cells were diluted with 12.5% Trypan blue solution and counted on a Neubauer counting chamber, using a microscope (10x magnification). This method discriminates between living and dead cells, as the dye only accumulates in dead cells due to a missing membrane integrity.

Cell numbers were assessed by using the following formula:

$$\frac{\text{Number of living cells}}{\text{Number of counted squares}} \times \text{dilution factor} \times 10^4 = \frac{\text{cell number}}{\text{ml}}$$

2.2.2.4 Freezing and thawing of cells

Isolated PBMCs were adjusted to $1x10^7$ cells/ ml with freshly prepared freezing medium (2.1.8) and aliquoted into 2 ml cryo vials. Afterwards, the vials were placed in a precooled (4°C) Mr. Frosty, stored for 24 hours at -80°C and then transferred for long-term storage into liquid nitrogen.

For the thawing of cryopreserved PBMCs, cells were transferred into preheated (37°C) cell culture medium, supplemented with Benzonase (2 µl for 10 ml of medium), and washed twice by centrifuging for 10 minutes at 700 g.

2.2.2.5 Resting of PBMCs for ICS

For the optimal stimulation of PBMCs and detection of produced cytokines by ICS, cells were rested for 18 hours at 37°C and 5% CO_2 in cell culture medium at a density of $2x10^6$ cells/ ml medium. For an optimal gas exchange, falcons were oriented in a 45° angle with a slightly opened lid (Kutscher et al., 2013).

2.2.3 QuantiFERON (QF) assay

The QF assay detects IFNγ-secretion of T cells after stimulation of whole blood with different peptides and was performed according to manufacturer's instructions and was summarized below.

2.2.3.1 Blood collection and stimulation of whole blood

For the stimulation of whole blood the QF-CMV Test Single Patient Pack (SPP) was used. This commercial available tests includes three different tubes. First, the NIL tube, which serves as a negative control. Second, the Mitogen tube, which serves as a positive control for the assessment of the overall stimulation capacity of the cells. Third, the CMV tube, provides CMV-specific stimulation of $CD8^+$ T cells via 22 different CMV-restricted peptides with HLA-restrictions representing > 98% of the world-wide MHC-haplotype (Giulieri & Manuel, 2011). Each tube was filled with 1 ml whole blood, intensively shaken and incubated for 16 to 24 hours at 37°C in an upright position. The next day, the tubes were centrifuged at 3000 g for 15 minutes and the supernatant was transferred into cryo vials for long-term storage at -80°C.

2.2.3.2 QuantiFERON-CMV enzyme-linked immunosorbent assay (ELISA)

The detection of secreted IFNγ, after MHC I-dependent stimulation (2.2.3.1), was performed with the QF-CMV ELISA according to the manufacturer's instructions. In brief, plasma and all reagents, except the 100x conjugate, were brought to RT for approximately one hour to ensure equilibration to RT. Afterwards, 50 µl of freshly prepared conjugate solution was transferred into a provided ELISA plate and 50 µl of respective plasma (NIL, CMV, CMV 1:10, Mitogen, Mitogen 1:10) and standard solution was added. The solution was intensively shaken for one minute and incubated for two hours at RT in the dark. Then all wells were washed six times with 400 µl wash buffer and plates were tapped face down on an absorbent towel to remove the residual liquid. 100 µl of enzyme substrate solution was added and incubated for 30 minutes at RT in the dark. To stop the reaction, the solution was mixed with 50 µl of enzyme stopping solution and the plate was immediately analyzed using an ELISA reader (Tecan). For the determination of the correct OD, a filter with 450nm filter and a reference filter of 620 to 650nm was used. The calculation of the readout was performed using the QuantiFERON-CMV Analysis Software (2.1.6).

2.2.4 Flow cytometry analyses

All experiments were performed with maximum care and acquired using a BD LSRII™ flow cytometer. All stainings were performed in a 96-well cell culture plate and for each well $1x10^6$ cells were used. If appropriate, a master mix of the respective antibodies was prepared. Flow cytometric analyses were performed with FlowJo 9.7.6.

2.2.4.1 Determination of absolute cell counts

The determination of absolute $CD45^+$, $CD3^+$ and $CD8^+$ cells was performed with the BD Trucount™ Tubes according to manufacturer's instructions (CLSI, 2007). In brief, 50 µl of whole blood was transferred into the BD Trucount™ Tubes and 20 µl of the Human BD Tritest™ was added and mixed. Suspension was incubated for 15 minutes at RT in the dark. Afterwards, 450 µl BD FACS lysing buffer was added and incubated for 15 minutes at RT in the dark, causing erythrocyte lysis and fixation of the cells. As a pipetting control, 50 µl of the corresponding BD Trucount™ Controls were added shortly before acquisition.

2.2.4.2 Detection of lymphocyte subpopulations

The determination of the different leucocyte populations was performed with the previously described antibody combination (Table 2.8) which were selected according to Autissier et al. (Autissier et al., 2010).

$1x10^6$ PBMCs were seeded into a 96-well plate and, for live/ dead discrimination, incubated for 10 minutes on ice with ethidium bromide monoazide (EMA) using strong light. Afterwards, cells were washed once with FACS buffer and thereafter incubated in 50 µl of the prepared antibody mixture for 30 minutes on ice and in the dark. Cells were washed again twice with PBS and fixed, using 100 µl of 2% PFA solution for 20 minutes on ice. Cells were once more washed with FACS buffer and resuspended in 250 µl FACS buffer for acquisition.

2.2.4.3 Detection of CMV-specific T cells by MHC-multimer staining

$1x10^6$ PBMCs were seeded into a 96-well plate and, for live/ dead discrimination, incubated for 10 minutes on ice with EMA using strong light. Cells were washed twice with FACS buffer and CCR7 staining was performed on 37°C for 25 minutes (Lugli et al., 2013b). Again cells were washed twice with FACS buffer and resuspended in 50 µl of MHC-multimer PE solution for 20 minutes on ice. Without any further washing step, 50 µl of the prepared antibody solution (Table 2.9) was added on top and incubated for a further 30 minutes on ice. Afterwards, cells

were washed twice with PBS and fixed, using 100 µl of 2% PFA solution for 20 minutes on ice. Cells were once more washed with FACS buffer and resuspended in 250 µl FACS buffer for acquisition.

On occasion, a MHC-multimer double staining was performed by increasing the incubation time of the PE multimer to 45min, followed by two washing steps with FACS buffer and an incubation with MHC-multimer APC solution for 20 minutes on ice followed by the surface staining with the respective antibodies.

2.2.4.4 Detection of CMV-specific T cells by ICS

In a first step, $1x10^6$ rested PBMCs (2.2.2.5) were seeded into a 96-well plate and resuspended in 150 µl cell culture medium, supplemented with 0.2 µl unlabeled antibodies for CD28 and CD49d and stimulated with 4 µl of peptide (2 µg/ ml peptide in the total volume of 200 µl after addition of Brefeldin A) (Table 2.13 or Table 2.14) or as a positive control with 3 µl of the prepared PMA/ Ionomycin working solution. Cells were incubated for one hour at 37°C at 5% CO_2. Then, 50 µl of freshly prepared BFA working solution (a Golgi apparatus inhibitor, leading to an accumulation of cytokines) was carefully added without mixing and further incubated for 3.5 hours at 37°C and 5% CO_2. Afterwards, stimulated cells were stored overnight at 4°C in the dark. The following day, cells were washed once with FACS buffer and incubated for 10 minutes on ice with EMA, for live/ dead discrimination using strong light. Afterwards, cells were washed once with FACS buffer, resuspended in 50 µl of the cell surface antibody mixture (Table 2.10) and incubated for 30 minutes on ice. Then, cells were washed twice with PBS, fixed and permeabilized using 100 µl of the BD Fixation/ Permeabilization Solution Kit for 20 minutes on ice. Again, the cells were washed twice with Perm/ Wash Solution and incubated with 50 µl of the intracellular cytokine antibody mixture (Table 2.10) for 30 minutes on ice. Afterwards, cells were washed once with Perm/ Wash Solution, once with FACS buffer and resuspended in 250 µl FACS buffer for acquisition.

2.2.5 Magnetic purification of *ex vivo* isolated CMV-specific T cells with MHC-*Strep*Tamers

2.2.5.1 Reversibility of MHC-*Strep*Tamers

The *Strep*-Tag II has a lower binding strength to *Strep*-Tactin than does biotin and therefore, biotin is able to disrupt the complex leading to a disassembly of the multimeric complex. Subsequently, the MHC-monomers dissociate from TCRs (Skerra & Schmidt, 1999).

In order to demonstrate the reversibility of the newly generated HLA-C*0702-restricted *Strep*Tamers, $5x10^6$ PBMCs were stained with 2 µg MHC-*Strep*Tamers multimerized to *Strep*-Tactin PE for 45 minutes on ice. For the detachment of MHC-multimers, the remaining $4x10^6$ cells were transferred into a 15 ml-Falcon. Then the cells were incubated for 10 minutes at RT with 10 ml detachment buffer (2.1.8) on a rotating mixer and centrifuged for 10 minutes at 700 g. These two steps were repeated once to ensure complete disruption of the MHC-*Strep*Tamer-complex. Afterwards, cells were incubated three times with FACS buffer for 10 minutes at RT on a rotating mixer, in order to dialyze all residual D-biotin. $1x10^6$ cells were distributed per well into a 96-well plate and stained with respective antibodies. As a control, cells were additionally labeled with *Strep*-Tactin PE or with HLA-C*0702-*Strep*Tamer. All different fractions were stained with CD158b FITC, CD8 A700 and CD3 eF450 (Table 2.7) for 30 minutes on ice and afterwards fixed with 2% PFA. Analysis was undertaken using a BD LSRII™ flow cytometer and analyzed with FlowJo 9.7.6.

2.2.5.2 Magnetic enrichment using microbead-coupled MHC-*Strep*Tamers

The magnetic enrichment of HLA-C*0702/IE-1-specific T cells was performed with *Strep*-Tactin Magnetic Microbeads in two serial enrichment steps (Stemberger et al., 2012) and of each fraction a sample was collected as purification controls. First, HLA-C*0702/IE-1-specific T cells were purified. In advance, for $1x10^7$ PBMCs 1 µg HLA-C*0702/IE-1 monomers were multimerized to 15 µl microbeads and 34 µl FACS buffer for 45 minutes at 4°C on a rotating mixer (for $1x10^8$ cells: 10 µg MHC-monomers, 150 µl beads and 340 µl FACS buffer). Afterwards, $1x10^8$ PBMCs were incubated in a 15 ml Falcon-tube with 500 µl of freshly generated MHC-multimers for 20 minutes on ice using a rotating mixer. 5 ml FACS buffer was added and the tube was placed firmly into the *Strep*Man Magnet for 3 minutes to ensure magnetic separation. Supernatant was carefully collected (negative fraction) and the tube was removed from the magnet. Positive fraction was washed with 5 ml FACS buffer and magnetic

separation was repeated. Afterwards, the positive fraction was incubated twice with 10 ml of detachment buffer for 10 minutes and washed twice with FACS buffer (2.2.5.1).
In a second step, depletion of HLA-C*0702/MAGE$^+$ T cells was performed. For 1x10^7 PBMCs, 2 µg HLA-C*0702/MAGE-monomers were multimerized with 30 µl microbeads and 18 µl FACS buffer for 45 minutes on ice. Cells were labeled for 20 minutes at 4°C using a rotating mixer. Magnetic separation was performed as previously described. Afterwards, all four fractions (1st run: positive/ negative; 2nd run: positive/ negative) were labeled with the respective MHC-multimers and labelled for surface markers (CD158b FITC, CD8 A700 and CD3 eF450; Table 2.7) and fixed using 2% PFA. Analysis was undertaken using a BD LSRII^{TM} flow cytometer and analyzed with FlowJo 9.7.6.

2.2.5.3 Depletion of KIR2DL2/3$^+$ cells followed by magnetic enrichment of CMV-specific CD8$^+$ T cells with MHC-*Strep*Tamers

The depletion of KIR$^+$ cells was performed according to manufacturer's instructions (Miltenyi Biotech). Again, of each fraction a sample was collected as purification controls. In brief, 5x10^7 PBMCs were stained with 100 µl CD158b PE antibodies and 400 µl of FACS buffer for 30 minutes at 4°C in the dark. Afterwards, the cells were washed once by adding 5 ml of FACS buffer and centrifuged for 10 minutes at 300 g. Then, the cells were resuspended in 400 µl of FACS buffer and 100 µl of Anti-PE MicroBeads (Miltenyi Biotech). The cell suspension was incubated for 15 minutes at 4°C in the dark. In order to remove unbound beads, 5 ml FACS buffer was added and centrifuged for 10 minutes at 300 g. Afterwards, the cells were resuspended in 500 µl FACS buffer and were passed through a presoaked LD Column attached to a Miltenyi QuadroMACS™ Separator. The unlabeled cell fraction, which had passed through the column, was collected. After depletion of KIR$^+$ cells, a positive magnetic enrichment of HLA-C*0702/IE-1-specific T cells was performed with *Strep*-Tactin® Magnetic Microbeads as previously described. As a purification control, all four fractions (1st run: positive/ negative; 2nd run: positive/ negative) were afterwards labelled with the respective MHC-multimers, stained for surface markers (CD158b FITC, CD8 A700 and CD3 eF450; Table 2.7) and fixed using 2% PFA. Analysis was undertaken using a BD LSRII^{TM} flow cytometer and analyzed with FlowJo 9.7.6.

2.2.6 Gating strategies

In order to specifically analyze CMV-specific T cells by MHC-multimer staining or ICS and the overall composition of the lymphocyte compartment, several different gating strategies were chosen according to the expression of specific cellular markers.

2.2.6.1 MHC-Multimer staining and T cell subpopulations

All MHC-multimer and phenotypical stainings were analyzed by a specific gating strategy. First, lymphocytes were selected by forward and side scatter, followed by exclusion of cell doublets. Separation of dead cells by live-dead discrimination was performed with EMA and exclusion of B cells by anti-CD19 staining. Afterwards, remaining cells were gated on $CD3^+$ T cells and selected for $CD8^+$ or $CD4^+$ T cells (Figure 2.3, A). Then, the presence of CMV-specific T cells within the $CD8^+$ T cell population was assessed (Figure 2.3, B). In addition, $CD8^+$ T cell subpopulations, namely T_{naive} ($CCR7^+CD45RO^-$), T_{CM} ($CCR7^+CD45RO^+$), T_{EM} ($CCR7^-CD45RO^+$) and T_{EMRA} cells, were analyzed (Figure 2.3, C). Furthermore, T_{SCM} ($CCR7^+CD95^+$) and T_{naive} cells ($CCR7^+CD95^-$) were separated within the T_{naive} cell population. (Figure 2.3, D). If applicable, MHC-multimer frequencies within the different T cell populations were analyzed.

The discrimination of $CD4^+$ T cell subpopulations was similarly achieved, by gating on T_{naive} ($CCR7^+CD45RO^-$), T_{CM} ($CCR7^+CD45RO^+$) and T_{EM} cells ($CCR7^-CD45RO^+$; Figure 2.3, E). Again, T_{SCM} ($CCR7^+CD95^+$) and T_{naive} cells ($CCR7^+CD95^-$) were separated within the T_{naive} cell population (Figure 2.3, F)

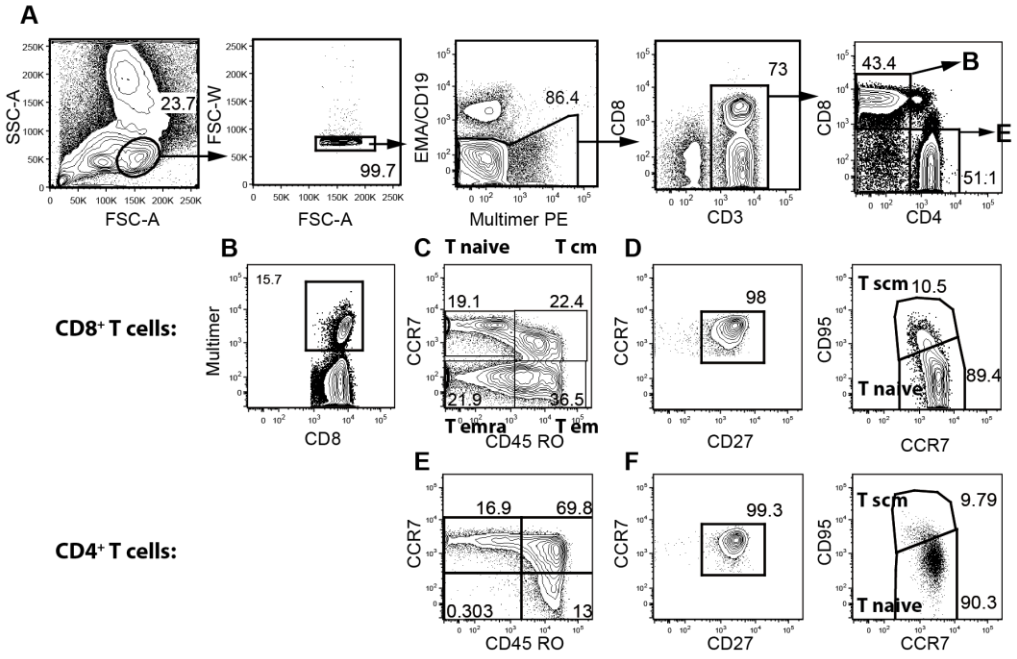

Figure 2.3: Gating strategy for MHC-multimer and phenotypical staining.
For the detection of CMV-specific T cells by MHC-multimer staining, 1x10^6 PBMCs were used. **(A)** Cells were gated according to their size and granulation, followed by exclusion of doublets, B cells and dead cells. Afterwards, cells were analyzed for the expression of CD3, CD4 and CD8. **(B)** Discrimination of MHC-multimer$^+$ CD8$^+$ T cells. **(C)** Memory phenotype of CD8$^+$ T cells. **(D)** Discrimination of T_{SCM}- and T_{naive} cells within CD8$^+$ T_{naive} cells. **(E)** Memory phenotype of CD4$^+$ T cells. **(F)** Discrimination of T_{SCM}- and T_{naive} cells within CD4$^+$ T_{naive} cells. If applicable, MHC-multimer binding was analyzed within the different CD8$^+$ T cell fractions.

2.2.6.2 Intracellular cytokine staining

For the detection of cytokine producing T cells after stimulation with CMV-restricted peptides the cells were again preselected on living lymphocytes. Afterwards, cells were gated on CD3$^+$ IFNγ$^+$ T cells and selected for CD8$^+$ or CD4$^+$ T cells (Figure 2.4, A). The production of cytokines (IFNγ, TNFα, IL-2 and GM-CSF) was assessed within all CD8$^+$ T cells (Figure 2.4, B) and if applicable within CD8$^+$ T cell memory subpopulations (Figure 2.4, C). In addition, the cytokine production of CD4$^+$ T cells was analyzed (Figure 2.4, D) and also within the CD4$^+$ T cell memory subpopulations (Figure 2.4, E).

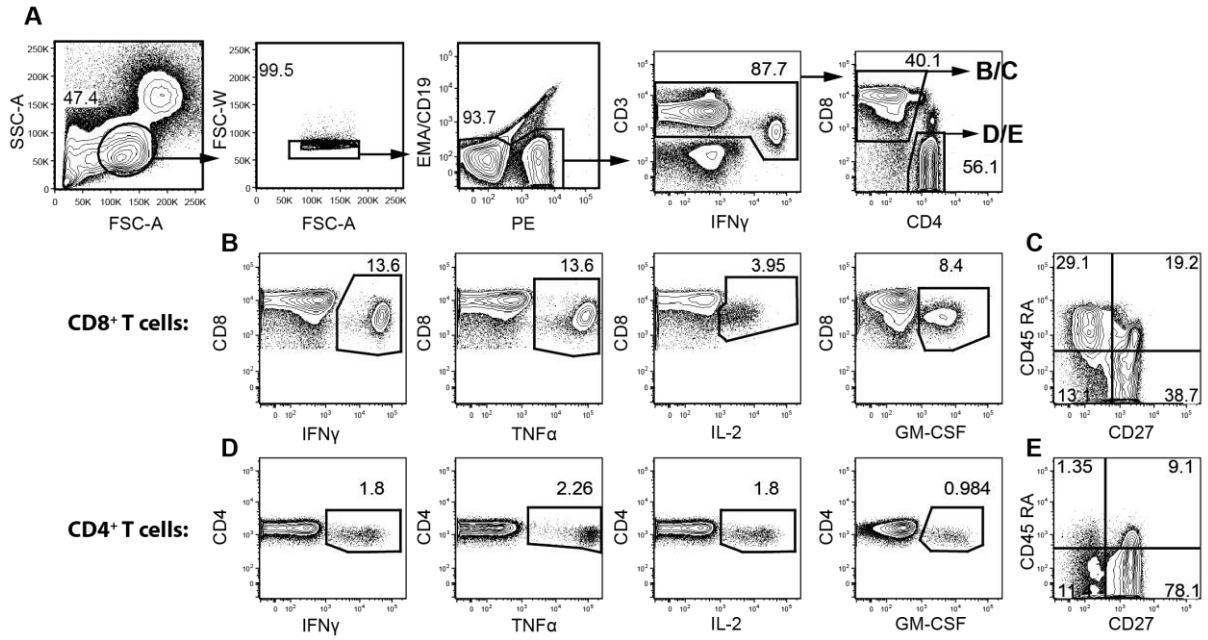

Figure 2.4: Gating strategy for intracellular cytokine staining
For the detection of cytokine production, 1x10^6 PBMCs were stimulated with CMV-restricted peptides (pp65 Mix) and an ICS was performed. **(A)** The cells were gated according to their size and granulation, followed by exclusion of doublets and dead cells. Afterwards, cells were gated on CD3$^+$ IFNγ$^+$ T cells and divided into CD4$^+$ or CD8$^+$ T cells. **(B)** Representative staining of IFNγ, TNFα, IL-2 and GM-CSF-producing CD8$^+$ T cells. **(C)** Memory phenotype of stimulated CD8$^+$ T cells. **(D)** Representative staining of IFNγ, TNFα, IL-2 and GM-CSF-producing CD4$^+$ T cells. **(E)** Memory phenotype of stimulated CD4$^+$ T cells.

2.2.6.3 Analysis of the lymphocyte compartment

The different lymphocyte subpopulations were analyzed according to forward and side scatter, followed by exclusion of cell doublets and separation of dead cells by live-dead staining with EMA (Figure 2.5, A). Afterwards, cells were chosen by the expression of CD3 and CD16 (Figure 2.5, B). As NK cells (CD16$^+$HLA-DR$^-$) and cDC (CD16$^+$HLA-DR$^+$) are CD3$^-$ but express both CD16 on the cell surface, the populations were discriminated by the expression of HLA-DR (Figure 2.5, C). Mucosal-associated invariant T cells (MAIT) express high levels of CD161 and were previously gated on CD8$^+$ T cells (Figure 2.5, D). B cells were previously gated of CD3$^-$ CD16$^-$ cells and visualized using CD19 and HLA-DR (Figure 2.5, F)

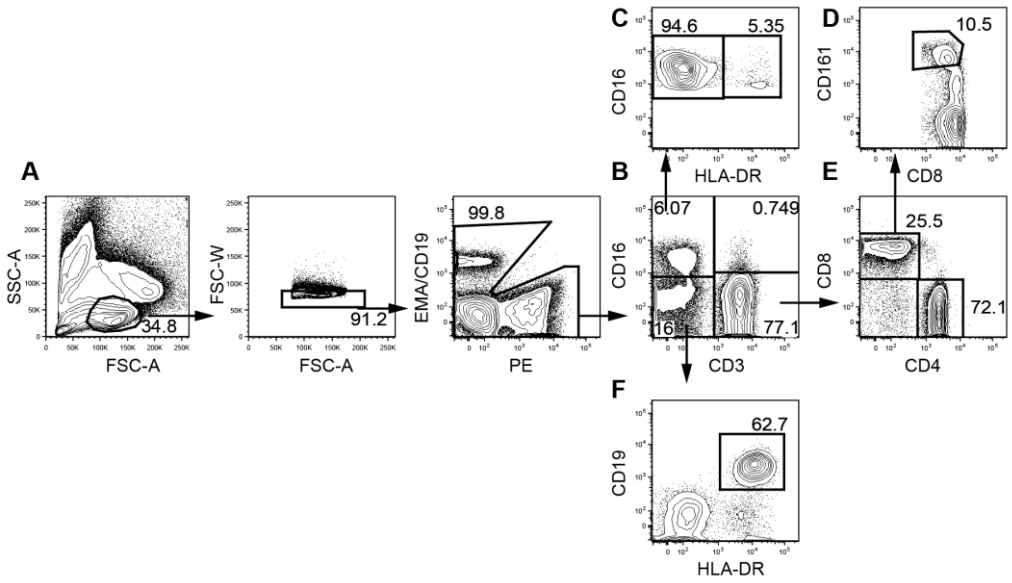

Figure 2.5: Gating strategy for the discrimination of different lymphocyte subpopulations
Flow cytometry analysis of lymphocyte populations from 1x10^6 PBMCs. **(A)** Gating on living lymphocytes. **(B)** T lymphocytes (CD3$^+$CD16$^-$) and NK cell (CD3$^-$CD16$^+$) populations were separated using CD3 and CD16. **(C)** NK cells (HLA-DR$^-$) and cDC (HLA-DR$^+$) were distinguished within the CD3$^-$ lymphocytes **(D)** MAIT cells were distinguished by the expression of CD161 within the CD3$^+$ CD8$^+$ T cell population. **(E)** Discrimination of CD4$^+$ and CD8$^+$ T cells within CD3$^+$ T cells. **(F)** Visualization of B cells within CD3$^-$CD16$^-$ lymphocytes.

2.2.6.4 Gating strategy for the assessment of absolute T cell numbers

For the calculation of absolute cell numbers, leucocytes were discriminated by the expression of CD45 (Figure 2.6, A) and the frequency of counting beads was analyzed (Figure 2.6, B). Finally, CD3$^+$ and CD3$^+$CD8$^+$ T cell frequencies were assessed (Figure 2.6, C).

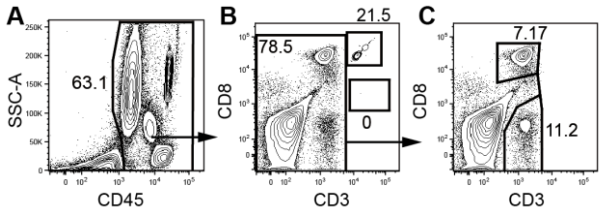

Figure 2.6: Gating strategy for the calculation of absolute cell numbers
For the calculation of absolute cell numbers, BD Trucount™ Tubes were used and whole blood was stained with CD3 and CD8 antibodies and thereafter, erythrocytes were lysed. **(A)** Discrimination of leucocytes by CD45 expression. **(B)** Exclusion of counting beads. **(C)** Separation of CD3$^+$ and CD3$^+$CD8$^+$ T cells.

3. Results

3.1 Generation of a novel HLA-C*0702-restricted multimer

$CD8^+$ T cells play a major role in the clearance of CMV-reactivations and viral suppression. New reagents, specifically MHC-multimers, enable the detection and characterization of $CD8^+$ T cell populations and increase further the ability to monitor immunocompetent and immunocompromised individuals for pathogen-specific T cells. In addition, MHC-multimers, in particular reversible MHC-*Strep*Tamers, enable the purification of CMV-specific $CD8^+$ T cells for further analysis, e.g. TCR sequencing, and ACT. Ameres et al. (Ameres et al., 2013) demonstrated the HLA-restriction of the IE-$1_{309-317}$ peptide to HLA-C*0702 and therefore the generation of an HLA-C-restricted *Strep*Tamer was commenced.

3.1.1 Cloning of the synthesized sequence into a bacterial expression vector.

The synthesized GeneArt vector, containing the sequence of the HLA-C*0702 heavy chain, did not comprise a suitable promoter region for expression in *E. coli.* Therefore, the StarGate vector (pASG-IBA-wt1) was chosen as a suitable expression vector. By homologous recombination, the HLA-C-sequence was cloned into the pASG-IBA-wt1 plasmid and sequenced for potential aberrations. The alignment of all three sequences, the published HLA-C*0702 sequence, the GeneArt vector sequence, and the pASG-IBA-wt1 expression vector showed no nonsynonymous mutations within the HLA-heavy chain (Figure 3.1). Furthermore, the expression vector, like the synthesized vector, contained the *Strep*-tag III without any protein deviations (Figure 3.1). After verifying successful cloning, heat competent *E. coli* (Top10) were transfected with the pASG-IBA-wt1 expression vector and a large scale bacterial culture for the expression of the HLA-C-heavy chain was initiated.

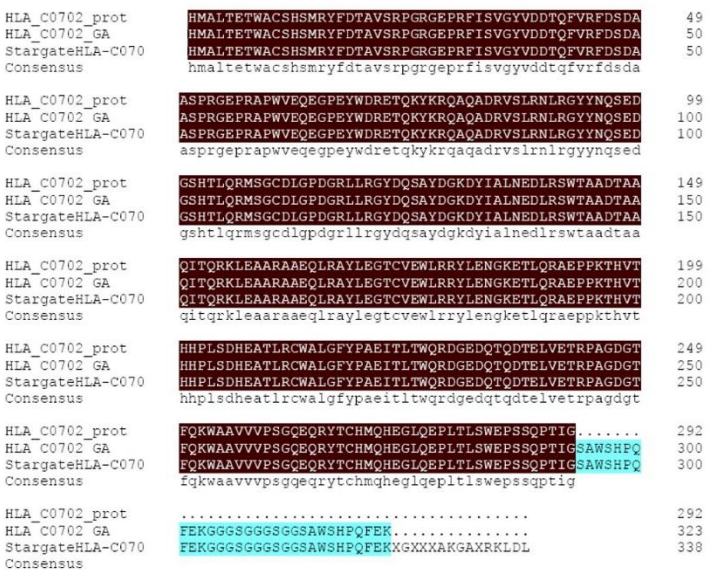

Figure 3.1: Sequence analysis of the published HLA-C*0702 sequence, the GeneArt vector, and the expression vector.
The sequences of the published HLA-C*0702 sequence (HLA_C0702_prot), the GeneArt sequence (HLA_C0702_GA), and the expression vector pASG-IBA-wt1 (StarGate HLA-C0702) were sequenced by GATC GmbH and analyzed with Vector NTI. The *Strep-t*ag sequence is depicted in blue.

3.1.2 Induction of expression and refolding of the HLA-C*0702-heavy chain with the IE-$1_{309-317}$ peptide

In order to achieve a sufficient protein amount of the HLA-heavy chain, six flasks, each with one liter of bacterial culture was set up. After an overnight incubation, the bacterial culture reached an OD_{600} of 0.7 and the expression of the plasmid was induced by the addition of tetracycline and the suspension was further incubated for 3h at 37°C. The expression of the HLA-heavy chain was analyzed by protein separation of unpurified samples with a SDS-page-gel. The HLA-heavy chain has a mass of approximately 39 kDa. After induction of expression (3h) a strong signal was detected around 39kD (Figure 3.2, A/ B) which was confirmed in a control gel using purified HLA-heavy chain protein (Figure 3.2, B, right). 66.5 mg/ml of protein in 18ml 8M Urea were obtained. These data verified the successful generation of the HLA-heavy chain.

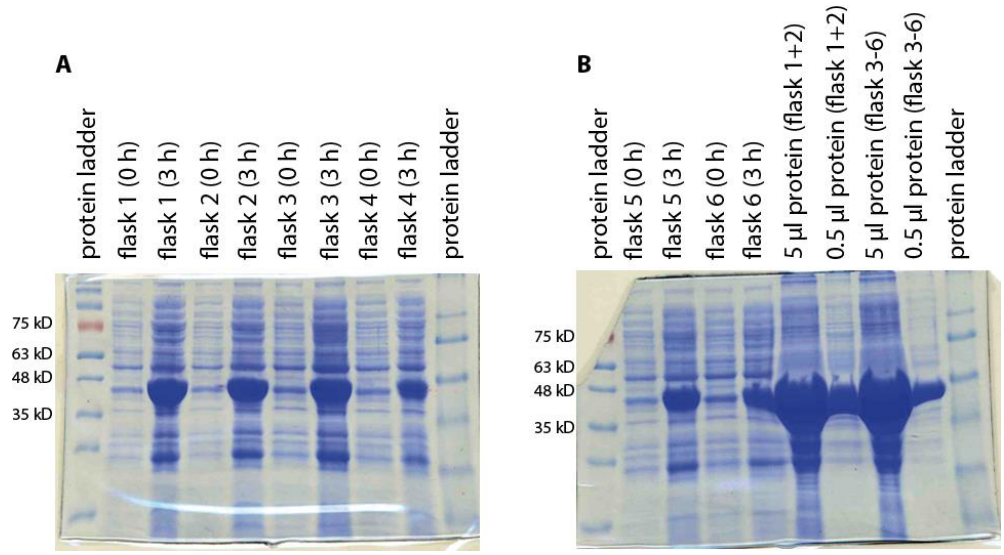

Figure 3.2: SDS-page for protein expression of the HLA-C-heavy chain.
Samples of the different bacterial culture flasks before (0h) and after (3h) induction of protein expression were loaded on the gels. (**A)** Flasks 1-4 and **(B, left)** flasks 5-6. **(B, right)** 5 µl and 0.5 µl of purified protein were loaded on the SDS-gel in combination with a protein ladder (10 to 180 kDa).

After successful expression, the protein was purified and the HLA-C-heavy chain was refolded with the IE-$1_{309\text{-}317}$ peptide in the presence of human β2 microglobulin (hβ2m). To achieve high purity of the pMHC-monomers the solution was injected into an ÄKTA Purifier 10 Protein Purification System and the fractions A7 to A11 were collected (Figure 3.3). The detection of a high and narrow peak indicated a successful MHC-monomer refolding with a high yield.

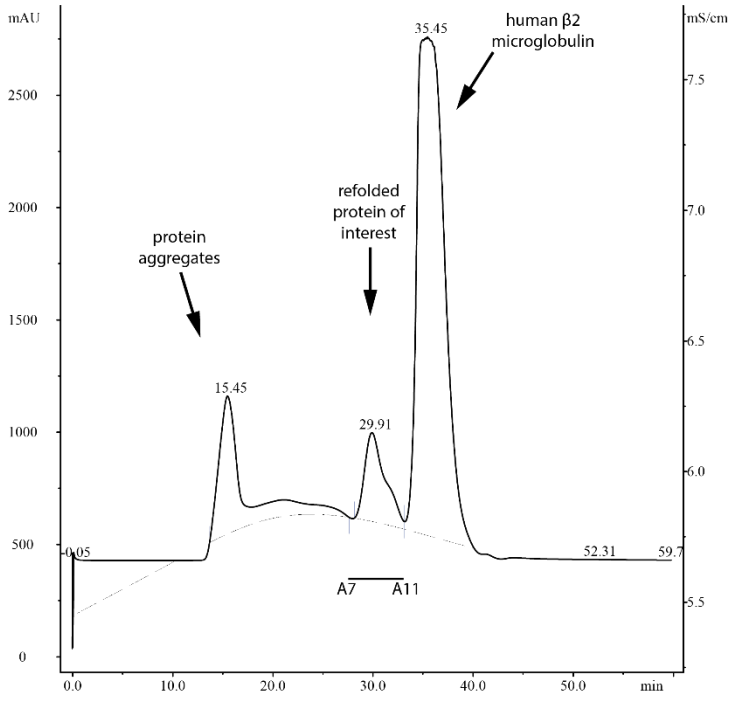

Figure 3.3: Histogram of the pMHC-monomer purification.
Refolded pMHC-solution was purified using an ÄKTA Protein Purification System. Segments A7 to A11 containing the MHC-monomers were collected for further use. Indicated are three peaks showing protein aggregates, the refolded protein of interest, and the human β2 microglobulin, respectively.

3.2 Verification of the functionality and specificity of the novel HLA-C*0702/IE-1 multimer

After successful generation of the novel MHC-multimer, the staining capabilities of the MHC-multimer were analyzed using PBMCs from healthy donors. The high linkage equilibrium of HLA-B*0702 and HLA-C*0702 (Schmidt et al., 2009) enabled the suitable donor selection according to the detection of HLA-B*0702/pp65$_{417-426}$-specific T cells, as available donors had not been HLA-typed. In addition, functional HLA-C*0702/IE-1 multimer staining was verified by detection of CMV-specific IFNγ-secretion after stimulation with the IE-1$_{309-317}$ peptide.

3.2.1 MHC-Multimer staining

In a first step, the staining ability of the new HLA-C*0702/IE-1 monomer was analyzed using PBMCs of a healthy donor. 0.4 µg of HLA-C*0702/IE-1 or HLA-B*0702/pp65 monomers were freshly multimerized by incubation with 0.2 µg *Strep*-Tactin PE. Afterwards, 1x10^6 PBMCs were stained with the respective MHC-multimers and analyzed by flow cytometry. The HLA-C*0702/IE-1 multimer revealed a frequency of 18.2% CMV-specific CD8$^+$ T cells (Figure 3.4, left), whereas HLA-B*0702/pp65-restricted T cells represented 0.347% of all CD8$^+$ T cells

(Figure 3.4, right). These data indicated a successful generation of the new reagent with good staining properties.

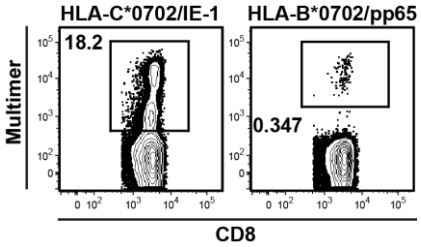

Figure 3.4: Verification of a positive staining by the novel HLA-C*0702/IE-1 multimer.
In order to verify the successful generation of the HLA-C*0702/IE-1 multimer, 0.4 µg of the HLA-C*0702/IE-1 or the HLA-B*0702/pp65 monomers were multimerized using 0.2 µg *Strep*-Tactin PE. Afterwards, 1x10^6 PBMCs of an HLA-B*0702-positive healthy donor were stained with the respective MHC-multimers and analyzed using a BD LSR II and FlowJo. The cells were pregated on living $CD3^+$ $CD8^+$ T cells (Figure 2.3, A).

In order to verify the apparent HLA-C*0702 status of the donor, 1x10^6 PBMCs were stimulated with 2 µg/ml of the respective peptides and an ICS was performed. Indeed, 1.48% of all $CD8^+$ T cells were restricted to the HLA-C*0702/IE-1 epitope (Figure 3.5, left). Interestingly, this frequency was much lower than the estimated 50% of MHC-multimer$^+$ $CD8^+$ T cells. This is a consistent ratio achieved for other CMV-restricted targets, e.g. HLA-A*0201/pp65 (data not shown). For the HLA-B*0702/pp65 epitope, a frequency of 0.23 % of all $CD8^+$ T cells was detected (Figure 3.5, right). This frequency was estimated to represent around half of the MHC-multimer$^+$ $CD8^+$ T cells.

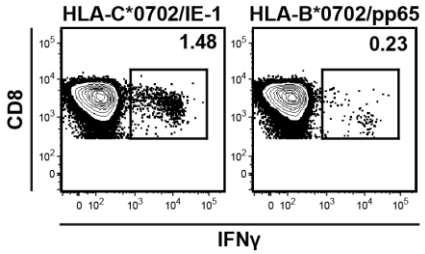

Figure 3.5: Verification of the HLA-C*0702/IE-1 and HLA-B*0702/pp65 multimer staining by ICS.
To verify the successful MHC-multimer staining of HLA-C*0702/IE-1 and HLA-B*0702/pp65, 1x10^6 PBMCs were stimulated with 2 µg/ml of the respective peptide and analyzed for the production of IFNγ. Cells were analyzed using a BD LSR II and FlowJo. The cells were pregated on living $CD3^+$ $IFN\gamma^+$ $CD8^+$ T cells (Figure 2.3, B).

Both experiments verify the successful generation of the HLA-C*0702/IE-1 multimer. Notably, there was a discrepancy of HLA-C*0702/IE-1 multimer$^+$ and $IFN\gamma^+$ T cells.

3.2.2 Evidence for the restriction of the IE-$1_{309-317}$ peptide to HLA-C*0702

Despite successful generation of the novel HLA-C*0702/IE-1 multimer, final evidence of the physiological HLA-restriction of the IE-$1_{309-317}$ peptide was still lacking. Fortunately, a Philippine donor belonging to an ethnic group with a different allelic linkage of HLA-molecules was HLA-C*0702-positive, but HLA-B*0702-negative (Figure 3.6, A). Strikingly, 0.438% of all $CD8^+$ T cells were positive for the HLA-C*0702/IE-1 multimer (Figure 3.6, B, middle) and 0.248% of all $CD8^+$ T cells produced IFNγ upon stimulation (Figure 3.6, C, middle). The HLA-B*0702/pp65 multimer staining showed only a background staining of 0.0321% (Figure 3.6, B, right) and no IFNγ-production after stimulation with the HLA-B*0702-restricted CMV pp$65_{417-426}$ peptide (Figure 3.6, C, right).

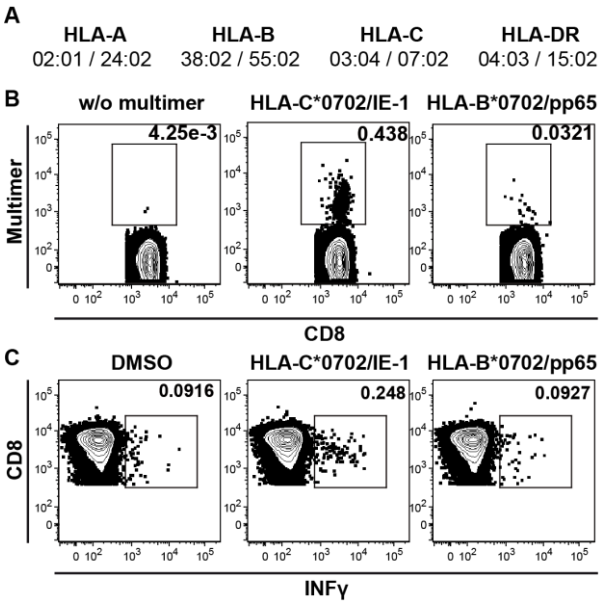

Figure 3.6: Confirmation of HLA-C*0702-restriction of IE-$1_{309-317}$ peptide by MHC-multimer and intracellular cytokine staining in an HLA-C*0702-positive/ HLA-B*0702-negative donor.
PBMCs form an HLA-typed healthy donor were used to proof the HLA-C*0702-restriction of IE-$1_{309-317}$ peptide. **(A)** Depiction of the HLA-type indicating that the donor is HLA-C*0702-postive but not HLA-B*0702. **(B)** $1x10^6$ PBMCs were stained with the respective MHC-multimers. As a negative control a FMO control was used. The cells were pregated on living $CD3^+CD8^+$ T cells. **(C)** $1x10^6$ PBMCs were stimulated with the respective peptides or as a negative control with DMSO and analyzed for the production of IFNγ. The cells were pregated on living $CD3^+IFN\gamma^+CD8^+$ T cells. The cells were analyzed using a BD LSR II and FlowJo.

These data provided evidence that IE-$1_{309-317}$ peptide is an HLA-C*0702-restricted and not HLA-B*0702-restricted T cell epitope as previously described by Kern et al (Kern et al., 1999).

3.3 Characterization of CMV-specific HLA-C*0702-restricted T cells

3.3.1 Distribution of HLA-C*0702/IE-1-restricted CD8+ T cells in healthy individuals

After demonstrating the successful generation of the HLA-C*0702/IE-1 multimer and the HLA-C*0702-restriction of the IE-$1_{309-317}$ peptide, a larger cohort of healthy individuals (n = 20) was analyzed for the distribution of HLA-C*0702/IE-1-restricted $CD8^+$ T cells. The donors had a median frequency within the $CD8^+$ T cell compartment of 11.35% (1.96 – 40.8%) for HLA-C*0702/IE-1 multimer and of 1.67% (0.239 – 9.98%) for the HLA-B*0702/pp65 multimer ($p < 0.0001$; Figure 3.7, A). In addition, stimulation with the respective peptides revealed intensive IFNγ production of $CD8^+$ T cells, especially for the IE-$1_{309-317}$ peptide. Median frequencies of 5.02% (0.04 – 22.5%) for HLA-C*0702/IE-1 and 1.07% (0.13 – 9.36%, $p = 0.0098$) for HLA-B*0702/pp65 were detected (Figure 3.7, B).

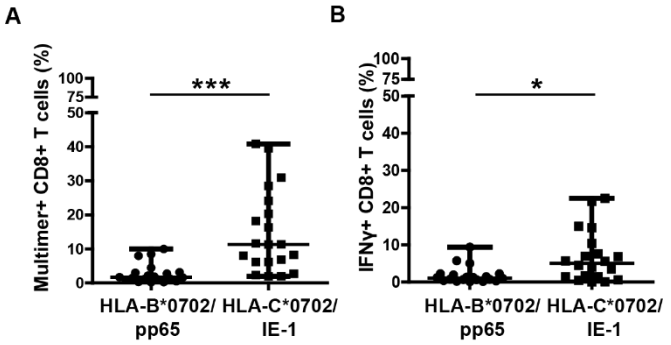

Figure 3.7: Comparison of HLA-B*0702/pp65- and HLA-C*0702/IE-1-restricted $CD8^+$ T cells in healthy donors.
T cell frequencies for HLA-B*0702/pp65 and HLA-C*0702/IE-1 epitopes were analyzed in a cohort of n = 20 healthy blood donors. All donors had CMV-specific $CD8^+$ T cells for both epitopes. **(A)** $1x10^6$ PBMCs of each donor were stained with the respective MHC-multimers. Median values are indicated, cells were pregated on living $CD3^+CD8^+$ T cells. **(B)** $1x10^6$ PBMCs of each donor were stimulated with the respective peptides and analyzed for the production of IFNγ. Median values are indicated, cells were pregated on living $CD3^+IFN\gamma^+CD8^+$ T cells. The cells were analyzed using a BD LSR II and FlowJo software. Statistical analyses were performed with the Mann-Whitney *U* test. * = $p < 0.05$, ** = $p < 0.01$, *** = $p < 0.001$.

Importantly, correlation of MHC-multimer+ and $IFN\gamma^+$ $CD8^+$ T cells revealed a reduced fit of $r^2 = 0.77$ for HLA-C*0702/IE-1-restricted T cells (Figure 3.8, A). In contrast, for the HLA-B*0702/pp65 epitope a very good fit of $r^2 = 0.90$ was detected (Figure 3.8, B).

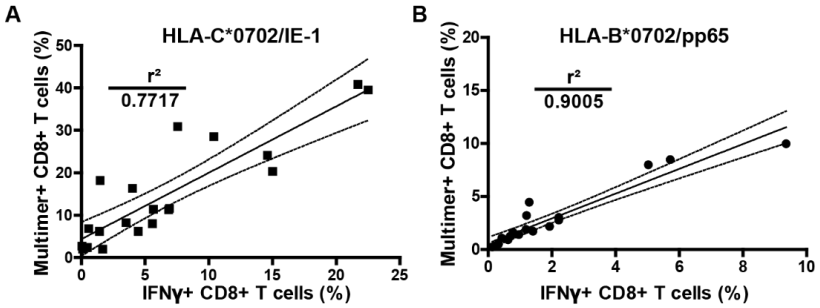

Figure 3.8: Correlation of MHC-multimer$^+$ and IFNγ$^+$CD8$^+$ T cells.
For a better overview of the distribution of HLA-C*0702/IE-1– or HLA-B*0702/pp65–specific T cells, the frequencies of MHC-multimer$^+$ and IFNγ$^+$ CD8$^+$ T cells of the previous experiment were correlated. **(A)** Correlation of HLA-C*0702/IE-1-specific CD8$^+$ T cells showed a fit of r^2 = 0.7717. **(B)** Correlation of HLA-B*0702/pp65-specific CD8$^+$ T cells showed a fit of r^2 = 0.9005.

In consequence, the lower correlation coefficient of HLA-C*0702/IE-1-specific CD8$^+$ T cells was interpreted as a potentially misbinding of the HLA-C*0702/IE-1 multimer.

3.3.2 Epitope independent binding of HLA-C-multimers by KIR2DL2/3-expressing CD8$^+$ T cells can be adjusted by MHC-multimer double staining

The potential misbinding of the new HLA-C7-multimer could be caused by KIR2DL2/3, a well-known binding partner of HLA-C*0702 by NK cells. Therefore, the expression of KIR2DL2/3 on CD8$^+$ T cells was analyzed and frequencies of 16.4% CD8$^+$ KIR2DL2/3$^+$ T cells were detected (Figure 3.9, A). After verifying the expression of the KIR2DL2/3 receptor on CD8$^+$ T cells, a MHC-multimer staining was performed. The previously detected frequencies were reproduced (Figure 3.9, B) and the KIR2DL2/3 binding was analyzed. The overlay of MHC-multimer$^+$ CD8$^+$ T cells (blue) on the overall CD8$^+$ T cell compartment (grey) revealed that the HLA-C*0702/IE-1-multimer was strongly bound by KIR2DL2/3 receptors (Figure 3.9, C, left). In contrast, no misbinding of HLA-B*0702/pp65 multimer$^+$ T cells was detected (Figure 3.9, C, right).

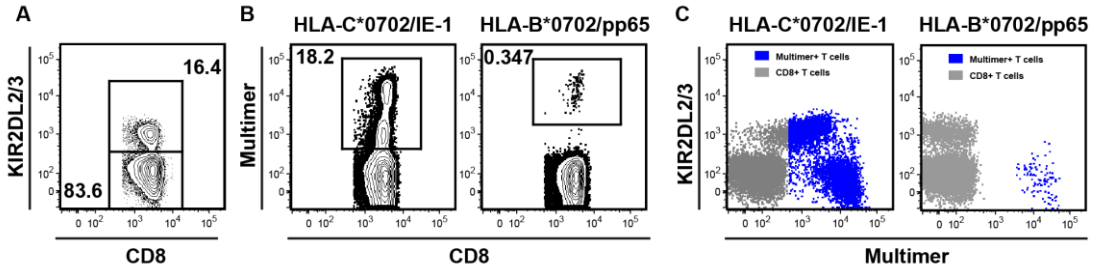

Figure 3.9: KIR2DL2/3 expression on CD8⁺ T cells and epitope-independent binding of HLA-C multimers by these receptors.
Illustration of an representative KIR2DL2/3 staining on CD8⁺ T cells and MHC-multimer combinatorial staining showing the epitope-independent binding of HLA-C*0702-multimers. **(A)** KIR2DL2/3 expression on CD8⁺ T cells. **(B)** MHC-multimer staining for HLA-C*0702/IE-1 and HLA-B*0702/pp65 of CD8⁺ T cells. **(C)** Overlay of corresponding MHC-multimer (blue) staining of KIR2DL2/3-expressing CD8⁺ T cells (grey). All cell were pregated on living CD3⁺CD8⁺ T cells.

In order to exclude these cells properly, a second HLA-C*0702-restricted multimer was generated by refolding the HLA-C*0702-heavy chain with the MAGE-A12$_{170\text{-}178}$ peptide. Combinatorial MHC-multimer double stainings with HLA-C*0702/MAGE PE and HLA-C*0702/IE-1 APC were performed and the gating strategy was adapted (Figure 3.10, A). Depending on the blood donor, large frequencies of HLA-C*0702/MAGE multimer⁺ CD8⁺ T cells were detected (Figure 3.10, A, left). In addition, the HLA-C7-multimer was used to exclude epitope-independent bound MHC-multimers enabling the visualization of KIR-adjusted CMV-specific CD8⁺ T cells (further named HLA-C*0702/IE-1^{MAGE-}) (Figure 3.10, A, right). As expected, all HLA-C*0702/MAGE⁺ T cells were additionally positive for the HLA-C*0702/IE-1 multimer (Figure 3.10, B, left) and were bound by the KIR2DL2/3 receptor (Figure 3.10, B, right, red). In contrast to this observation, a clear single positive HLA-C*0702/IE-1^{MAGE-} population was detected (Figure 3.10, B, left) which was negative for any KIR2DL2/3 staining (Figure 3.10, B, right, blue). The histogram for KIR2DL2/3 staining showed a clear distinction between pure HLA-C*0702/IE-1^{MAGE-} multimer single positive (blue) and HLA-C*0702/MAGE + IE-1 multimer double positive (red) CD8⁺ T cells (Figure 3.10, C). Taken together, these data verified the observation that HLA-C*0702-multimers were epitope-independently bound by KIR2DL2/3-expressing CD8⁺ T cells and that the novel HLA-C*0702/MAGE multimer enabled the visualization of HLA-C*0702/IE-1^{MAGE-}-specific T cells.

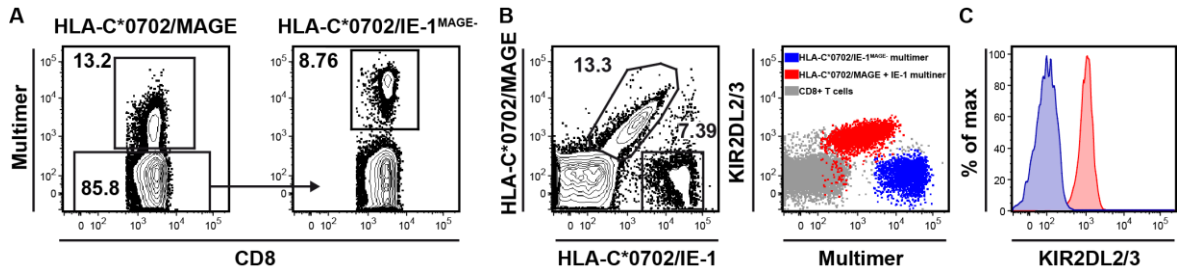

Figure 3.10: Exclusion of epitope-independent binding by HLA-C*0702/MAGE multimer staining.
Exclusion of KIR2DL2/3 bound MHC-multimers by MHC-multimer double staining with HLA-C*0702/MAGE and HLA-C*0702/IE-1 multimers. **(A)** Gating strategy for the exclusion of epitope-independently bound HLA-C*0702/IE-1 multimers. Cells were gated on living $CD3^+$ $CD8^+$ T cells, HLA-C*0702/$MAGE^+$ cells were excluded (left) and KIR-adjusted HLA-C*0702/IE-1^{MAGE-}-specific T cells were visualized (right). **(B)** MHC-multimer double staining of HLA-C*0702/MAGE and HLA-C*0702/IE-1 bound $CD8^+$ T cells. Overlay of KIR-adjusted HLA-C*0702/IE-1^{MAGE-} $multimer^+$ cells (blue) and HLA-C*0702/MAGE + IE-1 multimer double positive T cells (red) of corresponding MHC-multimer staining of KIR2DL2/3-expressing $CD8^+$ T cells (grey). **(C)** Histogram of KIR2DL2/3 for KIR-adjusted HLA-C*0702/IE-1^{MAGE-} $multimer^+$ cells (blue) and HLA-C*0702/MAGE + IE-1 multimer double positive T cells (red).

3.3.3 Distribution of KIR2DL2/3-adjusted HLA-C*0702/IE-1^{MAGE-} $multimer^+$ T cells in healthy donors

After exclusion of KIR2DL2/3-expressing $CD8^+$ T cells by MHC-multimer double stainings, the 20 healthy blood donors were reanalyzed for KIR-adjusted HLA-C*0702/IE-1^{MAGE-}-specific T cells. Notably, frequencies of KIR-adjusted HLA-C*0702/IE-1^{MAGE-} $multimer^+$ T cells were drastically reduced by 40% and showed a median level of 6.86% (0.04 – 37.59%, Figure 3.11 A). As expected, median frequencies of HLA-B*0702/pp65 $multimer^+$ T cells were 1.61% of $CD8^+$ T cells (0.22 – 9.7%, Figure 3.11, A) and comparable to previous experiments (Figure 3.7). Even though, HLA-C*0702/IE-1^{MAGE-}-specific T cells were reduced, there was still a significant difference in comparison to HLA-B*0702/pp65-specific $CD8^+$ T cells ($p = 0.0294$, Figure 3.11, A). Furthermore, the frequencies of MHC-$multimer^+$ and $IFN\gamma^+$ $CD8^+$ T cells were correlated and revealed an almost perfect fit of $r^2 = 0.965$ (Figure 3.11 B). Taken together, KIR-adjusted HLA-C*0702/IE-1^{MAGE-}-specific $CD8^+$ T cells represented a large fraction of $CD8^+$ CMV-specific T cells.

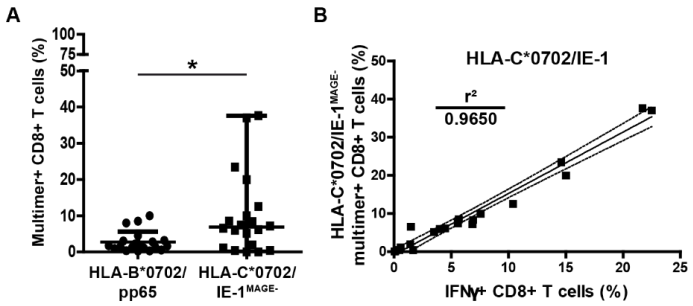

Figure 3.11: Reanalysis of KIR-adjusted HLA-C*0702/IE-1^{MAGE-}-specific T cells and correlation of MHC-multimer$^+$ and IFNγ$^+$ T cells.
The cohort of n = 20 healthy blood donors was reanalyzed for the existence of KIR-adjusted HLA-C*0702/IE-1^{MAGE-}-specific T cells and compared with the HLA-B*0702/pp65-epitope. **(A)** 1x10^6 PBMCs of each donor were stained by MHC-multimer single (HLA-B*0702/pp65) or MHC-multimer double staining (HLA-C*0702/MAGE + IE-1). Median values are indicated. Cells were pregated on living CD3$^+$CD8$^+$ T cells. The cells were analyzed using a BD LSR II and FlowJo. Statistical analyses were performed with the Mann-Whitney *U* test. * = p < 0.05, ** = p < 0.01, *** = p < 0.001. **(B)** Correlation of KIR-adjusted HLA-C*0702/IE-1^{MAGE-} multimer$^+$ and IFNγ$^+$ CD8$^+$ T cells showed a fit of r^2 = 0.9650.

3.3.4 KIR-adjusted HLA-C*0702/IE-1^{MAGE-} multimer$^+$ T cells in the early differentiated T_{CM} compartment

After analyzing the frequency and functionality of HLA-C*0702/IE-1-specific T cells in healthy blood donors their T cell memory phenotype was analyzed. The classification of the different CD8$^+$ subpopulations was set by the different expression of CCR7 and CD45RO: $T_{naïve}$ (CCR7$^+$CD45RO$^-$), T_{CM} (CCR7$^+$CD45RO$^+$), T_{EM} (CCR7$^-$CD45RO$^+$) and T_{EMRA} (CCR7$^-$CD45RO$^-$) cells. In some donors, frequencies of the HLA-C*0702/IE-1^{MAGE-}-specific T cells with an early differentiated T_{CM} phenotype were comparatively high. As exemplarily shown in Figure 3.12, 15.1% of the HLA-C*0702/IE-1^{MAGE-}-specific T cells (1.98% of CD8$^+$ T cells) had an early differentiated T_{CM} phenotype (Figure 3.12, A, left), while only 1.14% of the HLA-B*0702/pp65-specific T cells (4.46% of CD8$^+$ T cells) expressed a T_{CM} phenotype (Figure 3.12, A, right). Overall, after reanalyzing the 20 healthy donors, HLA-C*0702/IE-1^{MAGE-}-specific T cells had a median frequency of 0.172% (0 – 0.82%) within the whole CD8$^+$ T_{CM} compartment (Figure 3.12, B). In contrast, median frequency of HLA-B*0702/pp65-specific T cells within the CD8$^+$ T_{CM} compartment was with 0.049% (0 – 0.373%) significantly lower (p = 0.0186, Figure 3.12, B). However, significantly higher levels of HLA-C*0702/IE-1^{MAGE-}-specific T cells were also found in the T_{EM} (HLA-C*0702/IE-1^{MAGE-}: median 2.195%, 0.015 – 9.409%; HLA-B*0702/pp65: median 0.826%, 0.032 – 2.715%; p = 0.0962) and T_{EMRA} compartment HLA-C*0702/IE-1^{MAGE-}: median 4.626%, 0.002 – 31.086%; HLA-B*0702/pp65: median 0.64582%, 0.029 – 8.79%; p = 0.0239; data not shown). In summary, the overall high frequencies of the HLA-C*0702/IE-1^{MAGE-}-

specific T cells are reflected in all memory T cell fractions including the therapeutically important early T_{CM} subcompartment.

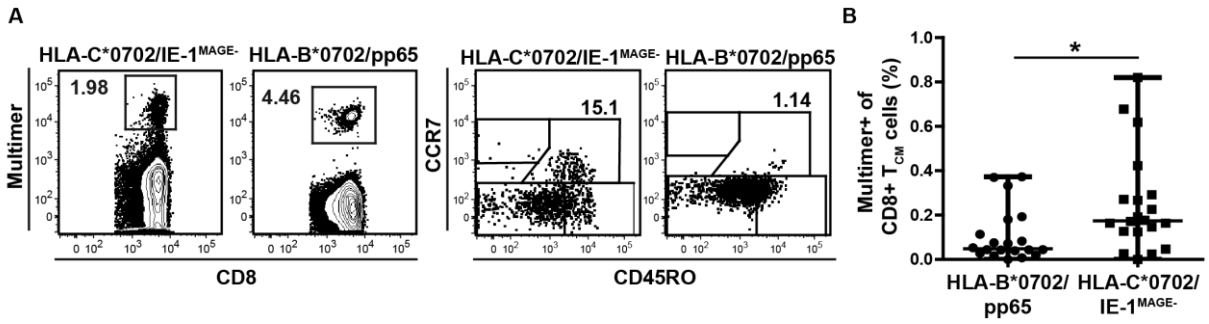

Figure 3.12: High content of central memory T cells within the KIR-adjusted HLA-C*0702/IE-1^{MAGE-}-specific T cell population.
Phenotypical analysis of HLA-C*0702/IE-1^{MAGE-}- or HLA-B*0702/pp65-specific $CD8^+$ $T_{naïve}$ ($CCR7^+CD45RO^-$), T_{CM} ($CCR7^+CD45RO^+$), T_{EM} ($CCR7^-CD45RO^+$) and T_{EMRA} ($CCR7^-CD45RO^-$) cells.
(A) Representative MHC-multimer staining for HLA-C*0702/IE-1^{MAGE-} and HLA-B*0702/pp65 $CD8^+$ T cells and phenotypical analysis with CCR7 and CD45RO of MHC-multimer$^+$ $CD8^+$ T cells. **(B)** Phenotypical analysis for n = 20 healthy donors. Frequencies are shown within the $CD8^+$ central memory T cell compartment. For all plots, cells were pregated on living $CD3^+CD8^+$ T cells. The cells were analyzed using a BD LSR II and FlowJo. Statistical analyses were performed with the Mann-Whitney *U* test. * = $p < 0.05$, ** = $p < 0.01$, *** = $p < 0.001$.

3.3.5 Expansion of HLA-C*0702/IE-1^{MAGE-}- and HLA-B*0702/pp65-specific T cells triggered by CMV-reactivation after kidney transplantation

In order to analyze the behavior and phenotype of HLA-C*0702/IE-1- and HLA-B*0702/pp65-specific T cells in a clinical situation, PBMCs of a 63 year old male kidney transplant recipient were used.

On postoperative day (POD) 33 a CMV viral load of 1010 copies/ml blood was detected by PCR. On POD 36 a MHC-multimer staining was performed and 0.278% of HLA-C*0702/IE-1^{MAGE-}-specific and 1.41% of HLA-B*0702/pp65-specific T cells were detected (Figure 3.13, A). Viral replication induced strong T cell proliferation against both viral epitopes. HLA-C*0702/IE-1^{MAGE-}-specific T cells proliferated extensively (35-fold) from POD 36 to 56 and subsequently declined until POD 79 (Figure 3.13, A). The peak of HLA-B*0702/pp65-specific T cells was reached after a 4-fold increase on POD 79 (Figure 3.13, A). In addition, absolute cell numbers were also determined. 0.27 HLA-C*0702/IE-1^{MAGE-}-specific cells/µl (solid line) and 1.39 HLA-B*0702/pp65-specific cells/µl (dotted line) were detected. Furthermore, absolute cell numbers of CMV-specific T cells strongly expanded showing 25.31 (HLA-C*0702/IE-1^{MAGE-}) and 21.36 (HLA-B*0702/pp65) cells/µl blood on POD 51. During expansion, CMV viral load decreased and protective immunity was generated. (Figure 3.13, B). Both CMV-specific

populations contained few $CD8^+$ T_{CM} cells on POD 36 and proliferated strongly. After viral clearance (POD 79) a high proportion of T_{CM} cells was reestablished for both CMV-specificities (HLA-C*0702/IE-1^{MAGE-}: 7.98%; HLA-B*0702/pp65: 6.09%; Figure 3.13, C), indicating the generation of a long lasting and protective T cell memory. In line with the detection of MHC-multimer$^+$ T cells, the frequencies of functional IFNγ-producing T cells increased from POD 36 (HLA-C*0702/IE-1: 0.107%; HLA-B*0702/pp65: 0.721%) to POD 79 (HLA-C*0702/IE-1: 3.47%; HLA-B*0702/pp65: 3.74 %) exemplifying the involvement of cytokines in viral control (Figure 3.13, D). Analyzing the absolute cell number of $IFN\gamma^+$ T cells in the peripheral blood, 10.36 cells/µl with specificity for HLA-C*0702/IE-1 and 8.04 cells/µl specificity for HLA-B*0702/pp65 were detected on POD 56. Coincidently the patient had a decline in viral load and further CMV-replications were not detected in the follow-up period (Figure 3.13, E).

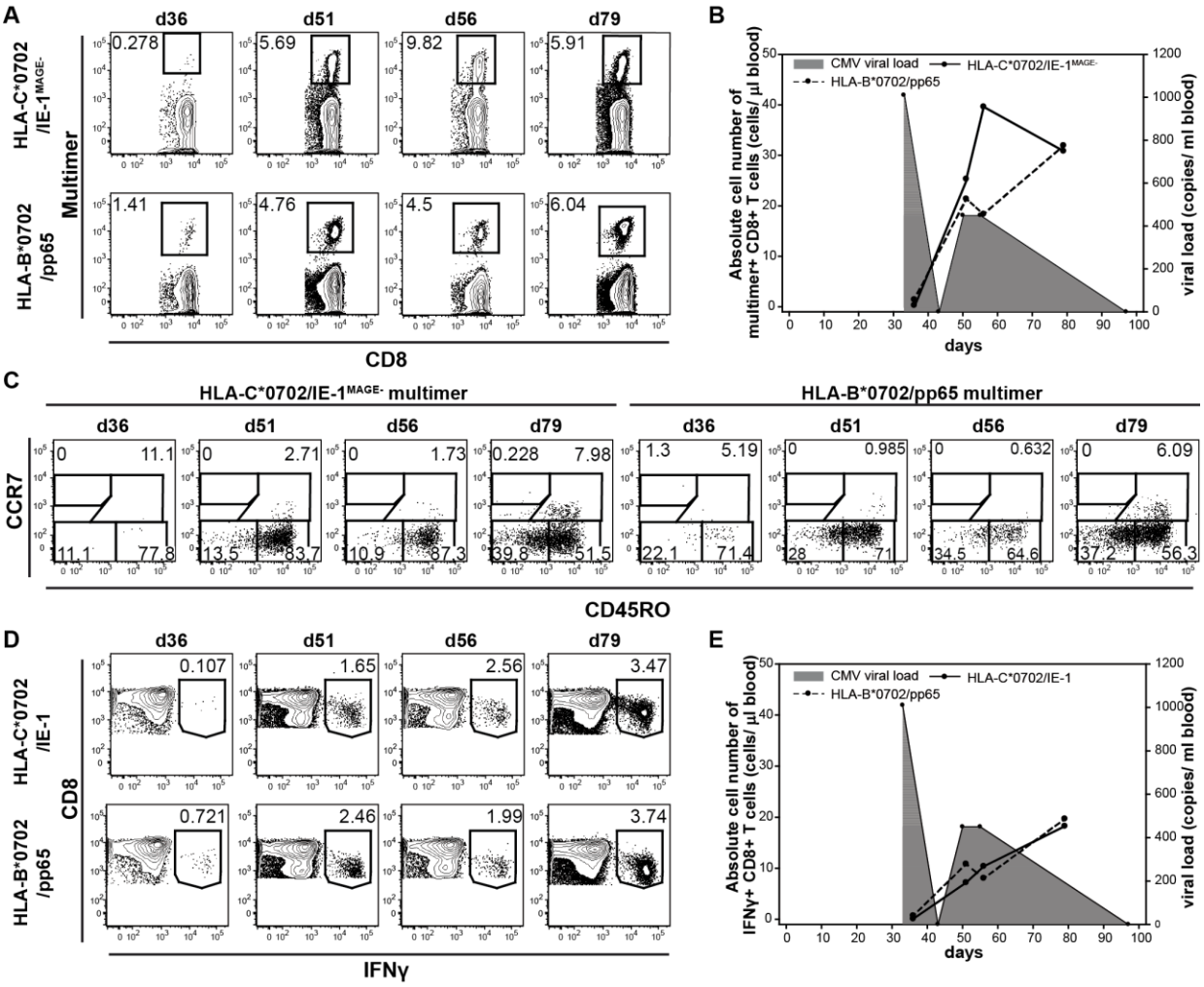

Figure 3.13: Immunmonitoring of HLA-C*0702/IE-1- and HLA-B*0702/pp65-specific T cells after kidney transplantation.

The expansion, functionality, and phenotype of HLA-C*0702/IE-1- and HLA-B*0702/pp65-specific $CD8^+$ T cells was monitored in a viremic kidney transplanted patient. CMV-reactivation was monitored in the peripheral blood by PCR. 30 ml of whole blood was collected on POD 36, 51, 56 and 79. **(A)** MHC-multimer staining of KIR-adjusted HLA-C*0702/IE-1^{MAGE-}- (top line) and HLA-B*0702/pp65-specific T cells (bottom line). Cells were pregated on living $CD3^+CD8^+$ T cells. **(B)** Absolute cell number of MHC-multimer$^+$ $CD8^+$ T cells for HLA-C*0702/IE-1 multimer (solid line) and HLA-B*0702/pp65 multimer (dotted line) in relationship to CMV-viral load (grey area). **(C)** Phenotypical characterization of MHC-multimer$^+$ T cells. Populations were divided into: $T_{naïve}$ ($CCR7^+CD45RO^-$), T_{CM} ($CCR7^+CD45RO^+$), T_{EM} ($CCR7^-CD45RO^+$), and T_{EMRA} ($CCR7^-CD45RO^-$) cells. **(D)** ICS of HLA-C*0702/IE-$1_{309-317}$ (top line) and HLA-B*0702/$pp65_{417-426}$ stimulated T cells (bottom line). Cells were pregated on living $CD3^+IFN\gamma^+CD8^+$ T cells. **(E)** Absolute cell number of $IFN\gamma^+CD8^+$ T cells stimulated with HLA-C*0702/IE-$1_{309-317}$ peptide (solid line) and HLA-B*0702/$pp65_{417-426}$ peptide (dotted line) in relationship to CMV-viral load (grey area).

Taken together, the immunmonitoring data of this kidney transplanted patient confirmed the strong expansion capacities of HLA-C*0702/IE-1-specific T cells and suggested the potential involvement of these cells in viral control.

3.4 Magnetic purification of pure HLA-C*0702/IE-1-specific CD8$^+$ T cells

In the previous experiments, the functionality of the new HLA-C7-multimer and the high central memory content within HLA-C*0702/IE-1^{MAGE-}-specific T cells was demonstrated. In addition, strong proliferation of HLA-C*0702/IE-1-specific T cells in a clinical situation could been shown. Consequently, HLA-C*0702/IE-1-restricted T cells might be a potent candidate for ACT in future. Due to KIR-associated epitope-independent binding, a two-step serial enrichment process was chosen (Stemberger et al., 2012) as classical one step magnetic enrichment of HLA-C*0702/IE-1-specific T cells was not feasible under these circumstances.

3.4.1 Reversibility of the generated HLA-C*0702/IE-1 and HLA-C*0702/MAGE *Strep*Tamers

In order to enrich minimally manipulated cells with MHC-*Strep*Tamers, the reagents had to be reversible. By adding D-biotin, the MHC-*Strep*Tamer complexes are disrupted and the MHC-monomers detach from the cells, due to low binding affinity.

In order to demonstrate the reversibility of the new reagents, PBMCs of a healthy donor were stained with HLA-C*0702/MAGE PE and HLA-C*0702/IE-1 APC and analyzed. The donor showed a frequency of 8.47% KIR-adjusted HLA-C*0702/IE-1^{MAGE-}-specific CD8$^+$ T cells (Figure 3.14, left). In a next step, D-biotin was used to disrupt the MHC-*Strep*Tamer complex. Excepting some background, due to *Strep*-Tactin APC usage, the staining was drastically diminished (Figure 3.14, center-left). As a control the cells were restained only with *Strep*-Tactin PE/APC showing a complete detachment of MHC-monomers (Figure 3.14, center-right). Finally, the PBMCs were relabeled with HLA-C*0702/MAGE PE and HLA-C*0702/IE-1 APC multimer verifying the complete reversibility, with almost the same frequency (8.02%) and intensity of labelling achieved (Figure 3.14, right).

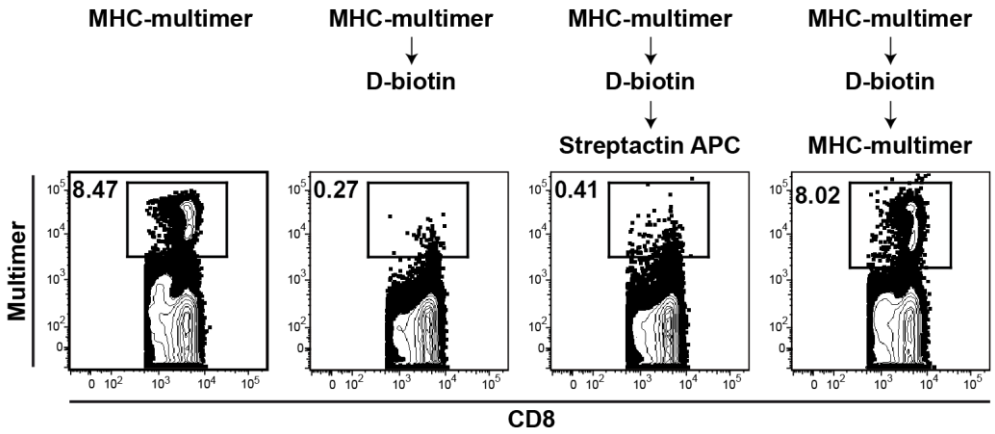

Figure 3.14: Detachment of MHC-*Strep*Tamers by supplementation of D-biotin.
In order to proof the reversibility of the HLA-C*0702/IE-1 and HLA-C*0702/MAGE *Strep*Tamers, a double staining was performed. PBMCs were stained with HLA-C*0702/MAGE PE and HLA-C*0702/IE-1 APC and the cell suspension was washed twice for 10 minutes with 10 ml dissociation buffer. Afterwards, the cells were labeled with HLA-C*0702/MAGE PE and HLA-C*0702/IE-1 APC or, as a control, only with *Strep*-Tactin PE or APC. For all plots, cells were pregated on living $CD3^+CD8^+$HLA-C*0702/$MAGE^-$ T cells.

Taken together, this experiment verified the reversibility of the novel HLA-C7-*Strep*Tamers enabling a clinical grade enrichment of HLA-C*0702/IE-1-specific T cells.

3.4.2 Serial magnetic enrichment for the purification of KIR-adjusted HLA-C*0702/IE-1^{MAGE-}-specific T cells with MHC-*Strep*Tamers

After demonstrating the reversibility of the HLA-C7-*Strep*Tamer a serial enrichment protocol was established. In a first step, the HLA-C*0702/IE-1 *Strep*Tamer was used for a positive enrichment step and afterwards the HLA-C*0702/MAGE *Strep*Tamer was used to deplete epitope-independently bound cells. According to previous published protocols (Stemberger et al., 2012), *Strep*-Tactin-labeled microbeads in combination with the *Strep*Man Magnet for 15 ml and 50 ml tubes (Table 2.2) were used to enrich cells of a health blood donor.

Before enrichment, the donor had a frequency of 9.08% of unspecific and 6.42% of KIR-adjusted CMV-specific $CD8^+$ T cells (Figure 3.15, A). After positive enrichment with the HLA-C*0702/IE-1 *Strep*Tamer, an almost 6-fold increased frequency of truly HLA-C*0702/IE-1^{MAGE-}-specific T cells (36.8%) was detected within the positive fraction indicating a successful enrichment step (Figure 3.15, C, upper row). Still, demonstrated by KIR2DL2/3 staining, most of the epitope-independent enriched cells were KIR^+ (Figure 3.15, C, lower row). However, the negative fraction contained still 2.44% HLA-C*0702/IE-1^{MAGE-}-specific T cells indicating a reduced yield of the enrichment process (Figure 3.15, B, upper row). In addition, this fraction

included several KIR$^+$ T cells (Figure 3.15, B, lower row). After depletion with the HLA-C*0702/MAGE *Strep*Tamer, only a poor purity of 52.1% of CMV-specific T cells was reached (Figure 3.15, D, upper row) containing a large fraction (34.5%) of potentially harmful KIR$^+$ T cells (Figure 3.15, D, lower row). The respective positive fraction comprised a high purity of either KIR2DL2/3$^+$ or HLA-C*0702/IE-1-specific T cells (93.8%, Figure 3.15, E, lower row).

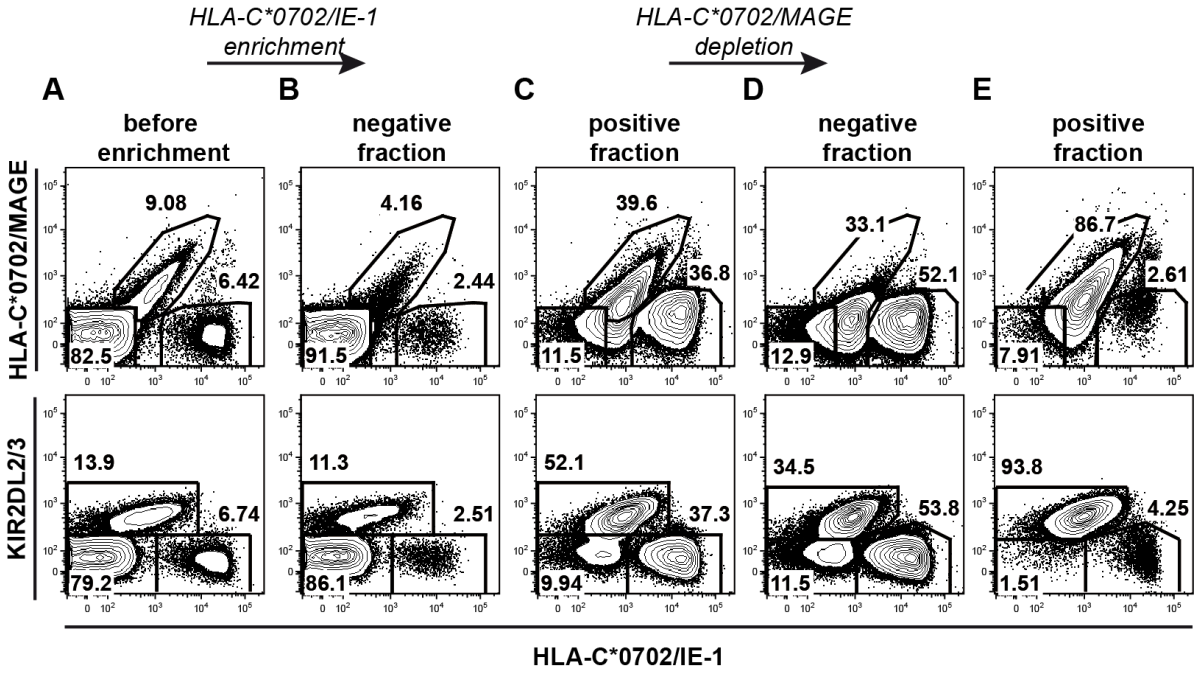

Figure 3.15: Magnetic enrichment of HLA-C*0702/IE-1-specific T cells and HLA-C*0702/MAGE depletion.
In order to purify pure HLA-C*0702/IE-1-specific T cells, a serial enrichment protocol was chosen. For a positive enrichment, 2,5x10^8 PBMCs were labeled with 25 µg HLA-C*0702/IE-1 monomers, multimerized with *Strep*-Tactin Microbeads, and purified with a *Strep*Man Magnet for 15 ml and 50 ml tubes. Afterwards, the multimeric complexes were cleansed away by using dissociation buffer. Then, 1.5 µg of HLA-C*0702/MAGE monomers, multimerized with *Strep*-Tactin Microbeads, were used to deplete epitope-independently bound cells. In order to control the enrichment efficiency, 1x10^6 PBMCs of each fraction were stained with HLA-C*0702/MAGE PE and HLA-C*0702/IE-1 APC multimer (upper row) in combination with the KIR2DL2/3 antibody (lower row). **(A)** Before enrichment. **(B)** HLA-C*0702/IE-1-negative fraction. **(C)** HLA-C*0702/IE-1-positive fraction. **(D)** HLA-C*0702/MAGE-negative fraction (cells of interest). **(E)** HLA-C*0702/MAGE-positive fraction. For all plots, cells were pregated on living CD3$^+$ T cells.

Taken together, the depletion step was insufficient and led to high levels of contamination by T cells with unknown specificity. In an adoptive transfer setting, these cells could cause potentially harmful side-effects, like GvHD. The HLA-C*0702/MAGE *Strep*Tamer was therefore inappropriate for the purification of CMV-specific T cells, but still can be used as a co-staining for the visualization of truly CMV-specific T cells.

3.4.3 Purification of KIR-adjusted HLA-C*0702/IE-1-specific T cells by depleting KIR2DL2/3$^+$ cells with MicroBeads

In order to improve the depletion of epitope-independently enriched T cells, the protocol was switched to primary KIR2DL2/3 depletion with MicroBeads. In a proof-of-concept experiment, the donor had a frequency of 3.13% HLA-C*0702/IE-1-specific T cells and 6.9% KIR2DL2/3$^+$ cells before depletion (Figure 3.16, A). The depleted fraction was almost free of KIR$^+$ cells, as only 0.512% KIR2DL2/3$^+$ cells were detected. Furthermore, the frequency of HLA-C*0702/IE-1-specific T cells was consistent (3.19%, Figure 3.16, C). Finally, a purity of 88.3% CMV-specific T cells was reached after the final enrichment step with HLA-C*0702/IE-1 (Figure 3.16, E). The contaminating cells detected in the final product consisted mainly of CD4$^+$ T cells (10.4%, data not shown) and a small fraction of 1.11% epitope-independently KIR$^+$-enriched cells (Figure 3.16, E). Consequently, the enrichment of HLA-C*0702/IE-1-specific T cells is feasible. At last, the KIR-positive fraction still contained 0.984% residual HLA-C*0702/IE-1-specitic T cells (Figure 3.16, B) and the respective final negative fraction contained 0.857% of HLA-C*0702/IE-1-specific T cells (Figure 3.16, D) indicating a slight loss of CMV-specific T cells. Nevertheless, the yield of 38.8% (% of the number of purified target cells in relation to the number of target cells in the original sample) was expected considering the purity of 88.3% and a cell loss of approximately 50% for each processing step (Stemberger et al., 2012).

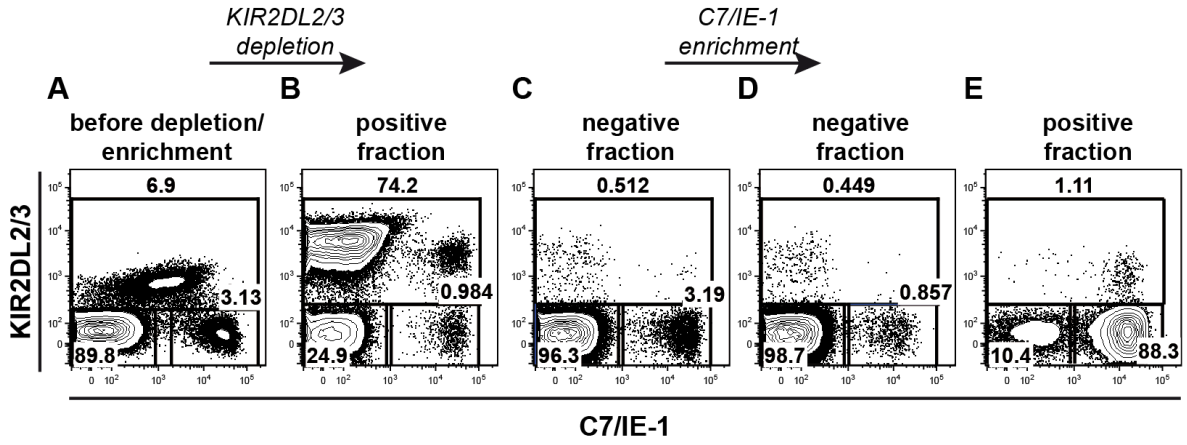

Figure 3.16: Magnetic enrichment of pure HLA-C*0702/IE-1 specific T cells by KIR2DL2/3 depletion. In order to purify pure HLA-C*0702/IE-1-specific T cells 5x10^7 PBMCs of a healthy donor were labeled with KIR2DL2/3 PE antibodies and labeled cells were depleted using Anti-PE MicroBeads. For the enrichment of pure HLA-C*0702/IE-1-specific T cells, 5µg HLA-C*0702/IE-1 monomers were multimerized with *Strep*-Tactin Microbeads and purified using the *Strep*Man Magnet for 15 ml and 50 ml tubes. In order to control the depletion and enrichment efficiency, 1x10^6 PBMCs of each fraction were stained with KIR2DL2/3 antibodies and HLA-C*0702/IE-1 APC multimer. **(A)** Before depletion. **(B)** KIR positive fraction. **(C)** KIR negative fraction. **(D)** HLA-C*0702/IE-1 negative fraction. **(E)** HLA-C*0702/IE-1 positive fraction (cells of interest). For all plots, cells were pregated on living CD3$^+$ T cells.

3.5 Characterization of CMV-specific T cell responses after kidney transplantation

The second part of this thesis is focused on the immunmonitoring of patients after kidney transplantation analyzing risk factors for primary CMV-infection or CMV-reactivation. The aim was to identify potentially predictive markers associated with consecutive CMV control. Therefore, a non-interventional immunmonitoring clinical trial was initiated with the aim to establish a risk-stratification concerning preemptive or prophylactic antiviral treatment. As the transplantation combination of D-/R- has a minimal risk for CMV-infection, only patients at risk for CMV-infection/ -reactivation were included: D+/R+, D-/R+ and D+/R-.

3.5.1 Longitudinal analysis of patients after kidney transplantation

The trial was based on a longitudinal setting where blood samples of patients at risk for CMV-infection/ -reactivation (D+/R+, D-/R+ and D+/R-) were collected. In order to harvest sufficient PBMCs, approximately 30 ml of NH_4-heparinized blood was collected before transplantation and on POD 28, 90, 180. For viremic patients an additional blood sample was collected on POD 270 and 360. All patients received an antiviral prophylaxis of 450 mg Valganciclovir three times per week for three months after transplantation. Patients were screened for CMV-infection/ -reactivation every two weeks in the first three months after transplantation using CMV polymerase chain reaction (PCR). Thereafter, every four weeks a CMV-screening was performed. In total, blood of 35 patients was collected, but 9 patients were excluded from data analysis. None of these patients had any detected viral load. In one patient concomitant Hepatitis C virus infection (n = 1) prevented sample testing and eight patients had missed the designated immune monitoring follow-up measurements (n = 8). In the remaining 26 patients with complete immunological data sets, 31% (n = 8) patients were at high risk (D+/R-) for CMV-infection and 18 patients had an intermediate (D+/R+; D-/R+) risk for CMV-reactivation. Patients' clinical and demographic data are summarized in Table 3.1.

Table 3.1: Clinical and demographic characteristics of longitudinal monitored kidney transplant recipients:

Characteristic	R– Patients (n = 8)	R+ Patients (n = 18)
Sex, male/ female, No.	4/4	12/6
Age, median ± Min/ Max, y	52.5 ± 40/62	60 ± 17/73
Type of transplant, kidney/ kidney-pancreas, No. (%)	7 (87.5)/ 1 (12.5)	18 (100)/ 0 (0)
Type of kidney transplant, living/ deceased donor, No. (%)	2 (25)/ 6 (75)	7 (39)/ 11 (61)
Donor CMV IgG serostatus		
Seronegative, No. (%)	0 (0)	8 (44)
Seropositive, No. (%)	8 (100)	10 (56)
Preventive therapy, prophylaxis, No. (%)	8 (100)	18 (100)
Maintenance IS, No. (%)		
CNI-based (TAC/ CsA)	7 (87.5)/ 1 (25)	16 (89)/ 2 (11)
MMF/ Steroid	3 (37.5)/ 8 (100)	16 (89)/ 17 (94)
Induction IS, No. (%)		
No induction/ rATG/ Basiliximab (anti-CD25)	2 (25)/ 6 (75)/ 0 (0)	10 (56)/ 5 (28)/ 3 (16)
CMV infection, yes/ no, No. (%)		
Viremia	4 (50)/ 4 (50)	3 (17)/ 15 (83)
Disease (part of viremia), yes/ no, No. (%)	3 (75)/ 1 (25)	0 (0)/ 3 (100)
Viral load <500/ >500 copies/ ml blood, No. (%)	0 (0)/ 4 (50)	3 (100)/ 0 (0)

Abbreviations: CMV = Cytomegalovirus; CNI = Calcineurin-inhibitors; CsA = Cyclosporine A; IgG = Immunoglobulin G; IS = immunosuppression; Min = minimum; Max = maximum; MMF = Mycophenolate mofetil; No = number; R = recipient; rATG = rabbit anti-thymocyte globulin; TAC = Tacrolimus; y = years;

3.5.2 Risk-assessment of D+/R+ and D-/R+ standard risk patients

18 patients with a standard risk for CMV-reactivation were included with a median follow-up time of 185.5 days (170-373 days). Three patients had confirmed borderline CMV-reactivation (≤ 500 copies/ml blood) detected by PCR. Median time of reactivation was 98 days (97 – 144 days) after transplantation. All viremic patients were treated by reduction of immunosuppression (short-time reduction of Tacrolimus by 50%). In none of the patients CMV-reactivation led to clinical manifestation of CMV-associated disease. Furthermore, two patients with CMV-reactivation had received an induction therapy with rATG (100 mg/225 mg).

3.5.2.1 Distribution of lymphocyte subpopulations in viremic and aviremic R+ standard risk patients

Alterations within the lymphocyte compartment might serve as a prognostic tool to predict recurrence from latency at an early stage. Immunological changes might already be visible at

the time of reactivation within the tissue, well before the virus becomes detectable in blood. Therefore, all viremic and aviremic patients were analyzed before transplantation, at the end of prophylaxis (POD 90), and on POD 180 with a broad spectrum of markers (Table 2.8) in order to analyze the main protagonists of the lymphocyte compartment (Table 3.2).

Interestingly, patients with subsequent viremia had significantly increased median frequencies of MAIT cells (3.26%; 1.32 – 2.68) on POD 90 whereas patients that remained aviremic had median frequencies of 0.64% (0.05 - 2.68%; p = 0.0178). Absolute number of MAIT cells were also increased (48.69 cells/µl blood; 6.51 – 50.53 cells/µl blood) in comparison to aviremic patients 6.48 cells/µl blood (0.64 - 31.61 cells/µl blood; p = 0.0756; Table 3.2). Frequencies and absolute cell numbers remained comparatively high in viremic patients till the end of follow-up.

In addition, NK cell frequencies and absolute cell numbers were reduced by up to 70% on POD 90 in patients with subsequent viremia (Table 3.2). B cells and cDCs were not altered during the observation period.

Table 3.2: Analysis of lymphocyte subpopulations:

	aviremic R+ Patients (n = 15) median (range)	viremic R+ Patients (n= 3) median (range)	*P* value
MAIT (% of living)			
pre Tx	0.49 (0.05 - 1.64)	1.22 (0.85 - 2.52)	*0.0580*
POD 90	0.64 (0.05 - 2.68)	3.26 (1.32 – 3.83)	**0.0178**
POD 180	0.71 (0.03 - 3.00)	2.40 (1.98 – 2.50)	**0.0244**
MAIT (cells/ µl blood)			
pre Tx	6.95 (1.17 - 32.03)	30.14 (4.56 - 70.64)	0.1551
POD 90	6.48 (0.64 - 31.61)	48.69 (6.51 - 50.53)	*0.0756*
POD 180	11.96 (0.89 - 29.20)	22.84 (15.99 - 52.30)	**0.0244**
B cells (% of living)			
pre Tx	5.43 (2.56 - 14.41)	8.00 (3.40 - 12.65)	0.5536
POD 90	8.86 (3.47 - 16.41)	9.24 (2.93 - 10.42)	0.6356
POD 180	4.60 (1.64 - 12.96)	6.03 (4.09 - 11.00)	0.3433
B cells (cells/ µl blood)			
pre Tx	77.79 (27.48 - 173.21)	94.43 (68.16 - 200.18)	0.9527
POD 90	96.19 (25.03 - 444.78)	55.47 (44.57 - 139.57)	0.9527
POD 180	67.93 (13.94 - 183.38)	76.36 (72.19 - 90.28)	0.9527
cDC (% of living)			
pre Tx	0.39 (0.02 - 2.52)	0.23 (0.12 - 0.25)	0.3433
POD 90	0.23 (0.02 - 1.95)	0.12 (0.03 - 0.26)	0.5536
POD 180	0.46 (0.03 - 1.57)	0.21 (0.01 - 0.60)	0.4069
cDC (cells/ µl blood)			
pre Tx	4.85 (0.15 - 20.70)	3.39 (1.25 - 6.14)	0.5536
POD 90	7.58 (0.91 - 45.30)	13.32 (2.09 - 16.21)	0.5536
POD 180	4.60 (0.87 - 24.38)	1.36 (0.21 - 7.55)	0.2361
NK cells (% of living)			
pre Tx	14.60 (6.76 - 32.67)	4.25 (2.15 - 8.28)	**0.0178**
POD 90	9.34 (4.56 - 27.94)	6.52 (2.76 - 8.22)	*0.0580*
POD 180	10.32 (4.60 - 28.99)	5.83 (2.24 - 11.38)	0.1551
NK cells (cells/ µl blood)			
pre Tx	201.75 (20.42 - 909.83)	117.92 (11.60 - 207.06)	0.1925
POD 90	122.17 (33.03 - 598.34)	43.76 (42.04 - 98.48)	*0.0972*
POD 180	154.85 (49.35 - 451.19)	49.35 (38.26 - 144.04)	*0.0580*

Abbreviations: cDC = classical dendritic cells; MAIT = Mucosal-Associated Invariant T Cells; NK cells = natural killer cells; pre Tx = prior to transplantation; Statistical analyses were performed using the Mann-Whitney *U* test (bold = statistical significant; italic = close to significance)

Then it was analyzed if key lymphocyte populations of the adaptive immune system ($CD3^+$, $CD4^+$, and $CD8^+$ T cells) were altered during of follow-up.

For CD3⁺ T cells no differences were detected except a trend towards increased frequencies and absolute cell numbers in patients becoming later on viremic (Figure 3.17, A). Interestingly, CD4⁺ T cell levels were comparable prior to transplantation and decreased before detection of viral replication on POD 90. At this time point, median CD4⁺ T cell frequencies of patients with viremia were 34.00% (29.90 – 46.30%) and significantly reduced in comparison to aviremic patients (median: 51.8%; 20 – 68.60%; p = 0.0440, Figure 3.17, B, top). In addition, absolute cell numbers of CD4⁺ T cells were reduced but without significance (Figure 3.17, B, bottom). CD8⁺ T cell levels were slightly increased on POD 90 in viremic patients (median: 57.10%; 42.80 – 64.10%) in comparison to aviremic patients (median: 43.30%; 42.80 -64.10%; p = 0.1549; Figure 3.17, C, top).

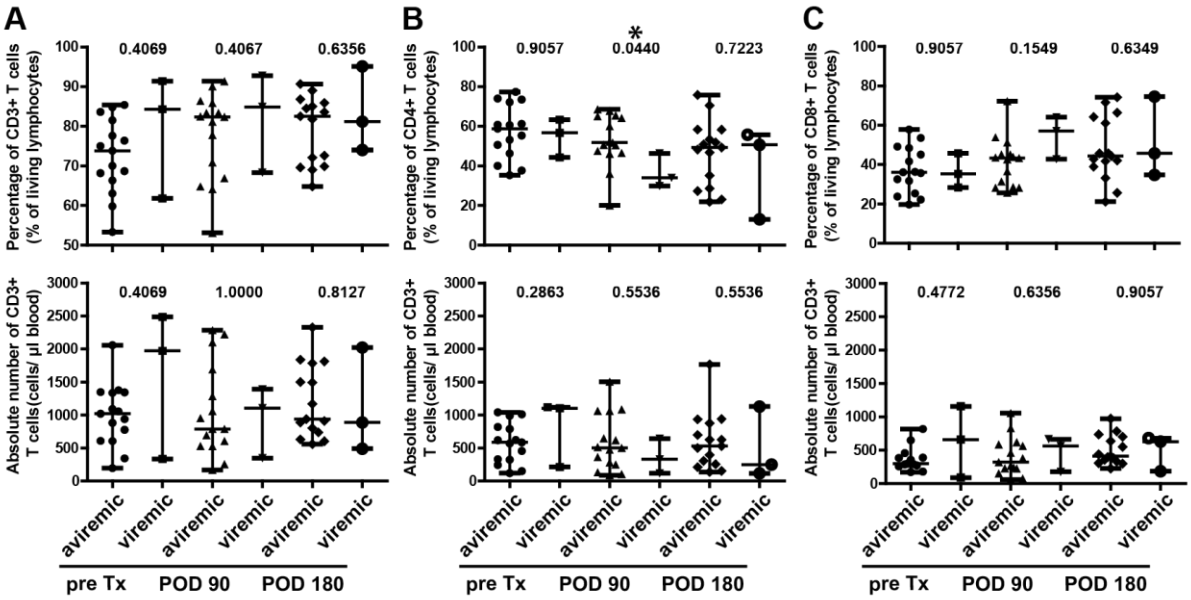

Figure 3.17: Frequencies and absolute cell numbers of CD3⁺, CD4⁺, and CD8⁺ T cells of aviremic and viremic patients.
For the determination of frequencies, PBMCs were stained with the respective antibodies and quoted as percentage of living lymphocytes. Absolute cell numbers were assed from whole blood staining using BD Trucount™ Tubes. **(A)** Frequencies (top) and absolute cell numbers (cells/µl blood; bottom) of CD3⁺ T cells. **(B)** Frequencies (top) and absolute cell numbers (cells/µl blood; bottom) of CD4⁺ T cells. **(C)** Frequencies (top) and absolute cell numbers (cells/µl blood, bottom) of CD8⁺ T cells. Statistical analyses were performed using the Mann-Whitney U test. Exact *p* values are indicated. * = p < 0.05, ** = p < 0.01, *** = p < 0.001.

3.5.2.2 Memory subpopulations of CD4⁺ and CD8⁺ T cells

As variations within CD4⁺ and CD8⁺ T cell populations were detected, the different memory subpopulations were characterized in detail.

First, the memory CD4⁺ T cell compartment was examined. Frequencies and absolute cell numbers of CD4⁺ T_{naive}, T_{SCM} and T_{EM} cells are summarized in Table 3.3. Even though there was

a trend to lower levels in $CD4^+$ T_{CM} frequencies in patients with viremia observable (Figure 3.18, left), statistically significant differences were due to small group sizes and high variability among R+ patients not detected.

Table 3.3: $CD4^+$ memory T cell populations:

	aviremic R+ Patients (n = 15) median (range)	viremic R+ Patients (n= 3) median (range)	*P* value
T_{naive} (% of CD4)			
pre Tx	33.47 (13.82 - 66.15)	41.30 (35.38 - 45.48)	0.3433
POD 90	44.39 (7.63 - 63.52)	24.87 (21.04 - 45.28)	0.3233
POD 180	36.31 (1.98 - 55.27)	30.79 (22.90 - 54.49)	1.0000
T_{naive} (cells/ µl blood)			
pre Tx	179.12 (33.58 - 511.52)	396.01 (87.79 - 501.41)	0.3433
POD 90	178.00 (6.74 - 788.89)	82.23 (24.87 - 291.56)	0.4772
POD 180	147.17 (2.75 - 853.88)	76.45 (26.48 - 614.42)	0.5536
T_{SCM} (% of CD4)			
pre Tx	2.61 (1.02 - 6.26)	3.14 (2.14 - 6.99)	0.3433
POD 90	2.52 (0.80 - 6.22)	3.55 (2.29 - 3.71)	0.4772
POD 180	2.33 (0.69 - 8.42)	3.70 (2.31 - 5.00)	0.2663
T_{SCM} (cells/ µl blood)			
pre Tx	14.36 (1.47 - 63.30)	23.62 (14.85 - 35.16)	0.2361
POD 90	12.68 (1.92 - 28.31)	11.75 (4.38 - 14.72)	0.5536
POD 180	12.78 (2.8 - 79.14)	12.43 (4.28 - 26.09)	1.0000
T_{EM} (% of CD4)			
pre Tx	14.10 (7.12 - 37.00)	17.40 (8.00 - 22.50)	1.0000
POD 90	13.30 (5.77 - 31.90)	17.50 (15.10 - 45.00)	0.1729
POD 180	12.70 (7.86 - 50.30)	26.50 (13.80 - 29.90)	0.1925
T_{EM} (cells/ µl blood)			
pre Tx	70.45 (25.54 - 210.91)	89.55 (47.83 - 191.84)	0.8127
POD 90	72.60 (15.99 - 196.64)	53.20 (49.92 - 112.68)	0.8127
POD 180	73.41 (19.42 - 193.10)	71.77 (30.65 - 155.61)	1.0000

Statistical analyses were performed using the Mann-Whitney U test. Exact p values are indicated.

In absolute cell numbers differences between both groups were not visible (Figure 3.18, right).

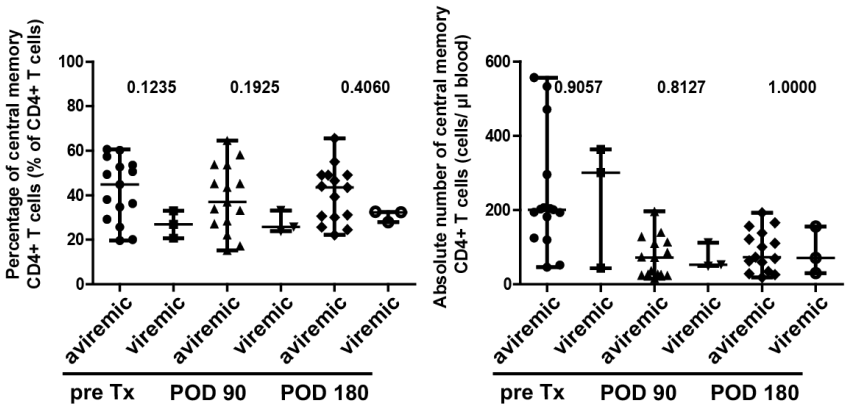

Figure 3.18: Frequencies and absolute cell numbers of $CD4^+$ T_{CM} cells.
For the determination of $CD4^+$ T_{CM} frequencies (left), PBMCs were gated as previously described. Absolute cell numbers of $CD4^+$ T_{CM} cells (right) were calculated from whole blood stainings using BD Trucount™ Tubes. Statistical analyses were performed using the Mann-Whitney U test. Exact *p* values are indicated.

In addition, the memory distribution of $CD8^+$ T cells was determined. Frequencies and absolute cell numbers of $CD8^+$ T_{naive}, T_{SCM}, T_{EM}, and T_{EMRA} cells are summarized in Table 3.4. No statistically significant changes were detectable.

Table 3.4: CD8$^+$ memory T cell populations:

	aviremic R+ Patients (n = 15) median (range)	viremic R+ Patients (n= 3) median (range)	*P* value
T_{naive} (% of CD8)			
pre Tx	11.61 (2.20 - 52.51)	21.61 (11.17 - 54.89)	0.2361
POD 90	17.10 (2.95 - 70.84)	10.11 (5.75 - 60.90)	0.9057
POD 180	13.69 (0.45 - 73.52)	21.45 (14.45 - 24.14)	0.2863
T_{naive} (cells/ µl blood)			
pre Tx	34.76 (6.29 - 692.49)	128.65 (19.33 - 361.19)	0.4069
POD 90	60.08 (6.01 - 272.24)	56.58 (10.06 - 401.48)	1.0000
POD 180	45.75 (1.87 - 2150.21)	141.36 (26.98 - 151.90)	0.4069
T_{SCM} (% of CD8)			
pre Tx	1.67 (0.55 - 3.68)	2.47 (0.61- 5.10)	0.6356
POD 90	1.71 (1.08 - 2.42)	0.84 (0.75 - 10.57)	0.4069
POD 180	1.71 (0.25 - 4.96)	1.27 (1.12 - 1.29)	0.1925
T_{SCM} (cells/ µl blood)			
pre Tx	6.34 (1.73 - 57.01)	6.82 (4.56 - 16.28)	0.7223
POD 90	6.32 (0.73 - 18.02)	4.66 (1.46 - 70.53)	1.0000
POD 180	9.63 (1.04 - 242.08)	7.98 (2.40 - 8.23)	0.3433
T_{EM} (% of CD8)			
pre Tx	23.10 (15.30 - 44.90)	20.30 (15.80 - 57.90)	1.0000
POD 90	22.90 (10.10 - 53.50)	23.60 (8.39 - 74.00)	0.9056
POD 180	22.50 (8.29 - 61.90)	32.70 (21.20 - 64.00)	0.3433
T_{EM} (cells/ µl blood)			
pre Tx	81.67 (45.51 - 206.46)	103.97 (51.78 -230.82)	0.6556
POD 90	63.85 (8.42 - 242.76)	129.52 (56.00 - 133.31)	0.7223
POD 180	103.79 (29.57 - 541.85)	146.90 (119.53 - 205.78)	0.6356
T_{EMRA} (% of CD8)			
pre Tx	40.60 (21.40 - 59.80)	15.60 (8.31 - 48.60)	0.1551
POD 90	34.20 (7.13 - 63.20)	15.60 (3.70 - 46.70)	0.2863
POD 180	41.50 (6.72 - 60.70)	30.70 (13.80 - 38.00)	0.2361
T_{EMRA} (cells/ µl blood)			
pre Tx	140.43 (36.86 - 388.23)	102.66 (7.43 - 571. 84)	0.8127
POD 90	128.01 (12.07 - 616.17)	27.30 (24.70 - 261.23)	0.5536
POD 180	178.24 (23.97 - 591.72)	193.20 (25.77 - 261.15)	0.9057

Statistical analyses were performed using the Mann-Whitney U test. Exact *p* values are indicated.

Interestingly, a reduced frequency of CD8$^+$ T_{CM} cells was measureable shortly before reactivation (POD 90; Figure 3.19, left). However, this was statistically not significant and a similar trend was not detectable in CD8$^+$ T_{CM} absolute cell numbers (Figure 3.19, right).

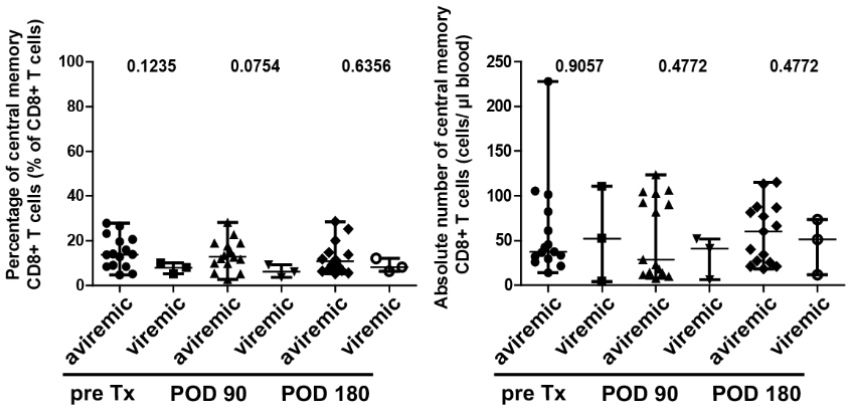

Figure 3.19: Frequencies and absolute cell numbers of CD8$^+$ T_{CM} cells
For the determination of CD8$^+$ T_{CM} frequencies (left), PBMCs were gated as previously described. Absolute cell numbers of CD8$^+$ T_{CM} cells (right) were calculated from whole blood stainings using BD Trucount™ Tubes. Statistical analyses were performed using the Mann-Whitney U test. Exact p values are indicated.

3.5.2.3 Analysis of CMV-specific T cells in viremic and aviremic R+ standard risk patients

In a next step CMV-specific T cells were closely analyzed. As MHC-multimers were not available for all D+/R+ and D-/R+ patients, the functional profile of CD4$^+$ and CD8$^+$ CMV-specific T cells was assessed.

In a first assay, whole blood was stimulated and analyzed using the CMV QuantiFERON assay. No differences between viremic and aviremic patients were detectable (Figure 3.20, A). Furthermore, 4 aviremic patients had no detectable response on POD 90, whereas only one viremic patient was unreactive at this time point. Interestingly, in all three patients showing CMV-reactivations an increase in IFNγ-secretion after reactivation was measurable (Figure 3.20, B) potentially leading to viral control.

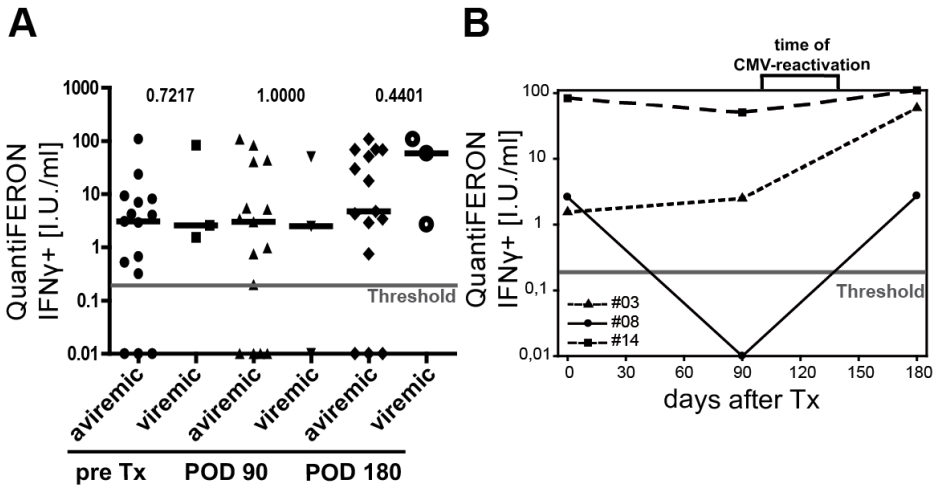

Figure 3.20: Analysis of IFNγ-secretion after stimulation using the QuantiFERON assay.
The IFNγ-secretion was measured after stimulation of whole blood with specific CMV-restricted peptides using the CMV QuantiFERON assay. The threshold of 0.2 I.U./ml for a positive QuantiFERON result is indicated. **(A)** Comparison of viremic and aviremic patients. **(B)** Analysis of viremic patients over time. Statistical analyses were performed using the Mann-Whitney U test. Exact p values are indicated.

In addition to the CMV-QuantiFERON assay, stimulation with CMV-specific peptide mixes was performed for all patients followed by ICS.

Between stimulated pp65 Mix-restricted $CD4^+$ T cells, no differences in frequencies (Figure 3.21, A) or absolute cell numbers (Figure 3.21, B) were detectable. If at all, slightly more $CD4^+$ T cells of viremic patients produced IFNγ on POD 90. Similar observation were made for TNFα, IL-2 and GM-CSF (data not shown). Interestingly, in all viremic patients $CD4^+$ pp65 Mix-specific T cells were detected, whereas 3 patients without detected viremia had no CMV-specific $CD4^+$ T cells

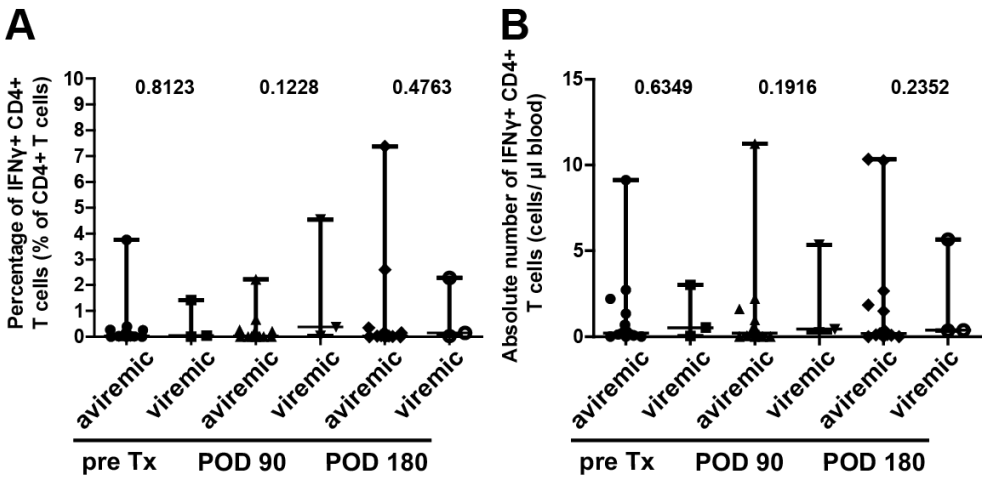

Figure 3.21: Analysis of stimulated and functional CD4⁺ T cells.
CMV-specific T cells were analyzed and quantified by IFNγ-secretion after restimulation with CMV-specific pp65 peptide mix. **(A)** Percentage of functional CD4⁺ T cells in viremic and aviremic patients. **(B)** Absolute cell number of IFNγ⁺ CD4⁺ T cells. Statistical analyses were performed using the Mann-Whitney U test. Exact p values are indicated.

Furthermore, the cytokine production of CD8⁺ T cells after stimulation with the viral epitopes for pp65 or IE-1 was analyzed. Comparisons of viremic and aviremic patients for pp65-specific CD8⁺ T cells revealed no differences with regard to frequency (Figure 3.22, A) or in absolute cell numbers (Figure 3.22, B).

Interestingly, viremic patients had increased frequencies of IE-1 Mix-specific CD8⁺ T cells at the time of monitoring. Especially on POD 90 viremic patients had an increased median frequency of 2.28% (0.96 – 14.57) whereas aviremic patients had a median frequency of 0.71% (0 – 5.95%; p = 0.0326, Figure 3.22, C). In absolute cell numbers viremic patients had increased cell numbers specific for IE-1 Mix (median: 12.66 cells/µl blood; 3.63 – 56.00 cells/µl blood) in comparison to aviremic patients (0.84 cells/µl blood; 0 – 16.43 cells/µl blood; p = 0.0575; Figure 3.22, D).

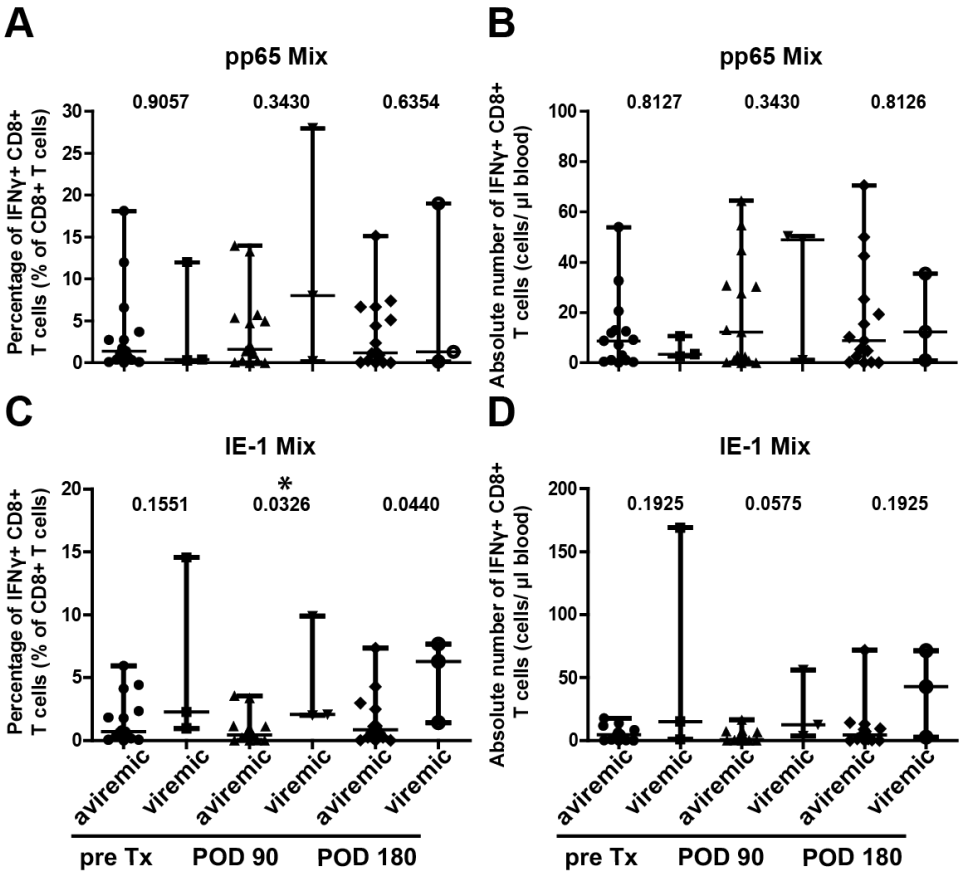

Figure 3.22: Analysis of stimulated and functional CD8⁺ T cells.
CMV-specific T cells were analyzed and quantified by IFNγ-secretion after restimulation with CMV-specific pp65 or IE-1 peptide mix. **(A)** Percentage of pp65 Mix-specific, functional CD8⁺ T cells in viremic and aviremic patients. **(B)** Absolute cell number of pp65 Mix-specific, IFNγ⁺CD8⁺ T cells. **(C)** Percentage of IE-1 Mix-specific, functional CD8⁺ T cells in viremic and aviremic patients. **(D)** Absolute cell number of IE-1 Mix-specific, IFNγ⁺ CD8⁺ T cells. Statistical analyses were performed using the Mann-Whitney U test. Exact p values are indicated. * = $p < 0.05$, ** = $p < 0.01$, *** = $p < 0.001$.

Notably, in contrast to the QuantiFERON data, after analyzing the individual viremic patients over time, no proliferation of pp65-specific CD4⁺ T cells was detected. Moreover, the frequency of CMV-specific CD4⁺ T cells declined in patient #03 and #08 (Figure 3.23, A). In case of pp65-specific CD8⁺ T cells, similar observations were made that demonstrated a decline in frequency for patients #03 and #08 (Figure 3.23, B). Furthermore, patient #08 was the only patient that showed proliferation of IE-1-specific CD8⁺ T cells after CMV-reactivation, whereas these frequencies declined in patient #03 and #14 (Figure 3.23, C).

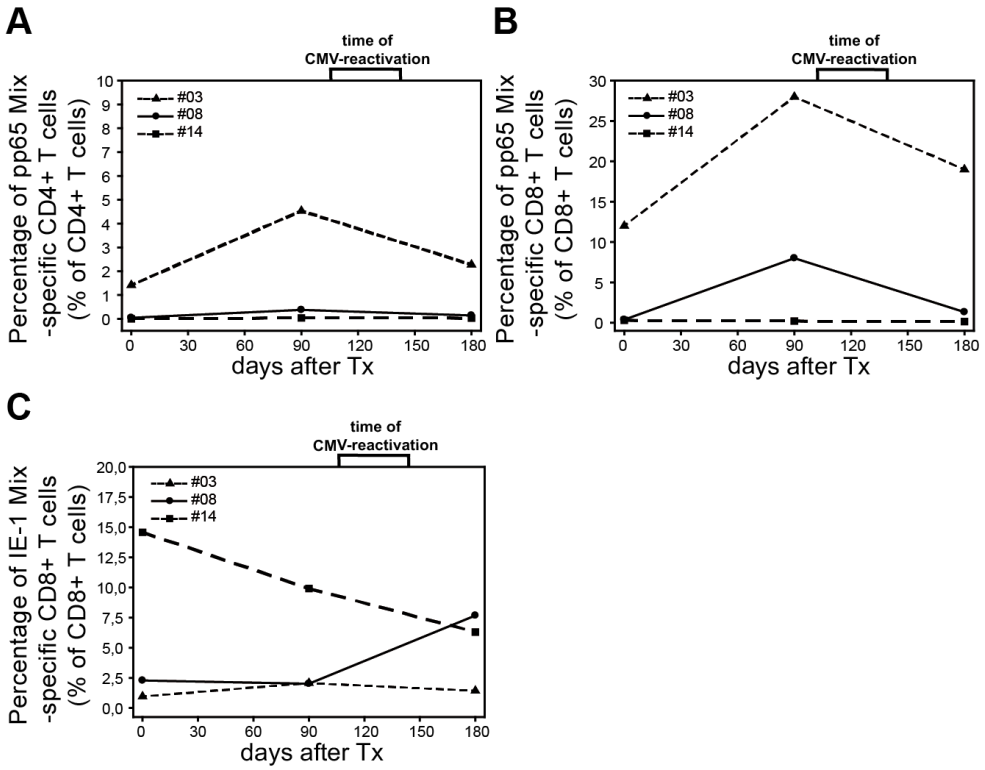

Figure 3.23: Analysis of functional CD4$^+$ and CD8$^+$ T cells over time.
Depicted are the percentage of functional CD4$^+$ and CD8$^+$ T cells of viremic patients #03, #08 and #14 at the given time of follow-up. **(A)** Percentage of pp65 Mix-specific, functional CD4$^+$ T cells. **(B)** Percentage of pp65 Mix-specific, functional CD8$^+$ T cells. **(C)** Percentage of IE-1 Mix-specific, functional CD8$^+$ T cells.

3.5.3 Risk-assessment of D+/R- high risk patients

8 patients with a high-risk (D+/R-) of CMV-infection were included and median follow-up time was 784 days (156-1155 days). Detailed clinical and demographic data are shown in Table 3.5.

Table 3.5: Detailed clinical and demographic data of D+/R- high risk patients:

Patient No.	#01	#02	#03	#04	#05	#06	#07	#08
Gender	f	m	f	m	m	m	f	f
Age	56	54	49	40	53	62	51	52
Type of transplant	K/P	K	K	K	K	K	K	K
Number of transplantations	1	2	1	1	1	1	1	2
ATG induction (mg)	300	200	125	100	225	200*	-	75
Cold ischemia time (min)	960	720	130	1080	660	1080	120	540
Warm ischemia time (min)	60	20	20	30	30	16	20	16
Underlying disease	DN	RN	DN/HN	DN	Fabry's disease	ADPKD	MPGN	HUS
Pretransplant renal replace-ment therapy	HD	HD	None	HD	HD	HD	None	HD
CMV infection	Yes	Yes	No	Yes	No	Yes	No	No
CMV-associated disease	Pneu-monitis	none	none	CMV syndrome/ Sepsis	none	Hepatitis	none	none

Abbreviations: f = female; m = male; K/P = kidney/pancreas transplantation; K = kidney transplantation, ATG = anti thymocyte globulin; DN = diabetic nephropathy; RN = reflux nephropathy; HN = hypertensive nephropathy; ADPKD = autosomal-dominant polycystic kidney disease; MPGN = membrano-proliferative glomerulonephritis; HUS = hemolytic-uremic-syndrome; HD = hemodialysis; * = post-transplant ATG treatment preceding CMV replication

3.5.3.1 CMV-infection causes severe clinical manifestations in D+/R- patients

Four of these 8 patients suffered from acute CMV-infection. Median time of detected viremia was 124.5 days (94 – 208 days) and three of the viremic patients had CMV-associated clinical manifestations needing additional antiviral treatment.

The first patient was a 56 year old female subject. After long term dialysis due to type I diabetes mellitus, the patient finally received a graft from a CMV-seropositive donor. The patient received 300 mg of rATG as an induction therapy and was treated with Tacrolimus and steroids in order to reduce graft rejection. After 90 days of antiviral prophylaxis, the patient developed an acute CMV-infection on POD 124, which led to a CMV-associated pneumonitis, requiring hospitalization admission to the intensive care unit (ICU) and additional antiviral treatment with intravenous ganciclovir. Three days after first detection of viremia (POD 127)

CMV-specific T cells directed against the viral epitopes pp65 (0.67 cells/µl blood) and IE-1 (55.2 cells/µl blood) were detected by ICS. In line with the generation of CMV-specific T cells, a seroconversion for CMV-specific IgM and IgG antibodies was detected (Table 3.6). After strong proliferation of CMV-specific $CD8^+$ T cells (pp65 Mix: POD 195, 20.6 cells/µl blood; IE-1 Mix; POD 371, 286.3 cells/µl blood) viral load decreased and protective T cell immunity was established, demonstrated by the absence of further CMV-reactivations (Figure 3.24, A). Similar observations were made using the CMV-QuantiFERON assay, indicating that the pp65 Mix-specific response was dominated by the A2pp65$_{495\text{-}503}$ epitope (Figure 3.24, B).

The second kidney transplant recipient was a 54 year old male with a reflux nephropathy. During transplantation, the patient received 200 mg rATG and Tacrolimus and steroids for long term immunosuppression. On POD 125 a borderline viral load of ≤500 copies/ml blood was detected. Interestingly, the viral episode lasted for almost 50 days and peaked on POD 171 with 871 copies/ml blood. On POD 177 a seroconversion to CMV-IgG was measurable (Table 3.6) and a small B7pp65-restriceted T cell population of 0.114 cells/µl blood was detected by MHC-multimer staining (data not shown). Neither by ICS (Figure 3.24, C) nor by the CMV-QuantiFERON assay (Figure 3.24, D) were any functional CMV-specific T cells detectable at this time point. In spite of this, viremia decreased and was controlled by POD 224. Proliferation of functional CMV-specific T cells directed against pp65 (100.2 cells/µl blood) and IE-1 (74.7 cells/µl blood) epitopes were confirmed on POD 849 by ICS (Figure 3.24, C) and by the CMV-QuantiFERON assay (Figure 3.24, D). The pp65-restricted response was dominated by the B7pp65$_{417\text{-}426}$ epitope and the IE-1-restricted response by the HLA-C*0702 IE-1$_{309\text{-}317}$ epitope (data not shown).

Patient #04, a 40 year old male, underwent kidney transplantation due to type I diabetes mellitus. Intraoperatively, the patient received 100 mg rATG and enduring immunosuppression consisted of Tacrolimus, MMF, and steroids. The patient had a delayed CMV-infection, leading to a CMV-syndrome which consisted of fever, leukopenia, and thrombocytopenia. On POD 208 a viral titer of more than 1.5 x 10^6 copies/ml blood was measured by an in-house PCR analysis. Shortly afterwards, the patient was found to be systemically infected by *S. aureus* and died 5 days later due to sepsis. No induction of a functional CMV-specific T cell response was detectable by ICS (Figure 3.24, E) or by the CMV-QuantiFERON assay (Figure 3.24, F). Nevertheless, on POD 208 the patient generated a CMV-

specific antibody response by synthesis of CMV-IgM antibodies (Table 3.6) but no class switch to CMV-IgG was detectable.

The fourth viremia patient (#06) was a 62 year old male who underwent kidney transplantation due to autosomal dominant polycystic kidney disease. Despite an immunosuppression consisting of Tacrolimus, MMF, and steroids the patient had a rejection episode that was treated with 200 mg rATG on POD 88. In between, no CMV-specific PCR was performed and on POD 123 the patient suffered from severe CMV-infection (11.900 copies/ml blood), leading to a CMV-associated hepatitis. The patient received medical treatment by administration of intravenous ganciclovir. On POD 94, a CMV-IgM antibody response was detected and a CMV-IgG class switch was observable on POD 135 (Table 3.6). In addition, on POD 94, a CMV-specific T cells response directed against the viral epitopes pp65 (8.3 cells/ µl blood) and IE-1 (0.04 cells/ µl blood) was detected by ICS. Afterwards, a decline of CMV-specific T cells in the peripheral blood till POD 125 (pp65 Mix: 6.8 cells/µl blood and IE-1 Mix 0.00 cells/ µl blood) was measured. Thereafter, extensive proliferation of functional CMV-specific T cells was recorded that correlated with control of CMV viremia (Figure 3.24, G). These results were verified by the CMV-QuantiFERON assay (Figure 3.24, H).

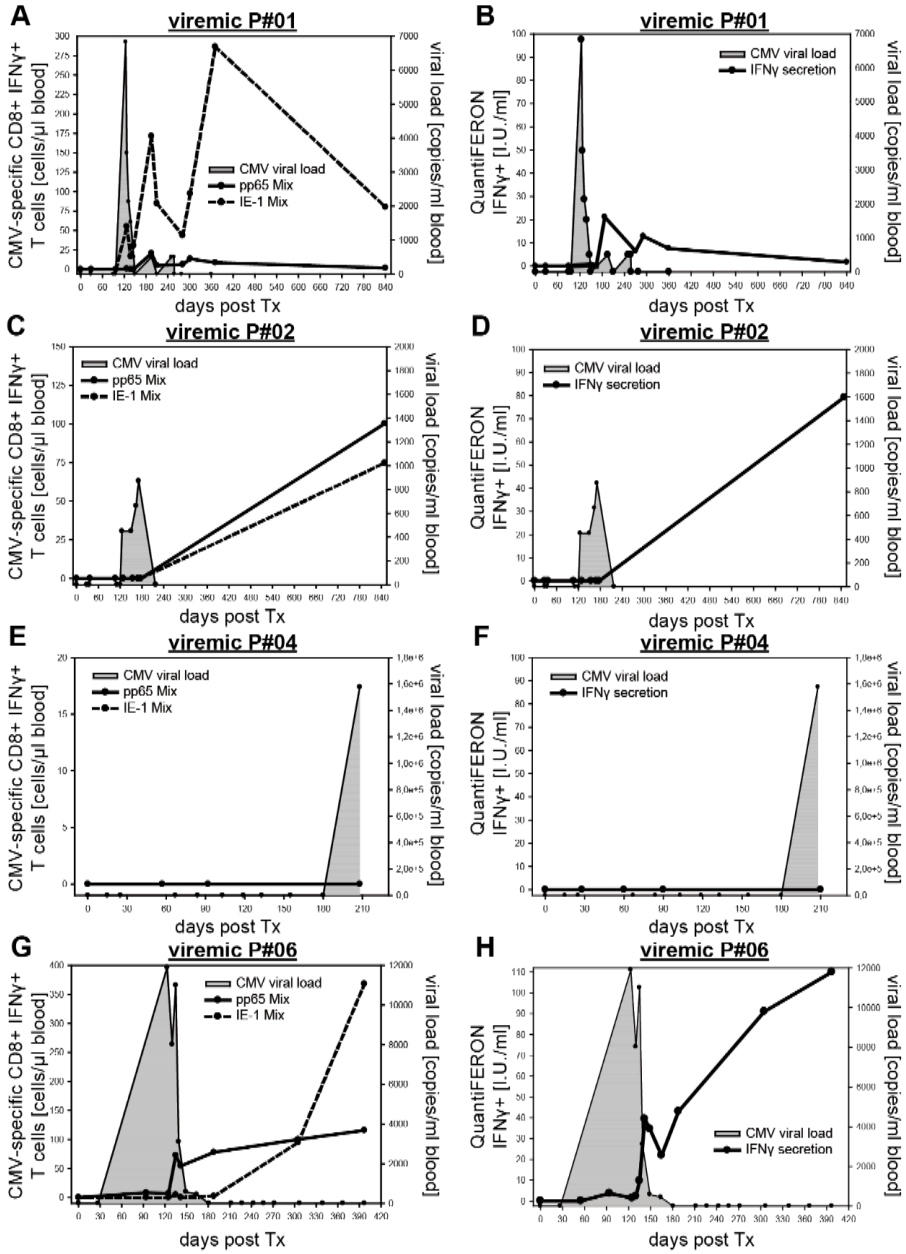

Figure 3.24: Immune monitoring of high-risk viremic patients.
High-risk D+/R- recipients were observed for a median follow-up time of 784 days (156-1155 days). CMV-viremia (grey area) was measured by quantitative PCR. CMV-specific T cells were quantified by IFNγ-secretion after restimulation with CMV-specific peptide mixes in ICS. Viremic patients are separately shown in (A), (C), (E), and (G). Kinetics of CMV-pp65- (solid line) or CMV-IE-1- (dashed line) specific $CD8^+$ T cells are indicated. (B), (D), (F) and (H) show the quantitative IFNγ-secretion measured by the CMV-QuantiFERON assay.

Table 3.6: Serostatus of viremic D+/R- patients:

Patient No.	POD	CMV-IgM serostatus	CMV-IgG serostatus
#01	127	positive	positive
#02	177	*negative*	positive
#04	208	positive	*negative*
#06	135	positive	positive

Taken together, primary CMV-infection led to severe clinical manifestations in most viremic D+/R- patients, underlining the high-risk potential of this patient subgroup. Conversely, viral replication led to induction of a protective T cell immunity, as demonstrated by detecting no further CMV-reactivations during of follow-up in three of four viremic patients.

3.5.3.2 No correlates of primary CMV-infection in aviremic patients

Even though, three of four viremic D+/R- patients suffered from severe clinical disease, no viremia was detected in the four remaining D+/R- patients. Since all three surviving viremic patients established a protective CMV-specific immunity, aviremic patients were screened for the generation of a CMV-specific T cell responses. Surprisingly, even after collecting PBMCs at very late time points, no IFNγ-producing CMV-specific T cells were detected after stimulation with the viral epitopes pp65 or IE-1 by ICS (Figure 3.25, A) or by the CMV-QuantiFERON assay (Figure 3.25, B).

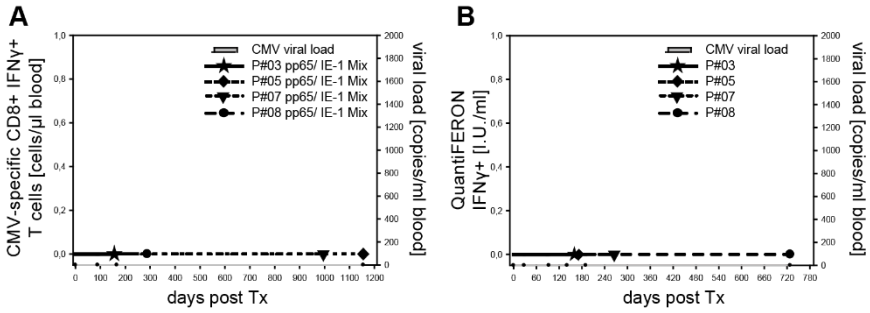

Figure 3.25: Immune monitoring of aviremic patients.
Aviremic high-risk D+/R- recipients were analyzed for the generation of CMV-specific T cells. **(A)** CMV-specific T cells were quantified by IFNγ-secretion after restimulation with CMV-specific peptide mixes by ICS. Last time points of negative T cell screenings are indicated. **(B)** Quantification of IFNγ-secretion using the CMV-QuantiFERON assay.

As none of the aviremic patients established a CMV-specific immunity, the serostatus of these patients was analyzed by ELISA. Interestingly, all aviremic patients were negative for CMV-IgM or -IgG antibodies (Table 3.7).

Table 3.7: Serostatus of aviremic D+/R- patients:

Patient No.	Days post Tx	CMV-IgM serostatus	CMV-IgG serostatus
#03	165	*negative*	*negative*
#05	1155	*negative*	*negative*
#07	995	*negative*	*negative*
#08	728	*negative*	*negative*

Taken together, aviremic D+/R- patients established no CMV-specific T cell response and remained permanently CMV-seronegative showing no correlate of an established primary CMV-infection.

3.5.3.3 Risk factors for primary CMV-infection in D+/R- patients

The assumption of a subgroup of patients that has no risk for primary CMV-infection is an interesting observation that could impact future clinical treatment dramatically. Therefore, known risk factors that are associated with viral replication, such as age, HLA mismatch, induction therapy, and immunosuppressive medication (Kotton, 2010; Shabir et al., 2013) were analyzed in order to dissect viremic from aviremic patients. The analyzed factors are summarized in Table 3.8. No significant differences were detected.

Table 3.8: Analyzes of known risk-factors for viral replication:

risk-factor	viremic patients median (range)	aviremic patients median (range)	*P* Value
Age (y)	55 (40 - 63)	51.5 (49 - 53)	0.34
Mismatches HLA class I	3 (2 - 4)	3 (2 - 4)	0.88
Mismatches HLA class II	2 (0 - 2)	1.5 (1 - 2)	0.87
rATG (mg)	200 (150 - 300)	100 (75 - 225)	0.20
IS:			
TAC POD 90 (ng/ml)	8.35 (0 – 9.2)	7.05 (5.5 – 10.5)	0.89
MMF POD 90 (mg/day)	0 (0 - 1000)	1500 (0 - 2000)	0.16
Steroids POD 90 (mg/d)	10 (5 - 20)	6.25 (2.5 – 7.5)	0.14

Abbreviations: HLA = human leukocyte antigen; IS = immunosuppression; MMF = Mycophenolate mofetil; POD = post-operative day; rATG = rabbit anti-thymocyte globulin; TAC = Tacrolimus; y = years; Statistical analyses were performed using the Mann-Whitney *U* test

Therefore, in a next step graft quality-related factors were analyzed. It is known that prolonged storage of organs in cold solution, termed cold ischemia time (CIT), influences severity of ischemia reperfusion injury (Ponticelli, 2015), a phenomenon which leads in turn to increased levels of inflammatory cytokines (e.g. tumor necrosis factor alpha (TNF-α)) (Ponticelli, 2015; Salvadori et al., 2015) and can induce viral replication in latently infected cells (Crough & Khanna, 2009). Therefore, CIT of viremic and aviremic patients was analyzed to characterize a potential role in primary CMV-infection of D+/R- high risk patients. Indeed, all patients with primary CMV-infection had received organs with significantly longer CIT (median = 1020 min; 720–1080 min) compared to patients without any correlate of infection (median = 335 min; 120–660 min; p = 0.0286; Figure 3.26, A). Warm ischemia time (WIT), known to drastically affect graft damage and survival (Tennankore et al., 2016), was comparable in this cohort of patients (Figure 3.26, B).

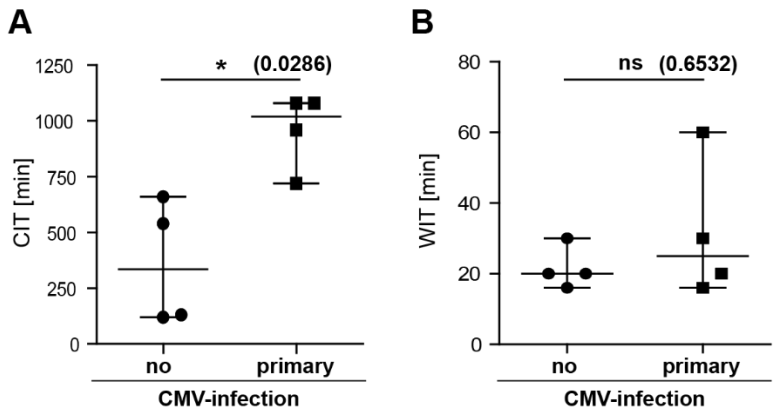

Figure 3.26: Comparison of CIT and WIT of viremic and aviremic patients.
(A) Cold ischemia time (CIT) and **(B)** warm ischemia time (WIT) was retrospectively analyzed in viremic and aviremic patients for a risk stratification regarding primary CMV-infection. Statistical analyses were performed using the Mann-Whitney *U* test: * = $p < 0.05$, ** = $p < 0.01$, *** = $p < 0.001$

Taken together, protracted CIT seemed to negatively influence the risk of primary CMV-infection in D+/R- high risk organ recipients and might serve as a prognostic marker.

4. Discussion

CMV is still a major cause for morbidity and mortality in immunocompromised individuals, such as patients after HSCT or SOT, and can lead to severe end-organ diseases. Furthermore, CMV-replication can cause indirect effects, such as secondary infections, immunosenescence, and acute or chronic graft rejection (M. Boeckh & Geballe, 2011; Crough & Khanna, 2009; Kotton, 2010, 2013; P. Ljungman et al., 2002; Moscarski et al., 2013; Moss & Rickinson, 2005). CMV-reactivations can be treated by prophylactic regiments, such as Ganciclovir/Valganciclovir prophylaxis, by preemptive therapy, or in the setting of HSCT by ACT (Brestrich et al., 2009; Coen & Richman, 2013; Einsele et al., 2002; Kotton, 2010, 2013; Moscarski et al., 2013; Moss & Rickinson, 2005; Riddell et al., 1992).

With this work, we provide a novel reversible HLA-C7-*Strep*Tamer, specific for the CMV IE-$1_{309-317}$ epitope and restricted to HLA-C*0702 with the potential to treat HSCT patients by ACT (Ameres et al., 2013). The analysis encompassed detailed characterization of frequency, functionality, and phenotype. Furthermore, the novel MHC-*Strep*Tamer was used for clinical monitoring and CMV-specific enrichment of HLA-C*0702/IE-1-restriced T cells.

Even though antiviral prophylaxis has reduced the incidence of CMV-reactivations, the optimal duration of prophylactic therapy is still intensively debated (Coen & Richman, 2013; Humar et al., 2010; KIDGO, 2009; Kotton, 2010, 2013; Kotton et al., 2013). In addition, risk factors predisposing for CMV-reactivation or primary CMV-infection are still not fully elucidated (Kotton, 2010; Shabir et al., 2013).

Therefore, a non-interventional clinical trial including 35 patients after kidney transplantation was conducted. Within this cohort, 8 D+/R- high-risk patients were enrolled and we were able to identify CIT as an important risk factor for primary CMV-infection giving the opportunity to segregate this previously homogenous patient group.

4.1 Characterization of HLA-C*0702/IE-1-restricted $CD8^+$ T cells

The treatment of CMV-reactivations in HSCT recipients by adoptive transfer of CMV-specific T cells was shown to be a feasible and safe therapeutic approach (Cobbold et al., 2005; Einsele et al., 2002; Leen et al., 2006; Micklethwaite et al., 2007; Peggs & Mackinnon, 2004; Riddell et al., 1992; Uhlin et al., 2012; Walter et al., 1995). This is although true for the transfer after purification of *ex vivo*-isolated and minimally manipulated CMV-specific T cells by reversible MHC-*Strep*Tamers (Schmitt et al., 2011). In this setting the identification of immunodominant

epitopes in combination with the generation of suitable reagents for the specific enrichment of these cells is an important task. The CMV-restricted peptide IE-$1_{309-317}$ with its restriction to HLA-C*0702 is therefore an interesting epitope for ACT (Ameres et al., 2013). Here we show, that HLA-C*0702/IE-1-specific T cells are a large, functional, and central memory rich population, which are an interesting target for ACT.

4.1.1 Large population size and high functionality of HLA-C*0702/IE-1-restricted T cell in healthy donors

The performed analysis for the characterization of the newly described HLA-C*0702/IE-$1_{309-317}$ population revealed high frequencies within healthy donors. This was also true after the exclusion of epitope-independently bound cells by MHC-multimer double staining. The large population size in combination with intensive cytokine secretion after stimulation supported the previously made observation that IE-$1_{309-317}$ is an immunodominant epitope and is thereby highly qualified for ACT (Ameres et al., 2013). Furthermore, several clinical trials have shown that the quality of T cells, especially in the setting of CMV, is associated with the ability of cells to secrete more than one cytokine upon stimulation (Boaz et al., 2002; Emu et al., 2005; Moscarski et al., 2013). The large frequencies of $CD8^+$ IFNγ-, TNFα-, IL-2-, and GM-SCF-secreting T cells detected after stimulation with the viral peptide IE-$1_{309-317}$ support the overall interesting characteristics of HLA-C*0702/IE-1-specific T cells. Furthermore, this viral epitope, if affixed to the CMV QuantiFERON assay, could enhance the predictions capacities of this commercial available test (Giulieri & Manuel, 2011).

In addition, the likelihood for the detection of this specific T cell population is high, as approximately 30% of the Caucasian population carry the HLA-C*0702 haplotype (Schmidt et al., 2009). Furthermore, the high linkage of HLA-B*0702 and HLA-C*0702 in the Caucasian population facilitates the monitoring of HLA-C*0702/IE-1-specific T cell populations, as the HLA-C loci are not always sequenced in the setting of transplantation whereas HLA-B is classically always analyzed (Schmidt et al., 2009).

It was reported that the efficiency of specific enrichment is increased in case of large population size (Odendahl et al., 2014). Therefore, the large detected frequencies in the cohort of healthy donors might facilitate the enrichment of a highly pure CMV-specific T cell population for the clinical application. In addition, approximately 1 to 5 $x10^5$ CMV-specific T cells per kg bodyweight are used for adoptive transfer of MHC-enriched T cells (Odendahl et

al., 2014; Schmitt et al., 2011). Hence, the large detected HLA-C*0702/IE-1-specific T cell populations might simplify the collection of sufficient *ex vivo* isolated virus-specific T cells for the usage in ACT. However, even low amounts of *ex vivo* isolated primary T cells can induce a protective pathogen-specific immunity. Specifically, single cell or low dose transfer of early differentiated T cells was able to induce a protective immunity in a murine *Listeria*-infection model and in refractory CMV-reactivations after HSCT (Stemberger et al., 2014; Stemberger et al., 2007). These data indicate that low-dose T cell transfer is successful if the optimal T cell population was selected. Therefore, the high T_{CM} content of HLA-C*0702/IE-1-specific T cells might enable a low-dose ACT.

4.1.2 KIR2DL2/3-associated binding of HLA-C-restricted *Strep*Tamers

NK cells express a wide variety of activating and inhibitory receptors. These receptors are essential for the regulation of NK cell activity. Inhibitory receptors interact with MHC I molecules in order to prevent the killing of cells expressing normal levels of MHC (Janeway, 2005). This is essential, as viruses, such as CMV, induce a downregulation of MHC I molecules in infected cells in order to evade the immune system (Ahn et al., 1996; Wiertz et al., 1996a; Wiertz et al., 1996b).

The expression of KIRs on $CD8^+$ T cells was reported by several groups. The precise mechanism of this phenomenon is still not yet fully elucidated (Arlettaz et al., 2004; Bjorkstrom et al., 2012; Byers et al., 2003; Huard & Karlsson, 2000; McMahon & Raulet, 2001; Mingari et al., 1998; Parham, 2005). The expression of an inhibitory KIR, such as KIR2DL2/3, is associated with the inhibition of different T cell functions with the aim to induce T-cell mediated tolerance to self-antigens (Huard & Karlsson, 2000). Nevertheless, the KIR-associated inhibition is abolished in case of high antigen burden (Huard & Karlsson, 2000). Furthermore, it was shown that activation-induced cell death is reduced in KIR-expressing T cells due to reduced activation by TCR signaling, leading to an accumulation of KIR-expression in late differentiated $CD8^+$ T_{EM} or T_{EMRA} cells (Arlettaz et al., 2004; Byers et al., 2003). Analysis of the expression pattern of KIRs on $CD8^+$ T cells revealed that there is classically one dominant activating or inhibitory KIR expressed on $CD8^+$ T cells that is linked to a similar expression on NK cells (Bjorkstrom et al., 2012). Similarly, the distribution of KIR-expressing T cells in the different healthy donors used in this work was also mainly found in late differentiated $CD8^+$ T cells, such as T_{EMRA} cells. Furthermore, the epitope-independent binding of HLA-C*0702-

multimers with KIR2DL2/3 might be associated with the reduced immunoevasion reported by Ameres et al. (Ameres et al., 2013).

Even though the expression of KIR on $CD8^+$ T cells is well known, the epitope-independent interaction of KIR2DL2/3 with the new synthesized HLA-C-*Strep*Tamer was unexpected and complicated the analysis. Several HLA-A, -B and -C molecules are ligands for inhibitory KIRs. These HLA molecules were, according to their KIR ligand, grouped in C1 (for example HLA-C*1, -C*3, -C*7, and -C*8), C2 (for example HLA-C*2, -C*4, -C*5, and –C*6), and Bw4 (for example HLA-A24 and HLA-B27) (Parham, 2005). An isoleucine residue at position 80 is one of the strongest interaction partners for the Bw4 ligands, whereas C1 ligand interaction is based on an Asparagine residue on position 80 (Cella et al., 1994; Parham, 2005). These different amino acid anchors could lead to a lower MHC-KIR interaction, explaining that in previously performed stainings using HLA-A24- or -B27-restricted MHC-multimers, refolded with CMV-specific peptides, no epitope-independent interaction was detected so far. In conclusion, the low number of available HLA-C-restricted multimers might explain that the epitope-independent interaction of KIRs and HLA-C-restricted multimers was not reported earlier. Nevertheless, the analysis of HLA-KIR interaction is essential as this could lead to a misinterpretation of population size or in the worst case scenario, the generated MHC-multimer is not specific at all. Therefore, the interaction of HLA-C multimers with KIRs for other restrictions than HLA-C*0702 needs to be analyzed.

4.1.3 Specific purification of HLA-C*0702/IE-1-restricted $CD8^+$ T cells

The utility of MHC-*Strep*Tamers for the enrichment of pathogen-specific $CD8^+$ T cells was shown by Knabel et al. (Knabel et al., 2002). The advantage of *ex vivo* MHC-*Strep*Tamer enrichment is the generation of minimally manipulated cells, thereby avoiding complex regulatory safety concerns. In addition, the adoptive transfer of MHC-*Strep*Tamer-enriched CMV-specific $CD8^+$ T cells into CMV-reactivating HSCT recipients performed by Schmitt et al. revealed good tolerance of the cells with minimal side-effects and the transferred cells caused a decrease in viral load (Schmitt et al., 2011). The used d-Biotin assay in this work verified the complete reversibility of the recently generated HLA-C*0702/IE-1 *Strep*Tamer. Interestingly, this was also true for KIR-associated epitope-independent interaction of the MHC-*Strep*Tamer. A potential explanation might be the lower binding strength of C1 group KIR-ligands caused by the Asparagine residue on position 80 (Parham, 2005). On the contrary, it is uncertain, if

MHC-*Strep*Tamers for HLA-types, such as HLA-C*2, -C*4, -C*5, and –C*6, also would reveal complete reversibility. Due to the reason that these HLA-types are members of the C2 group KIR-ligands which carry a Lysine at position 80 causing a stronger receptor-ligand interaction (Parham, 2005). Therefore, newly generated HLA-C7-*Strep*Tamers with HLA-restrictions to HLA-C*2, -C*4, -C*5, and –C*6 should be accurately investigated for reversibility in order to circumvent secondary enrichment problems.

The complete reversibility of the generated HLA-C*0702/IE-1 and MAGE *Strep*Tamers should enable in principal a serial enrichment strategy. The usage of both MHC-*Strep*Tamers was favored as the clinical grade generation of the reagents is already approved and was used in earlier clinical studies (Odendahl et al., 2014; Schmitt et al., 2011). Even though the primary enrichment step using the HLA-C*0702/IE-1 *Strep*Tamer was successful, the depletion of KIR-expressing cells with the HLA-C*0702/MAGE *Strep*Tamer was insufficient. The low staining intensity of KIR-expressing cells achieved with the MAGE *Strep*Tamer could be an explanation for this phenomenon but careful titration of the reagent did not influence the staining intensity. In line with that, earlier in-house experiments revealed approximately a minimum of one log step difference enabling a sufficient enrichment, respectively a depletion of cells (data not shown). On the other hand, the lower binding affinity by C1 group KIR-ligands as previously described might be responsible for the insufficient depletion using MHC-*Strep*Tamers (Parham, 2005). KIR interactions with C2 group KIR-ligands have not been shown so far, but theoretically the respective HLA-types with the expected higher binding strength might become suitable for such depletion steps.

In contrast to the first enrichment protocol, the primary depletion with an antibody specific for the KIR2DL2/3 epitope and a secondary positive selection of IE-1-specific T cells was successful. On drawback of this procedure is the missing clinical grade availability of KIR2DL2/3 antibodies generated by immortalized Hybridoma cell lines. The potential hazardous contaminants of these cells would require excessive and expensive validation and purification of the reagents. However, the generation of KIR2DL2/3-specific Fab-*Strep*Tamers would solve this problem. As shown by Stemberger et al. (Stemberger et al., 2012) Fab-*Strep*Tamers are easily generated according to GMP-compatible protocols and can be used in clinical settings. Furthermore, a KIR2DL2/3-Fab-*Strep*Tamer might also improve the purity of the final product by using Microbeads in combination with the large StrepMan Magnet avoiding Nanobead/column-interactions. In consequence, the final product might then comprise only

a minimal amount of cells that are enriched by unspecific interactions. The detected contaminates, seen in the proof of concept enrichment, consisted mainly of $CD4^+$ T cells, but were comparable to previously clinically applied cell products (Odendahl et al., 2014). In case of an envisioned usage of HLA-C*0702/IE-1-specific T cells for ACT, a generation of a KIR2DL2/3-specific Fab-*Strep*Tamer should be started in order to ensure an enrichment process based on reversible reagents.

4.1.4 Phenotypic characteristics and protective capacities of HLA-C*0702/IE-1-specific T cells

In recent years, it was suggested by several publications that early differentiated pathogen-specific T cells, such as T_{SCM} or T_{CM} cells, might be superior for ACT than transfer of late differentiated T_{EM} or T_{EMRA} cells. The advantage of these early differentiated T cells are the longevity, the differentiation capacities, and the high polyfunctional abilities (Appay et al., 2008; Buchholz et al., 2013; Gattinoni et al., 2011; Gattinoni & Restifo, 2013; Mahnke et al., 2013). In addition, the transfer of selected T cell populations, such as T_{naive}-depleted grafts, was associated with a reduction in GvHD in comparison to donor lymphocyte infusions (Bleakley et al., 2015).

In recent studies, especially T_{SCM} cells were promoted and thought to have increased anti-tumor effect but were also shown in the setting of CMV (Gattinoni et al., 2011; Lugli et al., 2013a; Sallusto & Lanzavecchia, 2011). Notably, even after excessive screening of healthy donors, no HLA-C*0702/IE-1-specific $CD8^+$ T_{SCM} cells were detectable. However, since these very early differentiated cells are only available in very low numbers in the peripheral blood, we cannot exclude that our used analytic methods were sensitive enough with the available cell numbers.

T_{CM} cells are also early differentiated and are able to establish a long lasting protective immunity in a non-human primate model (Berger et al., 2008). In addition, in several clinical trials using chimeric antigen receptor-transduced T_{CM} cells, these transferred cells were associated with a beneficial anti-tumor effect (Sommermeyer et al., 2016; X. Wang et al., 2016). In addition to anti-tumor effects, T_{CM} cells also comprise CMV-specific T cells in substantial numbers and are able to establish a functional pathogen-specific immunity. In a serial transfer mouse model using Listeria-specific T_{CM} cells, Graef et al. proved that these cells have a long-term survival and protective capacities in case of a lethal bacterial infection (Graef

et al., 2014). This underlines the positive features of T_{CM} cells and therefore, the high proportion of HLA-C*0702/IE-1-specific $CD8^+$ T cells within the central memory compartment makes these cells an attractive target for ACT. Even though the proportion of HLA-C*0702/IE-1-specific $CD8^+$ T cells was higher than for HLA-B*0702/pp65-specific T cells, this does not imply a superior role of the IE-1-specific T cells per se in case of viral control. But at least this enables already the co-transfer of these cells in a recently started clinical trial, called ”Prophylactic Central Memory Transfer” (PACT; EudraCT-No. 2015-001522-41). For the first time, in this clinical trial the HSCT recipient receives 30 days after primary stem cell transplantation a prophylactic application of low-dose, but purely enriched central memory T cells in order to prevent or attenuate potential pathogen-induced malignancies. The transferred product comprises the complete $CD4^+$ and $CD8^+$ central memory T cell compartment including all different pathogen specificities. Therefore, due to the high central memory proportion of HLA-C*0702/IE-1-specific T cells with the transferred T_{CM} compartment, this study will allow a detailed characterization of HLA-C*0702/IE-1-specific T cells *in vivo* and an analysis of their protective capacities in these highly vulnerable HCST recipients.

Even though the phenotypical characteristics of the HLA-C*0702/IE-1-specific T cell are promising, the protective capacities of CMV-restricted IE-1-specific $CD8^+$ T cells are still unclear. Immunmonitoring analysis of a kidney transplanted patient with CMV-reactivation indicated that both specificities (HLA-C*0702/IE-1 and HLA-B*0702/pp65) expanded strongly and were associated with further protection. As both specificities reached similar sizes and functional profiles, a prediction of the protective capacities of HLA-C*0702/IE-1-specific T cells was not possible. So far mainly pp65-specific T cells were used to treat severe CMV-replications in HSCT recipients or a combination of pp65- and IE-1-specific T cells was used (Cobbold et al., 2005; Einsele et al., 2002; Leen et al., 2006; Micklethwaite et al., 2007; Peggs & Mackinnon, 2004; Riddell et al., 1992; Schmitt et al., 2011; Uhlin et al., 2012; Walter et al., 1995). Even though the transfer of TCR-selected IE-1-specific T cells in mice was associated with a highly functional and long-lasting CMV-specific immunity (Pahl-Seibert et al., 2005), the transfer of IE-1-specific T cells might be more potent in a prophylactic setting. As IE-1 is one of the first proteins expressed by CMV (Crough & Khanna, 2009; Moscarski et al., 2013), transferred IE-1-specific T cells might be able to inhibit lytic reactivations within the tissue in the first place, thereby preventing serious uncontrolled CMV-reactivation, whereas pp65-

specific T cells might be more helpful in case of an acute viral replication when the tegument protein pp65 is already widely expressed. Therefore, the generated HLA-C*0702/IE-1 *Strep*Tamers might be useful for the isolation of IE-1-specific T cells and the prophylactic administration of these CMV-specific T cells, similar, to the different virus- and tumor-specificities used in the prophylactic administration in the ongoing clinical trial "T-control". So far, the epitopes used for this trial are mainly focused on HLA-A*0201, but in a potential extension of this trial, HLA-C*0702/IE-1-specific T cells might be an interesting target.

In addition to the transfer of the IE-1-specific T cells, further characterization of this T cell population might already give new insights into their potential protective capacities. One highly interesting new method is the "flow cytometry-based TCR-ligand K_{off}-rate assay" (Nauerth et al., 2016). This method would enable the measurement of the dissociation time of HLA-C*0702/IE-1-specific T cells, which is linked to the avidity of the TCR-ligand interaction. In previous studies, a high avidity was associated with increased pathogen or tumor protection (Derby et al., 2001; Nauerth et al., 2013; Zeh et al., 1999). Therefore, the avidity of HLA-C*0702/IE-1-specific T cells might correlate with viral control. In order to analyze the K_{off}-rate, only a minimal manipulation of the vector sequence is necessary, enabling the fusion of the Alexa488 maleimide fluorophore to the MHC-*Strep*Tamer and is therefore currently under investigation.

Taken together, HLA-C*0702/IE-1-specific T cells are a large and polyfunctional CMV-specific T cell population. The high proportion among T_{CM} cells in combination with the strong proliferation capacities upon CMV-reactivation identifies HLA-C*0702/IE-1-specific T cells as an interesting target for ACT. Furthermore, the high allelic frequency in the Caucasian population (30%) and the immuno dominance of the IE-$1_{309-317}$ epitope facilitates the usage in ACT (Ameres et al., 2013; Schmidt et al., 2009). In addition, the reversibility in combination with MHC- and Fab-*Strep*Tamers enables potentially the clinical grade isolation of these cells in order to transfer minimally manipulated CMV-specific T cells, most likely in a prophylactic setting.

4.2 Characterization of CMV-specific T cell responses after kidney transplantation

In addition to the generation of a reversible HLA-C*0702/IE-1-specific *Strep*Tamer, a non-interventional clinical trial encompassing patients after kidney transplantation was

conducted. The aim of this study was the characterization of CMV-specific immune responses in order to establish a risk-stratification for the preemptive antiviral treatment of these patients. So far, only the serostatus (CMV IgG) of the patients was used in order to determine future clinical interventions (KIDGO, 2009; Kotton, 2010). Based on this CMV-specific serostatus, three different risk groups were defined: low risk patients (D-/R-), standard risk patients (D+/R+; D-/R+), and high risk patients (D+/R-) (Kotton, 2013; Kotton et al., 2013).

4.2.1 Study design

Only patients at risk (standard and high risk) for CMV-reactivation were included. Blood collections were performed pre Tx, on POD 28, POD 90, POD180 and in case of viral reactivation. This study design was in line with several other non-interventional trials also analyzing predisposing risk factors for viral replication (Abate et al., 2010; Bestard et al., 2013; Calarota et al., 2012; Eid et al., 2010). All patients received a Valganciclovir prophylaxis for 90 days and viral replications under prophylaxis were expected to be most unlikely. Therefore, POD 90 was the most interesting time-point in order to detect differences concerning the immune system in patients with and without viral replication. This caused the exclusion of 8 from the previously 35 included patients, as those patients missed the blood collection on POD 90. Furthermore, one patient had in addition a HCV infection. This patient was also excluded from further analysis due to laboratory safety concerns.

4.2.2 Successful clinical management prevented serious CMV-reactivations in R+ standard risk patients

In the setting of kidney transplantation approximately 20% of standard risk patients suffer from CMV-reactivations (Kotton, 2010). Interestingly, only in 3 of 18 standard risk patients a CMV-viremia was detected and in all cases the measured viral load was only a minor borderline reactivation with less than 500 copies/ml. The occurrence of only low level reactivations might be due to the close screening and early intervention routine performed by the department of nephrology at the Klinikum rechts der Isar. All patients were screened every two weeks by CMV-specific PCR during prophylactic treatment and thereafter every four weeks or in case of a clinical visit. Recommendations suggest only viral screenings for preemptively treated patients or in case of clinical symptoms (KIDGO, 2009). The early detection of CMV-reactivation of low level viremia was treated by the clinicians with an

adaption of the immunosuppressive medication, mainly by halving the Tacrolimus dosage. Therefore, the early detection and intervention might be associated with a fast viral clearance avoiding high viral titers with serious side-effects, such as tissue-invasive CMV-disease. On the other side, the borderline reactivations might be associated with a more widespread persistence of the virus causing regular sub-clinical CMV-reactivations (Crough & Khanna, 2009). All other patients might also have experienced those recurrences from latency, but were simply not screened on those specific days. Therefore, viremic standard risk patients might also have solved viral titers by the patient's CMV-specific immune response without clinical interventions. In consequence, the rare and only minor CMV-reactivations in this patient cohort might justify a preemptive approach as no significant difference between prophylactic and preemptive treatment for R+ standard risk patients was observed. This might limit the drug-induced side-effects, late onset CMV, and potential resistance induction (Coen & Richman, 2013; Gohring et al., 2015; Jacobsen & Sifontis, 2010; KIDGO, 2009; Mengelle et al., 2015; Schoeppler et al., 2013).

4.2.3 Risk stratification for future CMV-reactivations

All patients were screened with large flow cytometric panels in order to identify lymphocyte subsets associated with protection. In case of CMV-reactivation the proliferative capacities and abilities to differentiate into effector T cell subsets might be essential as most standard risk patients and all high risk patients with ascertained viral load received ATG. Previous studies linked CD161-expressing $CD8^+$ T cells with increased protection and drug-resistance (Turtle et al., 2009). However, these cells were identified in the meanwhile as MAIT cells, responsible for fungal defense, but other subsets, such as T_{SCM} or T_{CM}, share respective attributes (Appay et al., 2008; Gattinoni et al., 2011; Mahnke et al., 2013). Therefore, the detected reduced T_{CM} proportions in reactivating patients might be an interesting observations for the prediction of upcoming CMV-reactivations.

In line with that, the proliferation of CMV-specific T cells in case of viral replication may be a relevant tool to determine future CMV-associated complications. In a clinical trial, transferring CMV-specific T cell from the stem cell donor in CMV-reactivating HSCT recipients, patients with proliferating CMV-specific T cells controlled viral replication, whereas, one patient with stagnant T cell numbers suffered from ongoing CMV-reactivations (Neuenhahn et al., 2016, unpublished results). In line with that, it was shown that patients with low numbers of CD28-

expressing CMV-specific $CD8^+$ T cells and missing proliferation of these cells were more likely to experience CMV viremia after kidney transplantation (Zieliński et al., 2016). This underlines that the proliferation and the overall competence to proliferate is essential, as CD28 is mainly expressed on T_{CM} and T_{EM} cells (Appay et al., 2008). Interestingly, most viremic D+/R- high risk patients developed eventually a CMV-specific T cell response with high proliferation rates. Notably, expanding T cells were uniformly associated with protection against further CMV-replications. However, with the small number of patients tested, this hypothesis needs further validation in larger cohorts. Importantly, this would also affect the current intention to use the CMV QuantiFERON assay. Previous studies correlated a positive assay result (> 0.1-0.2 I.U./ ml blood) with protection from CMV-reactivation (Fleming et al., 2010; D. Kumar et al., 2009; S. Walker et al., 2007). Therefore, if the proliferative capacity of virus-specific T cells were crucial, it might be essential to measure the CMV-specific response on two different time-points in order to predict the protective capacities of the T cells.

The control of CMV viral load in D+/R- patient was associated with the generation of T cells directed against the viral epitope pp65. This is in line with previous clinical trials, transferring pp65-specific T cells in reactivating HSCT recipients causing rapid viral control (Cobbold et al., 2005; Einsele et al., 2002; Leen et al., 2006; Micklethwaite et al., 2007; Peggs & Mackinnon, 2004; Riddell et al., 1992; Schmitt et al., 2011; Uhlin et al., 2012; Walter et al., 1995). On the other side, IE-1-specific T cells were also detected very early after viral replication (patient #01) with ongoing increase in viral titers or were detected after viral clearance (patient #06). Therefore, the lack of further viral replications could correlate with the generation of IE-1-specific T cells preventing tissue-specific CMV-reactivations. These data also support the hypothesis, that pp65-specific T cells are beneficial in currently proceeding viral replications, whereas IE-1-spcific T cells might be more suitable in prophylactic settings. Interestingly, two patients established a memory inflation of IE-1-specific T cells. As previously described, these inflating cells had indeed a terminal differentiated phenotype and produced large amount of effector cytokines, like IFNγ and TNFα (data not shown). Furthermore, the generation of an inflationary memory is associated with constant antigen exposure. As memory inflation seems to be dependent on constant antigen exposure (Hertoghs et al., 2010; Kim et al., 2015; Snyder et al., 2008), this could again indicate, that IE-1-spcific T cells control subclinical tissue-specific viral replications and are beneficial in prophylactic settings. Again, the respective role of pp65-

and IE-1 specific T cells in the control of CMV in kidney transplant recipients needs to be addressed in extended patient cohorts.

Concerning all other lymphocyte subpopulations, only slight differences in the analyzed standard risk patients were detected. The low reactivation rates in this group and the potential irrelevant viral titers limited the validity of the generated results. Therefore, the identification of potential prognostic candidates requires larger clinical trials. This has recently been started by collaborations with Hannover (Christine Falk) and Heidelberg (Thomas Giese). Each site collected samples of more than 100 kidney transplanted patients. Recently a harmonization of the flow cytometric antibody panels was achieved and therefore the samples will be soon evaluated retrospectively, with special interest in the proportion and occurrence of T_{CM} cells.

4.2.4 Prolonged CIT is associated with primary CMV-infection of D+/R-high risk patients

Within the small cohort of 8 D+/R- high risk patients, four patients with CIT of less than 12 hours had no detectable viral titers. In addition, none of these patients had any preformed CMV-specific memory T cells which were recently associated with the prevention of serious viral replications after transplantation (Lucia et al., 2014). On the contrary, none of these patients established any CMV-specific T cells nor generated a CMV-specific antibody response within up to three years of follow-up. Consequently, no primary CMV-infection was established implicating that CIT of less than 12 hours significantly reduce the incidence of viral transmission from latently CMV-infected donor kidneys. So far, the underlying molecular mechanisms preventing viral transmission are still unclear. Hypothetically, this phenomenon might be explained by the fact that short CIT induces little reperfusion injury of the donor organs and in consequence low levels of inflammatory cytokines are missing, which have been described to trigger CMV-reactivation from latency (Crough & Khanna, 2009; Salvadori et al., 2015). Therefore, CMV remains in organs with short CIT in a latent state and can be sufficiently suppressed by antiviral prophylaxis. Eventually, latently infected donor cells such as monocytes (Crough & Khanna, 2009), are substituted by uninfected recipient-derived monocytes and therefore, primary CMV-infection of the recipient will be permanently prevented (Figure 4.1, A). Consequently, the prophylactic regiment might be essential for the prevention of viral transmission. It is still elusive, if D+/R- high risk patients with short CIT need 90 days of antiviral prophylaxis in order to prevent primary CMV-infection. Monocytes have a

lifespan from development to differentiation of approximately 3 - 14 days (Reuter & Lang, 2009; Whitelaw & Bell, 1966) and therefore, it is justified to speculate about shorter prophylactic regiments still preventing viral transmission in this newly identified patient subgroup. A clinical trial treating patients with reduced risk for primary CMV-infection with different durations of prophylactic therapy might therefore be highly interesting.

On the contrary, D+/R- high risk patients with extended CIT (> 12 hours) suffered from primary CMV-infection with mostly serious clinical complications. Potentially, protracted CIT is primarily responsible for induction of viral replication due to high levels of induced inflammation (Salvadori et al., 2015). It might also be possible that ATG, as all patient received an induction therapy, in combination with long CIT increases the risk for primary CMV-infection. It needs to be determined, if donor-derived CMV-specific tissue-resident memory T cells (T_{RM}) (Klenerman & Oxenius, 2016; Park & Kupper, 2015) antagonizing CMV-replications in the tissue, were depleted by ATG or if ATG causes alternatively or synergistically an enduring unspecific inflammation leading to the viral transmission and infection of recipient-derived monocytes causing late onset CMV (Murray & Subramaniam, 2004) (Figure 4.1, B). One option for the investigation of ATG effects on T_{RM} cells, the hypothesis of the replacement of infected monocytes, or the recurrence from latency due to extended CIT are analysis of biopsies. Usually, from each kidney graft a biopsy is taken shortly before transplantation. These biopsies might potentially enable the detection of increased viral titers in donor organs with protracted CIT and thereby indicate potential molecular effects induced by CIT. In addition, biopsy sections might enable the determination of CMV-specific T_{RM} cells in the kidney and the depleting effects induced by ATG.

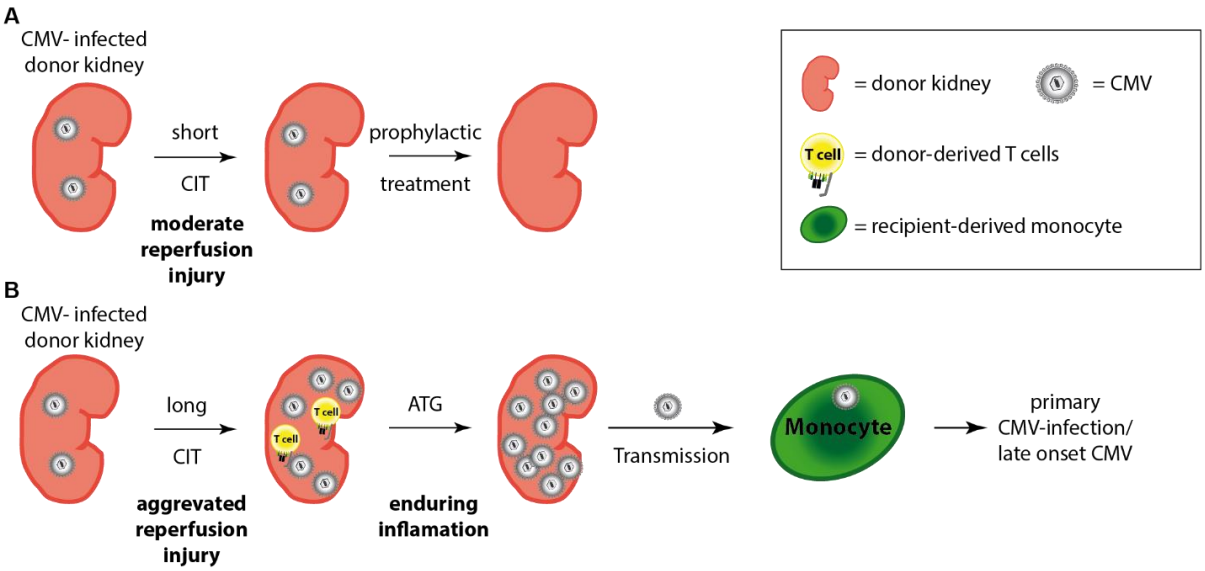

Figure 4.1: Influence of the CIT on the donor kidney leading to primary CMV-infection.
Depicted is a hypothetical explanation of the effects on the CMV-infected donor kidney induced by the CIT.
(A) A short CIT (< 12 hours) induces only moderate reperfusion injury, leading to low level inflammation without differentiation of CMV-infected donor cells, such as monocytes, thereby prohibiting viral replication. Under continuous suppression by prophylactic treatment infected donor-derived monocytes might be replaced by uninfected recipient cells leading to virus free organs.
(B) Long CIT (> 12 hours) cause serious reperfusion injury leading to monocyte differentiation and to CMV-reactivation. ATG treatment could lead to the depletion of donor-derived T_{RM} cells and moreover causes an enduring inflammation. High viral titers lead to the infection of recipient-derived monocytes and thereby to primary CMV-infection. After discontinuation of antiviral prophylaxis CMV is able to replicate and induces late-onset CMV.

Unlike in the setting of standard risk patients, the clinical management of high risk patients was less reliable, as two patients suffered from CMV-induced disease (pneumonia/ hepatitis) and a third patient died. Therefore, D+/R- high risk patients with increased risk for CMV-infection might benefit of an extended antiviral prophylaxis of 200 days. High risk kidney-transplanted recipients under 200 days Valganciclovir treatment had significantly less incidences of CMV-disease and CMV viremia in comparison to patients receiving 90 days of prophylaxis (Humar et al., 2010). On the contrary, a preemptive approach with continuous screening by PCR after discontinuation of 90 days prophylactic treatment might be superior. This approach would enable a clinically supervised and timely treated viral replication, triggering a protective CMV-specific immunity and thereby reduce fatal CMV complications.
In summary, the length of CIT might enable novel therapeutic approaches and clinical classifications of D+/R- high risk patients. These could alter the current prophylactic and preemptive regiments, even though these data still need further validation in larger D+/R- high risk patient cohorts.

5. Summary

CMV is a ubiquitous opportunistic pathogen that persists in infected individuals due to cellular latency. Primary CMV-infection of immunocompetent individuals, usually acquired at young age, proceeds mostly subclinical. However, primary CMV-infection or CMV-reactivation in immunocompromised patients, e.g. after SOT or allogeneic HSCT, can lead to severe clinical manifestations and remains a major source of morbidity and mortality. Complications comprise tissue-invasive end-organ diseases, acute or chronic graft rejection, immunosenescence, and secondary infections. Main protagonists in immunologic surveillance and viral control of this pathogen are CMV-specific T cells. Therefore, HSCT recipients are already treated by adoptive transfer of CMV-specific T cells, but the therapeutic efficiency might be counteracted by the expression of viral immunoevasins interfering with the host immunity. Interestingly, the HLA-C*0702-molecule is less prone to CMV-induced downregulation, potentially to retain NK cell-mediated cytotoxicity. In combination with the immunodominant epitope IE-$1_{309-317}$, HLA-C*0702/IE-1-restricted T cells are an attractive target for ACT.

Here, in order to enable the enrichment of *ex vivo* isolated HLA-C*0702/IE-1-specific T cells for clinical application, a reversible MHC-*Strep*Tamer was generated and used for the detailed characterization of this recently identified CMV-specific T cell population.

Analyses of 20 healthy blood donors revealed large MHC-multimer$^+$ T cell populations (median = 11.35%) and intense IFNγ-production after stimulation (IFNγ$^+$, median = 5.02%). Interestingly, flow cytometric analyses of KIR-expressing CD8$^+$ T cells showed an epitope-independent interaction of KIR2DL2/3 with HLA-C-*Strep*Tamers. A combinatorial staining with a tumor epitope-specific HLA-C-restricted *Strep*Tamer enabled the determination of KIR-adjusted CMV-specific T cells. Consequently, reduced frequencies (median = 6.86%) of HLA-C*0702/IE-1^{MAGE-} multimer$^+$ T cells were detected after reanalyzing the 20 healthy donors, correlating strongly ($r^2 = 0.96$) with IFNγ-production. Furthermore, substantial numbers of T_{CM} cells were detected within the KIR-adjusted HLA-C*0702/IE-1^{MAGE-}-specific T cell population, suggesting strong expansion capacity after ACT. In addition, a specific enrichment of 88.3% HLA-C*0702/IE-1-specific T cells and a yield of 38.8% was reached after circumventing epitope-independent interactions by depletion of KIR2DL2/3-expressing T cells.

In contrast to ACT after allogeneic HSCT, kidney transplant recipients are mainly treated by Ganciclovir/ Valganciclovir prophylaxis in order to prevent CMV recurrence from latency. According to the CMV-IgG-serostatus of donor and recipient, these patients are divided into different risk groups. Notably, D+/R- constellations have the highest risk for CMV-replication due to a missing CMV-specific immunity. However, it is still unknown which factors predispose for CMV-reactivation or primary CMV-infection.

Therefore, an observational trial including 26 standard risk (R+) and high risk (R-) kidney transplant recipients was conducted. Within the 18 R+ patients, three patients had detectable low level viremia. Intensive flow cytometric analyses revealed a potential trend to reduced T_{CM} frequencies prior to CMV-replication. In addition, over a period of 784 days (156-1155) eight D+/R- high risk patients were monitored carefully for CMV-viremia. Main focus of monitoring was the detection of CMV-specific T cells by ICS and CMV-serology measured by ELISA. Interestingly, CMV-viremia and thereafter seroconversion was detected only in four of eight D+/R- patients. Viremia mostly caused serious clinical manifestation underlining the increased risk of the recipient in a D+/R- constellation. Notably, viral control correlated with the expansion of functional CMV-specific T cells and protected from secondary CMV-reactivations. On the contrary, all other patients had no detectable viral load after discontinuation of prophylactic therapy and did not establish any CMV-specific immunological response over three years of follow-up. Importantly, primary CMV-infection significantly correlated with CIT as viremic recipients received donor-organs with extended CIT (median = 1020 min) whereas aviremic patients had a median CIT of 335 min ($p = 0.0286$).

In summary, we report with this work the generation of a novel HLA-C*0702/IE-1-specific reversible MHC-*Strep*Tamer suitable for *ex vivo* isolation of KIR-adjusted CMV-specific T cells. The high T_{CM} content qualifies these cells potentially for the prophylactic adoptive T cell therapy after allogeneic HSCT. Furthermore, we were able to identify CIT as an important risk factor for primary CMV-infection, which might become important for future SOT patient care.

6. Register

6.1 Register of figures

6.2 Register of tables

6.3 References

Abate, D., Saldan, A., Fiscon, M., Cofano, S., Paciolla, A., Furian, L., Ekser, B., Biasolo, M. A., Cusinato, R., Mengoli, C., Bonfante, L., Rossi, B., Rigotti, P., Sgarabotto, D., Barzon, L., & Palu, G. (2010). Evaluation of cytomegalovirus (CMV)-specific T cell immune reconstitution revealed that baseline antiviral immunity, prophylaxis, or preemptive therapy but not antithymocyte globulin treatment contribute to CMV-specific T cell reconstitution in kidney transplant recipients. *J Infect Dis, 202*(4), 585-594. doi:10.1086/654931

Abi-Rached, L., Jobin, M. J., Kulkarni, S., McWhinnie, A., Dalva, K., Gragert, L., Babrzadeh, F., Gharizadeh, B., Luo, M., Plummer, F. A., Kimani, J., Carrington, M., Middleton, D., Rajalingam, R., Beksac, M., Marsh, S. G., Maiers, M., Guethlein, L. A., Tavoularis, S., Little, A. M., Green, R. E., Norman, P. J., & Parham, P. (2011). The shaping of modern human immune systems by multiregional admixture with archaic humans. *Science, 334*(6052), 89-94. doi:10.1126/science.1209202

Adams, E. J., Thomson, G., & Parham, P. (1999). Evidence for an HLA-C-like locus in the orangutan Pongo pygmaeus. *Immunogenetics, 49*(10), 865-871.

Ahn, K., Angulo, A., Ghazal, P., Peterson, P. A., Yang, Y., & Fruh, K. (1996). Human cytomegalovirus inhibits antigen presentation by a sequential multistep process. *Proc Natl Acad Sci U S A, 93*(20), 10990-10995.

Akira, S., Uematsu, S., & Takeuchi, O. (2006). Pathogen recognition and innate immunity. *Cell, 124*(4), 783-801. doi:10.1016/j.cell.2006.02.015

Alford, C. A., & Pass, R. F. (1981). Epidemiology of chronic congenital and perinatal infections of man. *Clin Perinatol, 8*(3), 397-414.

Altman, J. D., Moss, P. A., Goulder, P. J., Barouch, D. H., McHeyzer-Williams, M. G., Bell, J. I., McMichael, A. J., & Davis, M. M. (1996). Phenotypic analysis of antigen-specific T lymphocytes. *Science, 274*(5284), 94-96.

Ameres, S., Besold, K., Plachter, B., & Moosmann, A. (2014). CD8 T cell-evasive functions of human cytomegalovirus display pervasive MHC allele specificity, complementarity, and cooperativity. *J Immunol, 192*(12), 5894-5905. doi:10.4049/jimmunol.1302281

Ameres, S., Mautner, J., Schlott, F., Neuenhahn, M., Busch, D. H., Plachter, B., & Moosmann, A. (2013). Presentation of an immunodominant immediate-early CD8+ T cell epitope resists human cytomegalovirus immunoevasion. *PLoS Pathog, 9*(5), e1003383. doi:10.1371/journal.ppat.1003383

Andrews, P. A., Emery, V. C., & Newstead, C. (2011). Summary of the British Transplantation Society Guidelines for the Prevention and Management of CMV Disease After Solid Organ Transplantation. *Transplantation, 92*(11), 1181-1187. doi:10.1097/TP.0b013e318235c7fc

Appay, V., Dunbar, P. R., Callan, M., Klenerman, P., Gillespie, G. M., Papagno, L., Ogg, G. S., King, A., Lechner, F., Spina, C. A., Little, S., Havlir, D. V., Richman, D. D., Gruener, N., Pape, G., Waters, A., Easterbrook, P., Salio, M., Cerundolo, V., McMichael, A. J., & Rowland-Jones, S. L. (2002a). Memory CD8+ T cells vary in differentiation phenotype in different persistent virus infections. *Nat Med, 8*(4), 379-385. doi:10.1038/nm0402-379

Appay, V., van Lier, R. A., Sallusto, F., & Roederer, M. (2008). Phenotype and function of human T lymphocyte subsets: consensus and issues. *Cytometry A, 73*(11), 975-983. doi:10.1002/cyto.a.20643

Appay, V., Zaunders, J. J., Papagno, L., Sutton, J., Jaramillo, A., Waters, A., Easterbrook, P., Grey, P., Smith, D., McMichael, A. J., Cooper, D. A., Rowland-Jones, S. L., & Kelleher, A. D. (2002b). Characterization of CD4(+) CTLs ex vivo. *J Immunol, 168*(11), 5954-5958.

Ariza-Heredia, E. J., Nesher, L., & Chemaly, R. F. (2014). Cytomegalovirus diseases after hematopoietic stem cell transplantation: A mini-review. *Cancer Letters, 342*(1), 1-8. doi:http://dx.doi.org/10.1016/j.canlet.2013.09.004

Arlettaz, L., Degermann, S., De Rham, C., Roosnek, E., & Huard, B. (2004). Expression of inhibitory KIR is confined to CD8+ effector T cells and limits their proliferative capacity. *Eur J Immunol, 34*(12), 3413-3422. doi:10.1002/eji.200324756

Arthurs, S. K., Eid, A. J., Pedersen, R. A., Kremers, W. K., Cosio, F. G., Patel, R., & Razonable, R. R. (2008). Delayed-onset primary cytomegalovirus disease and the risk of allograft failure and mortality after kidney transplantation. *Clin Infect Dis, 46*(6), 840-846. doi:10.1086/528718

Autissier, P., Soulas, C., Burdo, T. H., & Williams, K. C. (2010). Evaluation of a 12-color flow cytometry panel to study lymphocyte, monocyte, and dendritic cell subsets in humans. *Cytometry A, 77*(5), 410-419. doi:10.1002/cyto.a.20859

Backovic, M., & Jardetzky, T. S. (2009). Class III viral membrane fusion proteins. *Curr Opin Struct Biol, 19*(2), 189-196. doi:10.1016/j.sbi.2009.02.012

Barron, M. A., Gao, D., Springer, K. L., Patterson, J. A., Brunvand, M. W., McSweeney, P. A., Zeng, C., Baron, A. E., & Weinberg, A. (2009). Relationship of reconstituted adaptive and innate cytomegalovirus (CMV)-specific immune responses with CMV viremia in hematopoietic stem cell transplant recipients. *Clin Infect Dis, 49*(12), 1777-1783. doi:10.1086/648423

Bate, S. L., Dollard, S. C., & Cannon, M. J. (2010). Cytomegalovirus seroprevalence in the United States: the national health and nutrition examination surveys, 1988-2004. *Clin Infect Dis, 50*(11), 1439-1447. doi:10.1086/652438

Berger, C., Jensen, M. C., Lansdorp, P. M., Gough, M., Elliott, C., & Riddell, S. R. (2008). Adoptive transfer of effector CD8+ T cells derived from central memory cells establishes persistent T cell memory in primates. *The Journal of Clinical Investigation, 118*(1), 294-305. doi:10.1172/JCI32103

Bestard, O., Lucia, M., Crespo, E., Van Liempt, B., Palacio, D., Melilli, E., Torras, J., Llaudo, I., Cerezo, G., Taco, O., Gil-Vernet, S., Grinyo, J. M., & Cruzado, J. M. (2013). Pretransplant immediately early-1-specific T cell responses provide protection for CMV infection after kidney transplantation. *Am J Transplant, 13*(7), 1793-1805. doi:10.1111/ajt.12256

Biron, C. A., Byron, K. S., & Sullivan, J. L. (1989). Severe herpesvirus infections in an adolescent without natural killer cells. *N Engl J Med, 320*(26), 1731-1735. doi:10.1056/nejm198906293202605

Bitmansour, A. D., Douek, D. C., Maino, V. C., & Picker, L. J. (2002). Direct ex vivo analysis of human CD4(+) memory T cell activation requirements at the single clonotype level. *J Immunol, 169*(3), 1207-1218.

Bjorkstrom, N. K., Beziat, V., Cichocki, F., Liu, L. L., Levine, J., Larsson, S., Koup, R. A., Anderson, S. K., Ljunggren, H. G., & Malmberg, K. J. (2012). CD8 T cells express randomly selected KIRs with distinct specificities compared with NK cells. *Blood, 120*(17), 3455-3465. doi:10.1182/blood-2012-03-416867

Bleakley, M., Heimfeld, S., Loeb, K. R., Jones, L. A., Chaney, C., Seropian, S., Gooley, T. A., Sommermeyer, F., Riddell, S. R., & Shlomchik, W. D. (2015). Outcomes of acute

leukemia patients transplanted with naive T cell-depleted stem cell grafts. *J Clin Invest, 125*(7), 2677-2689. doi:10.1172/jci81229

Boaz, M. J., Waters, A., Murad, S., Easterbrook, P. J., & Vyakarnam, A. (2002). Presence of HIV-1 Gag-specific IFN-gamma+IL-2+ and CD28+IL-2+ CD4 T cell responses is associated with nonprogression in HIV-1 infection. *J Immunol, 169*(11), 6376-6385.

Boeckh, M., & Geballe, A. P. (2011). Cytomegalovirus: pathogen, paradigm, and puzzle. *J Clin Invest, 121*(5), 1673-1680. doi:10.1172/jci45449

Boeckh, M., & Nichols, W. G. (2004). The impact of cytomegalovirus serostatus of donor and recipient before hematopoietic stem cell transplantation in the era of antiviral prophylaxis and preemptive therapy. *Blood, 103*(6), 2003-2008. doi:10.1182/blood-2003-10-3616

Boehme, K. W., Guerrero, M., & Compton, T. (2006). Human cytomegalovirus envelope glycoproteins B and H are necessary for TLR2 activation in permissive cells. *J Immunol, 177*(10), 7094-7102.

Boppana, S. B., & Britt, W. J. (1996). Recognition of human cytomegalovirus gene products by HCMV-specific cytotoxic T cells. *Virology, 222*(1), 293-296. doi:10.1006/viro.1996.0424

Boppana, S. B., Pass, R. F., Britt, W. J., Stagno, S., & Alford, C. A. (1992). Symptomatic congenital cytomegalovirus infection: neonatal morbidity and mortality. *Pediatr Infect Dis J, 11*(2), 93-99.

Borysiewicz, L. K., Morris, S., Page, J. D., & Sissons, J. G. (1983). Human cytomegalovirus-specific cytotoxic T lymphocytes: requirements for in vitro generation and specificity. *Eur J Immunol, 13*(10), 804-809. doi:10.1002/eji.1830131005

Bratcher, D. F., Bourne, N., Bravo, F. J., Schleiss, M. R., Slaoui, M., Myers, M. G., & Bernstein, D. I. (1995). Effect of passive antibody on congenital cytomegalovirus infection in guinea pigs. *J Infect Dis, 172*(4), 944-950.

Brestrich, G., Zwinger, S., Fischer, A., Schmuck, M., Rohmhild, A., Hammer, M. H., Kurtz, A., Uharek, L., Knosalla, C., Lehmkuhl, H., Volk, H. D., & Reinke, P. (2009). Adoptive T-cell therapy of a lung transplanted patient with severe CMV disease and resistance to antiviral therapy. *Am J Transplant, 9*(7), 1679-1684. doi:10.1111/j.1600-6143.2009.02672.x

Britt, W. (2007). Virus entry into host, establishment of infection, spread in host, mechanisms of tissue damage. In A. Arvin, G. Campadelli-Fiume, E. Mocarski, P. S. Moore, B. Roizman, R. Whitley, & K. Yamanishi (Eds.), *Human Herpesviruses: Biology, Therapy, and Immunoprophylaxis*. Cambridge.

Browne, H., Smith, G., Beck, S., & Minson, T. (1990). A complex between the MHC class I homologue encoded by human cytomegalovirus and beta 2 microglobulin. *Nature, 347*(6295), 770-772. doi:10.1038/347770a0

Buchholz, V. R., Flossdorf, M., Hensel, I., Kretschmer, L., Weissbrich, B., Graf, P., Verschoor, A., Schiemann, M., Hofer, T., & Busch, D. H. (2013). Disparate individual fates compose robust CD8+ T cell immunity. *Science, 340*(6132), 630-635. doi:10.1126/science.1235454

Busch, D. H., Frassle, S. P., Sommermeyer, D., Buchholz, V. R., & Riddell, S. R. (2016). Role of memory T cell subsets for adoptive immunotherapy. *Semin Immunol, 28*(1), 28-34. doi:10.1016/j.smim.2016.02.001

Busch, D. H., Pilip, I. M., Vijh, S., & Pamer, E. G. (1998). Coordinate regulation of complex T cell populations responding to bacterial infection. *Immunity, 8*(3), 353-362.

Buxmann, H., Stackelberg, O. M., Schlosser, R. L., Enders, G., Gonser, M., Meyer-Wittkopf, M., Hamprecht, K., & Enders, M. (2012). Use of cytomegalovirus hyperimmunoglobulin for

prevention of congenital cytomegalovirus disease: a retrospective analysis. *J Perinat Med, 40*(4), 439-446. doi:10.1515/jpm-2011-0257

Byers, Anthony M., Kemball, Christopher C., Andrews, Nicolas P., & Lukacher, Aron E. (2003). Regulation of antiviral CD8+ T cells by inhibitory natural killer cell receptors. *Microbes and Infection, 5*(2), 169-177. doi:http://dx.doi.org/10.1016/S1286-4579(02)00086-2

Calarota, S. A., Zelini, P., De Silvestri, A., Chiesa, A., Comolli, G., Sarchi, E., Migotto, C., Pellegrini, C., Esposito, P., Minoli, L., Tinelli, C., Marone, P., & Baldanti, F. (2012). Kinetics of T-lymphocyte subsets and posttransplant opportunistic infections in heart and kidney transplant recipients. *Transplantation, 93*(1), 112-119. doi:10.1097/TP.0b013e318239e90c

Cannon, M. J., Hyde, T. B., & Schmid, D. S. (2011). Review of cytomegalovirus shedding in bodily fluids and relevance to congenital cytomegalovirus infection. *Rev Med Virol, 21*(4), 240-255. doi:10.1002/rmv.695

Cella, M., Longo, A., Ferrara, G. B., Strominger, J. L., & Colonna, M. (1994). NK3-specific natural killer cells are selectively inhibited by Bw4-positive HLA alleles with isoleucine 80. *J Exp Med, 180*(4), 1235-1242.

Charpentier, B., Rostaing, L., Berthoux, F., Lang, P., Civati, G., Touraine, J. L., Squifflet, J. P., Vialtel, P., Abramowicz, D., Mourad, G., Wolf, P., Cassuto, E., Moulin, B., Rifle, G., Pruna, A., Merville, P., Mignon, F., Legendre, C., Le Pogamp, P., Lebranchu, Y., Toupance, O., Hurault De Ligny, B., Touchard, G., Olmer, M., Purgus, R., Pouteil-Noble, C., Glotz, D., Bourbigot, B., Leski, M., Wauters, J. P., & Kessler, M. (2003). A three-arm study comparing immediate tacrolimus therapy with antithymocyte globulin induction therapy followed by tacrolimus or cyclosporine A in adult renal transplant recipients. *Transplantation, 75*(6), 844-851. doi:10.1097/01.tp.0000056635.59888.ef

Chee, M. S., Bankier, A. T., Beck, S., Bohni, R., Brown, C. M., Cerny, R., Horsnell, T., Hutchison, C. A., 3rd, Kouzarides, T., Martignetti, J. A., & et al. (1990). Analysis of the protein-coding content of the sequence of human cytomegalovirus strain AD169. *Curr Top Microbiol Immunol, 154*, 125-169.

Cheung, A. K., Abendroth, A., Cunningham, A. L., & Slobedman, B. (2006). Viral gene expression during the establishment of human cytomegalovirus latent infection in myeloid progenitor cells. *Blood, 108*(12), 3691-3699. doi:10.1182/blood-2005-12-026682

CLSI. (2007). Enumeration of Immunologically Defined Cell Populations by Flow Cytometry; Approved Guideline-Second Edition. *CLSI document H42-A2. Wayne, PA: Clinical and Laboratory Standards Institute*.

Cobbold, M., Khan, N., Pourgheysari, B., Tauro, S., McDonald, D., Osman, H., Assenmacher, M., Billingham, L., Steward, C., Crawley, C., Olavarria, E., Goldman, J., Chakraverty, R., Mahendra, P., Craddock, C., & Moss, P. A. (2005). Adoptive transfer of cytomegalovirus-specific CTL to stem cell transplant patients after selection by HLA-peptide tetramers. *J Exp Med, 202*(3), 379-386. doi:10.1084/jem.20040613

Coen, D. M., & Richman, D. D. (2013). Antiviral Agents. In D. M. Knipe & P. M. Hawley (Eds.), *Fields Virology* (6th ed., Vol. 1, pp. 338-373). Philadelphia: Wolters Kluwer Health/Lippincott Williams & Wilkins.

Compton, T., Nepomuceno, R. R., & Nowlin, D. M. (1992). Human cytomegalovirus penetrates host cells by pH-independent fusion at the cell surface. *Virology, 191*(1), 387-395.

Crocchiolo, R., Ciceri, F., Fleischhauer, K., Oneto, R., Bruno, B., Pollichieni, S., Sacchi, N., Sormani, M. P., Fanin, R., Bandini, G., Bonifazi, F., Bosi, A., Rambaldi, A., Alessandrino, P. E., Falda, M., & Bacigalupo, A. (2009). HLA matching affects clinical outcome of adult

patients undergoing haematopoietic SCT from unrelated donors: a study from the Gruppo Italiano Trapianto di Midollo Osseo and Italian Bone Marrow Donor Registry. *Bone Marrow Transplant, 44*(9), 571-577. doi:10.1038/bmt.2009.67

Crough, T., & Khanna, R. (2009). Immunobiology of human cytomegalovirus: from bench to bedside. *Clin Microbiol Rev, 22*(1), 76-98, Table of Contents. doi:10.1128/cmr.00034-08

Davison, A. J. (2010). Herpesvirus systematics. *Vet Microbiol, 143*(1), 52-69. doi:10.1016/j.vetmic.2010.02.014

Davison, A. J., Dolan, A., Akter, P., Addison, C., Dargan, D. J., Alcendor, D. J., McGeoch, D. J., & Hayward, G. S. (2003). The human cytomegalovirus genome revisited: comparison with the chimpanzee cytomegalovirus genome. *J Gen Virol, 84*(Pt 1), 17-28. doi:10.1099/vir.0.18606-0

Derby, M., Alexander-Miller, M., Tse, R., & Berzofsky, J. (2001). High-avidity CTL exploit two complementary mechanisms to provide better protection against viral infection than low-avidity CTL. *J Immunol, 166*(3), 1690-1697.

Diamond, D. J., York, J., Sun, J. Y., Wright, C. L., & Forman, S. J. (1997). Development of a candidate HLA A*0201 restricted peptide-based vaccine against human cytomegalovirus infection. *Blood, 90*(5), 1751-1767.

Dolan, A., Cunningham, C., Hector, R. D., Hassan-Walker, A. F., Lee, L., Addison, C., Dargan, D. J., McGeoch, D. J., Gatherer, D., Emery, V. C., Griffiths, P. D., Sinzger, C., McSharry, B. P., Wilkinson, G. W., & Davison, A. J. (2004). Genetic content of wild-type human cytomegalovirus. *J Gen Virol, 85*(Pt 5), 1301-1312. doi:10.1099/vir.0.79888-0

Douek, D. C., Vescio, R. A., Betts, M. R., Brenchley, J. M., Hill, B. J., Zhang, L., Berenson, J. R., Collins, R. H., & Koup, R. A. (2000). Assessment of thymic output in adults after haematopoietic stem-cell transplantation and prediction of T-cell reconstitution. *Lancet, 355*(9218), 1875-1881. doi:10.1016/s0140-6736(00)02293-5

Dumont-Girard, F., Roux, E., van Lier, R. A., Hale, G., Helg, C., Chapuis, B., Starobinski, M., & Roosnek, E. (1998). Reconstitution of the T-cell compartment after bone marrow transplantation: restoration of the repertoire by thymic emigrants. *Blood, 92*(11), 4464-4471.

Dunn, W., Chou, C., Li, H., Hai, R., Patterson, D., Stolc, V., Zhu, H., & Liu, F. (2003). Functional profiling of a human cytomegalovirus genome. *Proc Natl Acad Sci U S A, 100*(24), 14223-14228. doi:10.1073/pnas.2334032100

Dzabic, M., Rahbar, A., Yaiw, K. C., Naghibi, M., Religa, P., Fellstrom, B., Larsson, E., & Soderberg-Naucler, C. (2011). Intragraft cytomegalovirus protein expression is associated with reduced renal allograft survival. *Clin Infect Dis, 53*(10), 969-976. doi:10.1093/cid/cir619

Eid, A. J., Brown, R. A., Arthurs, S. K., Lahr, B. D., Eckel-Passow, J. E., Larson, T. S., & Razonable, R. R. (2010). A prospective longitudinal analysis of cytomegalovirus (CMV)-specific CD4+ and CD8+ T cells in kidney allograft recipients at risk of CMV infection. *Transpl Int, 23*(5), 506-513. doi:10.1111/j.1432-2277.2009.01017.x

Eid, A. J., Brown, R. A., Hogan, W. J., Lahr, B. D., Eckel-Passow, J. E., Litzow, M. R., & Razonable, R. R. (2009). Kinetics of interferon-gamma producing cytomegalovirus (CMV)-specific CD4+ and CD8+ T lymphocytes and the risk of subsequent CMV viremia after allogeneic hematopoietic stem cell transplantation. *Transpl Infect Dis, 11*(6), 519-528. doi:10.1111/j.1399-3062.2009.00446.x

Einsele, H., Roosnek, E., Rufer, N., Sinzger, C., Riegler, S., Loffler, J., Grigoleit, U., Moris, A., Rammensee, H. G., Kanz, L., Kleihauer, A., Frank, F., Jahn, G., & Hebart, H. (2002).

Infusion of cytomegalovirus (CMV)-specific T cells for the treatment of CMV infection not responding to antiviral chemotherapy. *Blood, 99*(11), 3916-3922.

Elkington, R., Walker, S., Crough, T., Menzies, M., Tellam, J., Bharadwaj, M., & Khanna, R. (2003). Ex vivo profiling of CD8+-T-cell responses to human cytomegalovirus reveals broad and multispecific reactivities in healthy virus carriers. *J Virol, 77*(9), 5226-5240.

Emery, V. C. (2012). Cytomegalovirus: recent progress in understanding pathogenesis and control. *QJM, 105*(5), 401-405. doi:10.1093/qjmed/hcr262

Emu, B., Sinclair, E., Favre, D., Moretto, W. J., Hsue, P., Hoh, R., Martin, J. N., Nixon, D. F., McCune, J. M., & Deeks, S. G. (2005). Phenotypic, functional, and kinetic parameters associated with apparent T-cell control of human immunodeficiency virus replication in individuals with and without antiretroviral treatment. *J Virol, 79*(22), 14169-14178. doi:10.1128/jvi.79.22.14169-14178.2005

Eriksson, B., Oberg, B., & Wahren, B. (1982). Pyrophosphate analogues as inhibitors of DNA polymerases of cytomegalovirus, herpes simplex virus and cellular origin. *Biochim Biophys Acta, 696*(2), 115-123.

Fishman, J. A. (2007). Infection in solid-organ transplant recipients. *N Engl J Med, 357*(25), 2601-2614. doi:10.1056/NEJMra064928

Fleming, T., Dunne, J., & Crowley, B. (2010). Ex vivo monitoring of human cytomegalovirus-specific CD8(+) T-Cell responses using the QuantiFERON-CMV assay in allogeneic hematopoietic stem cell transplant recipients attending an Irish hospital. *J Med Virol, 82*(3), 433-440. doi:10.1002/jmv.21727

Fletcher, J. M., Prentice, H. G., & Grundy, J. E. (1998). Natural killer cell lysis of cytomegalovirus (CMV)-infected cells correlates with virally induced changes in cell surface lymphocyte function-associated antigen-3 (LFA-3) expression and not with the CMV-induced down-regulation of cell surface class I HLA. *J Immunol, 161*(5), 2365-2374.

Fortun, J., Martin-Davila, P., Pascual, J., Cervera, C., Moreno, A., Gavalda, J., Aguado, J. M., Pereira, P., Gurgui, M., Carratala, J., Fogueda, M., Montejo, M., Blasco, F., Bou, G., & Torre-Cisneros, J. (2010). Immunosuppressive therapy and infection after kidney transplantation. *Transpl Infect Dis, 12*(5), 397-405. doi:10.1111/j.1399-3062.2010.00526.x

Frascaroli, G., Varani, S., Blankenhorn, N., Pretsch, R., Bacher, M., Leng, L., Bucala, R., Landini, M. P., & Mertens, T. (2009). Human cytomegalovirus paralyzes macrophage motility through down-regulation of chemokine receptors, reorganization of the cytoskeleton, and release of macrophage migration inhibitory factor. *J Immunol, 182*(1), 477-488.

Freeman, R. B., Jr. (2009). The 'indirect' effects of cytomegalovirus infection. *Am J Transplant, 9*(11), 2453-2458. doi:10.1111/j.1600-6143.2009.02824.x

Freitas, M. C. (2011). Kidney transplantation in the US: an analysis of the OPTN/UNOS registry. *Clin Transpl*, 1-16.

Gamadia, L. E., Remmerswaal, E. B., Weel, J. F., Bemelman, F., van Lier, R. A., & Ten Berge, I. J. (2003). Primary immune responses to human CMV: a critical role for IFN-gamma-producing CD4+ T cells in protection against CMV disease. *Blood, 101*(7), 2686-2692. doi:10.1182/blood-2002-08-2502

Garboczi, D. N., Hung, D. T., & Wiley, D. C. (1992). HLA-A2-peptide complexes: refolding and crystallization of molecules expressed in Escherichia coli and complexed with single antigenic peptides. *Proc Natl Acad Sci U S A, 89*(8), 3429-3433.

Gattinoni, L., Lugli, E., Ji, Y., Pos, Z., Paulos, C. M., Quigley, M. F., Almeida, J. R., Gostick, E., Yu, Z., Carpenito, C., Wang, E., Douek, D. C., Price, D. A., June, C. H., Marincola, F. M.,

Roederer, M., & Restifo, N. P. (2011). A human memory T cell subset with stem cell-like properties. *Nat Med, 17*(10), 1290-1297. doi:10.1038/nm.2446

Gattinoni, L., & Restifo, N. P. (2013). Moving T memory stem cells to the clinic. *Blood, 121*(4), 567-568. doi:10.1182/blood-2012-11-468660

Gaytant, M. A., Steegers, E. A., Semmekrot, B. A., Merkus, H. M., & Galama, J. M. (2002). Congenital cytomegalovirus infection: review of the epidemiology and outcome. *Obstet Gynecol Surv, 57*(4), 245-256.

Genini, E., Percivalle, E., Sarasini, A., Revello, M. G., Baldanti, F., & Gerna, G. (2011). Serum antibody response to the gH/gL/pUL128-131 five-protein complex of human cytomegalovirus (HCMV) in primary and reactivated HCMV infections. *J Clin Virol, 52*(2), 113-118. doi:10.1016/j.jcv.2011.06.018

Gerna, G., Percivalle, E., Lilleri, D., Lozza, L., Fornara, C., Hahn, G., Baldanti, F., & Revello, M. G. (2005). Dendritic-cell infection by human cytomegalovirus is restricted to strains carrying functional UL131-128 genes and mediates efficient viral antigen presentation to CD8+ T cells. *J Gen Virol, 86*(Pt 2), 275-284. doi:10.1099/vir.0.80474-0

Gewurz, B. E., Wang, E. W., Tortorella, D., Schust, D. J., & Ploegh, H. L. (2001). Human cytomegalovirus US2 endoplasmic reticulum-lumenal domain dictates association with major histocompatibility complex class I in a locus-specific manner. *J Virol, 75*(11), 5197-5204. doi:10.1128/jvi.75.11.5197-5204.2001

Giulieri, S., & Manuel, O. (2011). QuantiFERON(R)-CMV assay for the assessment of cytomegalovirus cell-mediated immunity. *Expert Rev Mol Diagn, 11*(1), 17-25. doi:10.1586/erm.10.109

Goderis, J., De Leenheer, E., Smets, K., Van Hoecke, H., Keymeulen, A., & Dhooge, I. (2014). Hearing loss and congenital CMV infection: a systematic review. *Pediatrics, 134*(5), 972-982. doi:10.1542/peds.2014-1173

Gohring, K., Hamprecht, K., & Jahn, G. (2015). Antiviral Drug- and Multidrug Resistance in Cytomegalovirus Infected SCT Patients. *Comput Struct Biotechnol J, 13*, 153-159. doi:10.1016/j.csbj.2015.01.003

Gondos, A., Dohler, B., Brenner, H., & Opelz, G. (2013). Kidney graft survival in Europe and the United States: strikingly different long-term outcomes. *Transplantation, 95*(2), 267-274. doi:10.1097/TP.0b013e3182708ea8

Graef, P., Buchholz, V. R., Stemberger, C., Flossdorf, M., Henkel, L., Schiemann, M., Drexler, I., Hofer, T., Riddell, S. R., & Busch, D. H. (2014). Serial transfer of single-cell-derived immunocompetence reveals stemness of CD8(+) central memory T cells. *Immunity, 41*(1), 116-126. doi:10.1016/j.immuni.2014.05.018

Gratama, J. W., Brooimans, R. A., van der Holt, B., Sintnicolaas, K., van Doornum, G., Niesters, H. G., Lowenberg, B., & Cornelissen, J. J. (2008). Monitoring cytomegalovirus IE-1 and pp65-specific CD4+ and CD8+ T-cell responses after allogeneic stem cell transplantation may identify patients at risk for recurrent CMV reactivations. *Cytometry B Clin Cytom, 74*(4), 211-220. doi:10.1002/cyto.b.20420

Grundy, J. E., Trapman, J., Allan, J. E., Shellam, G. R., & Melief, C. J. (1982). Evidence for a protective role of interferon in resistance to murine cytomegalovirus and its control by non-H-2-linked genes. *Infect Immun, 37*(1), 143-150.

Guethlein, L. A., Flodin, L. R., Adams, E. J., & Parham, P. (2002). NK cell receptors of the orangutan (Pongo pygmaeus): a pivotal species for tracking the coevolution of killer cell Ig-like receptors with MHC-C. *J Immunol, 169*(1), 220-229.

Hanley, P. J., & Bollard, C. M. (2014). Controlling cytomegalovirus: helping the immune system take the lead. *Viruses, 6*(6), 2242-2258. doi:10.3390/v6062242

Hecker, M., Qiu, D., Marquardt, K., Bein, G., & Hackstein, H. (2004). Continuous cytomegalovirus seroconversion in a large group of healthy blood donors. *Vox Sang, 86*(1), 41-44.

Helantera, I., Schachtner, T., Hinrichs, C., Salmela, K., Kyllonen, L., Koskinen, P., Lautenschlager, I., & Reinke, P. (2014). Current characteristics and outcome of cytomegalovirus infections after kidney transplantation. *Transpl Infect Dis, 16*(4), 568-577. doi:10.1111/tid.12247

Hertoghs, K. M., Moerland, P. D., van Stijn, A., Remmerswaal, E. B., Yong, S. L., van de Berg, P. J., van Ham, S. M., Baas, F., ten Berge, I. J., & van Lier, R. A. (2010). Molecular profiling of cytomegalovirus-induced human CD8+ T cell differentiation. *J Clin Invest, 120*(11), 4077-4090. doi:10.1172/jci42758

Hochrein, H., Schlatter, B., O'Keeffe, M., Wagner, C., Schmitz, F., Schiemann, M., Bauer, S., Suter, M., & Wagner, H. (2004). Herpes simplex virus type-1 induces IFN-alpha production via Toll-like receptor 9-dependent and -independent pathways. *Proc Natl Acad Sci U S A, 101*(31), 11416-11421. doi:10.1073/pnas.0403555101

Huard, B., & Karlsson, L. (2000). KIR expression on self-reactive CD8+ T cells is controlled by T-cell receptor engagement. *Nature, 403*(6767), 325-328. doi:http://www.nature.com/nature/journal/v403/n6767/suppinfo/403325a0_S1.html

Huber, M. T., & Compton, T. (1998). The human cytomegalovirus UL74 gene encodes the third component of the glycoprotein H-glycoprotein L-containing envelope complex. *J Virol, 72*(10), 8191-8197.

Humar, A., Lebranchu, Y., Vincenti, F., Blumberg, E. A., Punch, J. D., Limaye, A. P., Abramowicz, D., Jardine, A. G., Voulgari, A. T., Ives, J., Hauser, I. A., & Peeters, P. (2010). The efficacy and safety of 200 days valganciclovir cytomegalovirus prophylaxis in high-risk kidney transplant recipients. *Am J Transplant, 10*(5), 1228-1237. doi:10.1111/j.1600-6143.2010.03074.x

IBA-GmbH, I. (2016). StarGate Expression Vectors. Retrieved from http://www.iba-lifesciences.com/Acceptor_vectors_E._coli_Technology.html

Isaacson, M. K., & Compton, T. (2009). Human cytomegalovirus glycoprotein B is required for virus entry and cell-to-cell spread but not for virion attachment, assembly, or egress. *J Virol, 83*(8), 3891-3903. doi:10.1128/jvi.01251-08

Jacobsen, T., & Sifontis, N. (2010). Drug interactions and toxicities associated with the antiviral management of cytomegalovirus infection. *Am J Health Syst Pharm, 67*(17), 1417-1425. doi:10.2146/ajhp090424

Janeway, C. (2005). *Immunobiology : the immune system in health and disease* (6th ed.). New York: Garland Science.

Jonjic, S., Mutter, W., Weiland, F., Reddehase, M. J., & Koszinowski, U. H. (1989). Site-restricted persistent cytomegalovirus infection after selective long-term depletion of CD4+ T lymphocytes. *J Exp Med, 169*(4), 1199-1212.

Kalejta, R. F. (2008). Functions of human cytomegalovirus tegument proteins prior to immediate early gene expression. *Curr Top Microbiol Immunol, 325*, 101-115.

Kenneson, A., & Cannon, M. J. (2007). Review and meta-analysis of the epidemiology of congenital cytomegalovirus (CMV) infection. *Rev Med Virol, 17*(4), 253-276. doi:10.1002/rmv.535

Kern, F., Bunde, T., Faulhaber, N., Kiecker, F., Khatamzas, E., Rudawski, I. M., Pruss, A., Gratama, J. W., Volkmer-Engert, R., Ewert, R., Reinke, P., Volk, H. D., & Picker, L. J. (2002). Cytomegalovirus (CMV) phosphoprotein 65 makes a large contribution to

shaping the T cell repertoire in CMV-exposed individuals. *J Infect Dis, 185*(12), 1709-1716. doi:10.1086/340637

Kern, F., Surel, I. P., Faulhaber, N., Frommel, C., Schneider-Mergener, J., Schonemann, C., Reinke, P., & Volk, H. D. (1999). Target structures of the CD8(+)-T-cell response to human cytomegalovirus: the 72-kilodalton major immediate-early protein revisited. *J Virol, 73*(10), 8179-8184.

Khan, N., Cobbold, M., Keenan, R., & Moss, P. A. (2002a). Comparative analysis of CD8+ T cell responses against human cytomegalovirus proteins pp65 and immediate early 1 shows similarities in precursor frequency, oligoclonality, and phenotype. *J Infect Dis, 185*(8), 1025-1034. doi:10.1086/339963

Khan, N., Shariff, N., Cobbold, M., Bruton, R., Ainsworth, J. A., Sinclair, A. J., Nayak, L., & Moss, P. A. (2002b). Cytomegalovirus seropositivity drives the CD8 T cell repertoire toward greater clonality in healthy elderly individuals. *J Immunol, 169*(4), 1984-1992.

KIDGO. (2009). KDIGO (KIDNEY DISEASE | IMPROVING GLOBAL OUTCOMES) clinical practice guideline for the care of kidney transplant recipients. *Am J Transplant, 9 Suppl 3*, S1-155. doi:10.1111/j.1600-6143.2009.02834.x

Kim, J., Kim, A. R., & Shin, E. C. (2015). Cytomegalovirus Infection and Memory T Cell Inflation. *Immune Netw, 15*(4), 186-190. doi:10.4110/in.2015.15.4.186

Klenerman, P., & Oxenius, A. (2016). T cell responses to cytomegalovirus. *Nat Rev Immunol, 16*(6), 367-377. doi:10.1038/nri.2016.38

Knabel, M., Franz, T. J., Schiemann, M., Wulf, A., Villmow, B., Schmidt, B., Bernhard, H., Wagner, H., & Busch, D. H. (2002). Reversible MHC multimer staining for functional isolation of T-cell populations and effective adoptive transfer. *Nat Med, 8*(6), 631-637. doi:10.1038/nm0602-631

Koch, S., Larbi, A., Ozcelik, D., Solana, R., Gouttefangeas, C., Attig, S., Wikby, A., Strindhall, J., Franceschi, C., & Pawelec, G. (2007). Cytomegalovirus infection: a driving force in human T cell immunosenescence. *Ann N Y Acad Sci, 1114*, 23-35. doi:10.1196/annals.1396.043

Kotton, C. N. (2010). Management of cytomegalovirus infection in solid organ transplantation. *Nat Rev Nephrol, 6*(12), 711-721. doi:10.1038/nrneph.2010.141

Kotton, C. N. (2013). CMV: Prevention, Diagnosis and Therapy. *Am J Transplant, 13 Suppl 3*, 24-40; quiz 40. doi:10.1111/ajt.12006

Kotton, C. N., Kumar, D., Caliendo, A. M., Asberg, A., Chou, S., Danziger-Isakov, L., & Humar, A. (2013). Updated international consensus guidelines on the management of cytomegalovirus in solid-organ transplantation. *Transplantation, 96*(4), 333-360. doi:10.1097/TP.0b013e31829df29d

Krol, L., Stuchly, J., Hubacek, P., Keslova, P., Sedlacek, P., Stary, J., Hrusak, O., & Kalina, T. (2011). Signature profiles of CMV-specific T-cells in patients with CMV reactivation after hematopoietic SCT. *Bone Marrow Transplant, 46*(8), 1089-1098. doi:10.1038/bmt.2010.261

Krug, A., French, A. R., Barchet, W., Fischer, J. A., Dzionek, A., Pingel, J. T., Orihuela, M. M., Akira, S., Yokoyama, W. M., & Colonna, M. (2004). TLR9-dependent recognition of MCMV by IPC and DC generates coordinated cytokine responses that activate antiviral NK cell function. *Immunity, 21*(1), 107-119. doi:10.1016/j.immuni.2004.06.007

Krzyzaniak, M. A., Mach, M., & Britt, W. J. (2009). HCMV-encoded glycoprotein M (UL100) interacts with Rab11 effector protein FIP4. *Traffic, 10*(10), 1439-1457. doi:10.1111/j.1600-0854.2009.00967.x

Kumar, D., Chernenko, S., Moussa, G., Cobos, I., Manuel, O., Preiksaitis, J., Venkataraman, S., & Humar, A. (2009). Cell-mediated immunity to predict cytomegalovirus disease in high-risk solid organ transplant recipients. *Am J Transplant, 9*(5), 1214-1222. doi:10.1111/j.1600-6143.2009.02618.x

Kumar, V., & McNerney, M. E. (2005). A new self: MHC-class-I-independent natural-killer-cell self-tolerance. *Nat Rev Immunol, 5*(5), 363-374. doi:10.1038/nri1603

Kutscher, S., Dembek, C. J., Deckert, S., Russo, C., Korber, N., Bogner, J. R., Geisler, F., Umgelter, A., Neuenhahn, M., Albrecht, J., Cosma, A., Protzer, U., & Bauer, T. (2013). Overnight resting of PBMC changes functional signatures of antigen specific T- cell responses: impact for immune monitoring within clinical trials. *PLoS One, 8*(10), e76215. doi:10.1371/journal.pone.0076215

Lanier, L. L. (2005). NK cell recognition. *Annu Rev Immunol, 23*, 225-274. doi:10.1146/annurev.immunol.23.021704.115526

Lanier, L. L. (2008). Up on the tightrope: natural killer cell activation and inhibition. *Nat Immunol, 9*(5), 495-502. doi:10.1038/ni1581

Lanier, L. L. (2009). DAP10- and DAP12-associated receptors in innate immunity. *Immunol Rev, 227*(1), 150-160. doi:10.1111/j.1600-065X.2008.00720.x

Leen, A. M., Myers, G. D., Sili, U., Huls, M. H., Weiss, H., Leung, K. S., Carrum, G., Krance, R. A., Chang, C. C., Molldrem, J. J., Gee, A. P., Brenner, M. K., Heslop, H. E., Rooney, C. M., & Bollard, C. M. (2006). Monoculture-derived T lymphocytes specific for multiple viruses expand and produce clinically relevant effects in immunocompromised individuals. *Nat Med, 12*(10), 1160-1166. doi:10.1038/nm1475

Legendre, C., Canaud, G., & Martinez, F. (2014). Factors influencing long-term outcome after kidney transplantation. *Transpl Int, 27*(1), 19-27. doi:10.1111/tri.12217

Li, L., Coelingh, K. L., & Britt, W. J. (1995). Human cytomegalovirus neutralizing antibody-resistant phenotype is associated with reduced expression of glycoprotein H. *J Virol, 69*(10), 6047-6053.

Li Pira, G., Bottone, L., Ivaldi, F., Pelizzoli, R., Del Galdo, F., Lozzi, L., Bracci, L., Loregian, A., Palu, G., De Palma, R., Einsele, H., & Manca, F. (2004). Identification of new Th peptides from the cytomegalovirus protein pp65 to design a peptide library for generation of CD4 T cell lines for cellular immunoreconstitution. *Int Immunol, 16*(5), 635-642. doi:10.1093/intimm/dxh065

Lilleri, D., Kabanova, A., Lanzavecchia, A., & Gerna, G. (2012). Antibodies against neutralization epitopes of human cytomegalovirus gH/gL/pUL128-130-131 complex and virus spreading may correlate with virus control in vivo. *J Clin Immunol, 32*(6), 1324-1331. doi:10.1007/s10875-012-9739-3

Linares, L., Sanclemente, G., Cervera, C., Hoyo, I., Cofan, F., Ricart, M. J., Perez-Villa, F., Navasa, M., Marcos, M. A., Anton, A., Pumarola, T., & Moreno, A. (2011). Influence of cytomegalovirus disease in outcome of solid organ transplant patients. *Transplant Proc, 43*(6), 2145-2148. doi:10.1016/j.transproceed.2011.05.007

Lisboa, L. F., Kumar, D., Wilson, L. E., & Humar, A. (2012). Clinical utility of cytomegalovirus cell-mediated immunity in transplant recipients with cytomegalovirus viremia. *Transplantation, 93*(2), 195-200. doi:10.1097/TP.0b013e31823c1cd4

Ljungman, P. (2002). Beta-herpesvirus challenges in the transplant recipient. *J Infect Dis, 186 Suppl 1*, S99-s109. doi:10.1086/342962

Ljungman, P., Griffiths, P., & Paya, C. (2002). Definitions of Cytomegalovirus Infection and Disease in Transplant Recipients. *Clinical Infectious Diseases, 34*(8), 1094-1097. doi:10.1086/339329

Ljungman, P., Griffiths, P., & Paya, C. (2002). Definitions of cytomegalovirus infection and disease in transplant recipients. *Clin Infect Dis, 34*(8), 1094-1097. doi:10.1086/339329

Long, E. O. (2008). Negative signaling by inhibitory receptors: the NK cell paradigm. *Immunol Rev, 224*, 70-84. doi:10.1111/j.1600-065X.2008.00660.x

Longmate, J., York, J., La Rosa, C., Krishnan, R., Zhang, M., Senitzer, D., & Diamond, D. J. (2001). Population coverage by HLA class-I restricted cytotoxic T-lymphocyte epitopes. *Immunogenetics, 52*(3-4), 165-173.

Lowance, D., Neumayer, H. H., Legendre, C. M., Squifflet, J. P., Kovarik, J., Brennan, P. J., Norman, D., Mendez, R., Keating, M. R., Coggon, G. L., Crisp, A., & Lee, I. C. (1999). Valacyclovir for the prevention of cytomegalovirus disease after renal transplantation. International Valacyclovir Cytomegalovirus Prophylaxis Transplantation Study Group. *N Engl J Med, 340*(19), 1462-1470. doi:10.1056/nejm199905133401903

Lucia, M., Crespo, E., Melilli, E., Cruzado, J. M., Luque, S., Llaudo, I., Niubo, J., Torras, J., Fernandez, N., Grinyo, J. M., & Bestard, O. (2014). Preformed frequencies of cytomegalovirus (CMV)-specific memory T and B cells identify protected CMV-sensitized individuals among seronegative kidney transplant recipients. *Clin Infect Dis, 59*(11), 1537-1545. doi:10.1093/cid/ciu589

Lugli, E., Dominguez, M. H., Gattinoni, L., Chattopadhyay, P. K., Bolton, D. L., Song, K., Klatt, N. R., Brenchley, J. M., Vaccari, M., Gostick, E., Price, D. A., Waldmann, T. A., Restifo, N. P., Franchini, G., & Roederer, M. (2013a). Superior T memory stem cell persistence supports long-lived T cell memory. *J Clin Invest, 123*(2), 594-599. doi:10.1172/jci66327

Lugli, E., Gattinoni, L., Roberto, A., Mavilio, D., Price, D. A., Restifo, N. P., & Roederer, M. (2013b). Identification, isolation and in vitro expansion of human and nonhuman primate T stem cell memory cells. *Nat Protoc, 8*(1), 33-42. doi:10.1038/nprot.2012.143

Luo, X. H., Huang, X. J., Liu, K. Y., Xu, L. P., & Liu, D. H. (2010). Protective immunity transferred by infusion of cytomegalovirus-specific CD8(+) T cells within donor grafts: its associations with cytomegalovirus reactivation following unmanipulated allogeneic hematopoietic stem cell transplantation. *Biol Blood Marrow Transplant, 16*(7), 994-1004. doi:10.1016/j.bbmt.2010.02.007

Mach, M., Kropff, B., Dal Monte, P., & Britt, W. (2000). Complex formation by human cytomegalovirus glycoproteins M (gpUL100) and N (gpUL73). *J Virol, 74*(24), 11881-11892.

Mach, M., Kropff, B., Kryzaniak, M., & Britt, W. (2005). Complex formation by glycoproteins M and N of human cytomegalovirus: structural and functional aspects. *J Virol, 79*(4), 2160-2170. doi:10.1128/jvi.79.4.2160-2170.2005

Mahnke, Y. D., Brodie, T. M., Sallusto, F., Roederer, M., & Lugli, E. (2013). The who's who of T-cell differentiation: human memory T-cell subsets. *Eur J Immunol, 43*(11), 2797-2809. doi:10.1002/eji.201343751

McGeoch, D. J., Dolan, A., & Ralph, A. C. (2000). Toward a comprehensive phylogeny for mammalian and avian herpesviruses. *J Virol, 74*(22), 10401-10406.

McMahon, C. W., & Raulet, D. H. (2001). Expression and function of NK cell receptors in CD8+ T cells. *Curr Opin Immunol, 13*(4), 465-470. doi:http://dx.doi.org/10.1016/S0952-7915(00)00242-9

Mengelle, C., Rostaing, L., Weclawiak, H., Rossignol, C., Kamar, N., & Izopet, J. (2015). Prophylaxis versus pre-emptive treatment for prevention of cytomegalovirus infection in CMV-seropositive orthotopic liver-transplant recipients. *J Med Virol, 87*(5), 836-844. doi:10.1002/jmv.23964

Micklethwaite, K., Hansen, A., Foster, A., Snape, E., Antonenas, V., Sartor, M., Shaw, P., Bradstock, K., & Gottlieb, D. (2007). Ex vivo expansion and prophylactic infusion of CMV-pp65 peptide-specific cytotoxic T-lymphocytes following allogeneic hematopoietic stem cell transplantation. *Biol Blood Marrow Transplant, 13*(6), 707-714. doi:10.1016/j.bbmt.2007.02.004

Mingari, M. C., Moretta, A., & Moretta, L. (1998). Regulation of KIR expression in human T cells: a safety mechanism that may impair protective T-cell responses. *Immunology Today, 19*(4), 153-157. doi:http://dx.doi.org/10.1016/S0167-5699(97)01236-X

Moins-Teisserenc, H., Busson, M., Scieux, C., Bajzik, V., Cayuela, J. M., Clave, E., de Latour, R. P., Agbalika, F., Ribaud, P., Robin, M., Rocha, V., Gluckman, E., Charron, D., Socie, G., & Toubert, A. (2008). Patterns of cytomegalovirus reactivation are associated with distinct evolutive profiles of immune reconstitution after allogeneic hematopoietic stem cell transplantation. *J Infect Dis, 198*(6), 818-826. doi:10.1086/591185

Monforte, V., Lopez, C., Santos, F., Zurbano, F., de la Torre, M., Sole, A., Gavalda, J., Ussetti, P., Lama, R., Cifrian, J., Borro, J. M., Pastor, A., Len, O., Bravo, C., & Roman, A. (2009). A multicenter study of valganciclovir prophylaxis up to day 120 in CMV-seropositive lung transplant recipients. *Am J Transplant, 9*(5), 1134-1141. doi:10.1111/j.1600-6143.2009.02574.x

Morton, R. L., Howard, K., Webster, A. C., Wong, G., & Craig, J. C. (2009). The cost-effectiveness of induction immunosuppression in kidney transplantation. *Nephrol Dial Transplant, 24*(7), 2258-2269. doi:10.1093/ndt/gfp174

Moscarski, E. S., Shenk, T., Griffiths, P. D., & Pass, R. E. (2013). Cytomegalovirus. In D. M. Knipe & P. M. Hawley (Eds.), *Fields Virology* (6th ed., Vol. 2, pp. 1960-2014). Philadelphia: Wolters Kluwer Health/Lippincott Williams & Wilkins.

Moss, P., & Rickinson, A. (2005). Cellular immunotherapy for viral infection after HSC transplantation. *Nat Rev Immunol, 5*(1), 9-20. doi:10.1038/nri1526

Munoz-Cobo, B., Solano, C., Benet, I., Costa, E., Remigia, M. J., de la Camara, R., Nieto, J., Lopez, J., Amat, P., Garcia-Noblejas, A., Bravo, D., Clari, M. A., & Navarro, D. (2012). Functional profile of cytomegalovirus (CMV)-specific CD8+ T cells and kinetics of NKG2C+ NK cells associated with the resolution of CMV DNAemia in allogeneic stem cell transplant recipients. *J Med Virol, 84*(2), 259-267. doi:10.1002/jmv.22254

Murphy, E., Yu, D., Grimwood, J., Schmutz, J., Dickson, M., Jarvis, M. A., Hahn, G., Nelson, J. A., Myers, R. M., & Shenk, T. E. (2003). Coding potential of laboratory and clinical strains of human cytomegalovirus. *Proc Natl Acad Sci U S A, 100*(25), 14976-14981. doi:10.1073/pnas.2136652100

Murray, B. M., & Subramaniam, S. (2004). Late cytomegalovirus infection after oral ganciclovir prophylaxis in renal transplant recipients. *Transpl Infect Dis, 6*(1), 3-9. doi:10.1111/j.1399-3062.2004.00043.x

Naing, Z. W., Scott, G. M., Shand, A., Hamilton, S. T., van Zuylen, W. J., Basha, J., Hall, B., Craig, M. E., & Rawlinson, W. D. (2016). Congenital cytomegalovirus infection in pregnancy: a review of prevalence, clinical features, diagnosis and prevention. *Aust N Z J Obstet Gynaecol, 56*(1), 9-18. doi:10.1111/ajo.12408

Nauerth, M., Stemberger, C., Mohr, F., Weissbrich, B., Schiemann, M., Germeroth, L., & Busch, D. H. (2016). Flow cytometry-based TCR-ligand Koff -rate assay for fast avidity screening of even very small antigen-specific T cell populations ex vivo. *Cytometry A*. doi:10.1002/cyto.a.22933

Nauerth, M., Weissbrich, B., Knall, R., Franz, T., Dossinger, G., Bet, J., Paszkiewicz, P. J., Pfeifer, L., Bunse, M., Uckert, W., Holtappels, R., Gillert-Marien, D., Neuenhahn, M.,

Krackhardt, A., Reddehase, M. J., Riddell, S. R., & Busch, D. H. (2013). TCR-ligand koff rate correlates with the protective capacity of antigen-specific CD8+ T cells for adoptive transfer. *Sci Transl Med, 5*(192), 192ra187. doi:10.1126/scitranslmed.3005958

Nebbia, G., Mattes, F. M., Smith, C., Hainsworth, E., Kopycinski, J., Burroughs, A., Griffiths, P. D., Klenerman, P., & Emery, V. C. (2008). Polyfunctional cytomegalovirus-specific CD4+ and pp65 CD8+ T cells protect against high-level replication after liver transplantation. *Am J Transplant, 8*(12), 2590-2599. doi:10.1111/j.1600-6143.2008.02425.x

Neuenhahn, M., Albrecht, J., Odendahl, M., Schlott, F., Dössinger, G., Schiemann, M., Lakshmipathi, S., Martin, K., Bunjes, D., Harsdorf, S., Weissinger, E. M., Menzel, H., Verbeek, M., Uharek, L., Kröger, N., Wagner, E., Kobbe, G., Schroeder, T., Schmitt, M., Held, G., Herr, W., Germeroth, L., Bonig, H., Tonn, T., Einsele, H., Busch, D. H., & Grigoleit, G. U. (2016). Transfer of minimally manipulated CMV-specific T cells from stem cell or third-party donors to treat CMV infection after alloHSCT. *unbublished manuscript*.

Nigro , G., Adler , S. P., La Torre , R., & Best , A. M. (2005). Passive Immunization during Pregnancy for Congenital Cytomegalovirus Infection. *New England Journal of Medicine, 353*(13), 1350-1362. doi:doi:10.1056/NEJMoa043337

Nigro, G., Adler, S. P., Parruti, G., Anceschi, M. M., Coclite, E., Pezone, I., & Di Renzo, G. C. (2012). Immunoglobulin therapy of fetal cytomegalovirus infection occurring in the first half of pregnancy--a case-control study of the outcome in children. *J Infect Dis, 205*(2), 215-227. doi:10.1093/infdis/jir718

Odendahl, M., Grigoleit, G. U., Bönig, H., Neuenhahn, M., Albrecht, J., Anderl, F., Germeroth, L., Schmitz, M., Bornhäuser, M., Einsele, H., Seifried, E., Busch, D. H., & Tonn, T. (2014). Clinical-scale isolation of 'minimally manipulated' cytomegalovirus-specific donor lymphocytes for the treatment of refractory cytomegalovirus disease. *Cytotherapy, 16*(9), 1245-1256. doi:http://dx.doi.org/10.1016/j.jcyt.2014.05.023

Pahl-Seibert, M.-F., Juelch, M., Podlech, J., Thomas, D., Deegen, P., Reddehase, M. J., & Holtappels, R. (2005). Highly Protective In Vivo Function of Cytomegalovirus IE1 Epitope-Specific Memory CD8 T Cells Purified by T-Cell Receptor-Based Cell Sorting. *J Virol, 79*(9), 5400-5413. doi:10.1128/JVI.79.9.5400-5413.2005

Paraskeva, M., Bailey, M., Levvey, B. J., Griffiths, A. P., Kotsimbos, T. C., Williams, T. P., Snell, G., & Westall, G. (2011). Cytomegalovirus replication within the lung allograft is associated with bronchiolitis obliterans syndrome. *Am J Transplant, 11*(10), 2190-2196. doi:10.1111/j.1600-6143.2011.03663.x

Parham, P. (2005). MHC class I molecules and KIRs in human history, health and survival. *Nat Rev Immunol, 5*(3), 201-214. doi:10.1038/nri1570

Park, C. O., & Kupper, T. S. (2015). The emerging role of resident memory T cells in protective immunity and inflammatory disease. *Nat Med, 21*(7), 688-697. doi:10.1038/nm.3883

Pass, R. F., Zhang, C., Evans, A., Simpson, T., Andrews, W., Huang, M. L., Corey, L., Hill, J., Davis, E., Flanigan, C., & Cloud, G. (2009). Vaccine prevention of maternal cytomegalovirus infection. *N Engl J Med, 360*(12), 1191-1199. doi:10.1056/NEJMoa0804749

Passweg, J. R., Baldomero, H., Peters, C., Gaspar, H. B., Cesaro, S., Dreger, P., Duarte, R. F., Falkenburg, J. H., Farge-Bancel, D., Gennery, A., Halter, J., Kroger, N., Lanza, F., Marsh, J., Mohty, M., Sureda, A., Velardi, A., & Madrigal, A. (2014). Hematopoietic SCT in Europe: data and trends in 2012 with special consideration of pediatric transplantation. *Bone Marrow Transplant, 49*(6), 744-750. doi:10.1038/bmt.2014.55

Patrone, M., Secchi, M., Bonaparte, E., Milanesi, G., & Gallina, A. (2007). Cytomegalovirus UL131-128 products promote gB conformational transition and gB-gH interaction during entry into endothelial cells. *J Virol, 81*(20), 11479-11488. doi:10.1128/jvi.00788-07

Peggs, K. S., & Mackinnon, S. (2004). Augmentation of virus-specific immunity after hematopoietic stem cell transplantation by adoptive T-cell therapy. *Hum Immunol, 65*(5), 550-557. doi:10.1016/j.humimm.2004.02.016

Pellett, P. E., & Roizman, B. (2013). Herpesviridae. In D. M. Knipe & P. M. Hawley (Eds.), *Fields Viology* (6th ed., pp. 1802-1822). Philadelphia: Wolters Kluwer Health/Lippincott Williams & Wilkins.

Polic, B., Hengel, H., Krmpotic, A., Trgovcich, J., Pavic, I., Luccaronin, P., Jonjic, S., & Koszinowski, U. H. (1998). Hierarchical and redundant lymphocyte subset control precludes cytomegalovirus replication during latent infection. *J Exp Med, 188*(6), 1047-1054.

Ponticelli, C. E. (2015). The impact of cold ischemia time on renal transplant outcome. *Kidney Int, 87*(2), 272-275. doi:10.1038/ki.2014.359

Prod'homme, V., Tomasec, P., Cunningham, C., Lemberg, M. K., Stanton, R. J., McSharry, B. P., Wang, E. C., Cuff, S., Martoglio, B., Davison, A. J., Braud, V. M., & Wilkinson, G. W. (2012). Human cytomegalovirus UL40 signal peptide regulates cell surface expression of the NK cell ligands HLA-E and gpUL18. *J Immunol, 188*(6), 2794-2804. doi:10.4049/jimmunol.1102068

Reddehase, M. J., Mutter, W., Munch, K., Buhring, H. J., & Koszinowski, U. H. (1987). CD8-positive T lymphocytes specific for murine cytomegalovirus immediate-early antigens mediate protective immunity. *J Virol, 61*(10), 3102-3108.

Reeves, M., & Sinclair, J. (2008). Aspects of human cytomegalovirus latency and reactivation. *Curr Top Microbiol Immunol, 325*, 297-313.

Reeves, M. B., MacAry, P. A., Lehner, P. J., Sissons, J. G., & Sinclair, J. H. (2005). Latency, chromatin remodeling, and reactivation of human cytomegalovirus in the dendritic cells of healthy carriers. *Proc Natl Acad Sci U S A, 102*(11), 4140-4145. doi:10.1073/pnas.0408994102

Reid, R., Mar, E. C., Huang, E. S., & Topal, M. D. (1988). Insertion and extension of acyclic, dideoxy, and ara nucleotides by herpesviridae, human alpha and human beta polymerases. A unique inhibition mechanism for 9-(1,3-dihydroxy-2-propoxymethyl)guanine triphosphate. *J Biol Chem, 263*(8), 3898-3904.

Reischig, T., Hribova, P., Jindra, P., Hes, O., Bouda, M., Treska, V., & Viklicky, O. (2012). Long-term outcomes of pre-emptive valganciclovir compared with valacyclovir prophylaxis for prevention of cytomegalovirus in renal transplantation. *J Am Soc Nephrol, 23*(9), 1588-1597. doi:10.1681/asn.2012010100

Reischig, T., Jindra, P., Hes, O., Bouda, M., Kormunda, S., & Treska, V. (2009). Effect of cytomegalovirus viremia on subclinical rejection or interstitial fibrosis and tubular atrophy in protocol biopsy at 3 months in renal allograft recipients managed by preemptive therapy or antiviral prophylaxis. *Transplantation, 87*(3), 436-444. doi:10.1097/TP.0b013e318192ded5

Remberger, M., Watz, E., Ringden, O., Mattsson, J., Shanwell, A., & Wikman, A. (2007). Major ABO blood group mismatch increases the risk for graft failure after unrelated donor hematopoietic stem cell transplantation. *Biol Blood Marrow Transplant, 13*(6), 675-682. doi:10.1016/j.bbmt.2007.01.084

Rentenaar, R. J., Gamadia, L. E., van DerHoek, N., van Diepen, F. N., Boom, R., Weel, J. F., Wertheim-van Dillen, P. M., van Lier, R. A., & ten Berge, I. J. (2000). Development of virus-specific CD4(+) T cells during primary cytomegalovirus infection. *J Clin Invest, 105*(4), 541-548. doi:10.1172/jci8229

Reuter, S., & Lang, D. (2009). Life span of monocytes and platelets: importance of interactions. *Front Biosci (Landmark Ed), 14*, 2432-2447.

Reyburn, H. T., Mandelboim, O., Vales-Gomez, M., Davis, D. M., Pazmany, L., & Strominger, J. L. (1997). The class I MHC homologue of human cytomegalovirus inhibits attack by natural killer cells. *Nature, 386*(6624), 514-517. doi:10.1038/386514a0

Riddell, S. R., Watanabe, K. S., Goodrich, J. M., Li, C. R., Agha, M. E., & Greenberg, P. D. (1992). Restoration of viral immunity in immunodeficient humans by the adoptive transfer of T cell clones. *Science, 257*(5067), 238-241.

Roizman, B., Carmichael, L. E., Deinhardt, F., de-The, G., Nahmias, A. J., Plowright, W., Rapp, F., Sheldrick, P., Takahashi, M., & Wolf, K. (1981). Herpesviridae. Definition, provisional nomenclature, and taxonomy. The Herpesvirus Study Group, the International Committee on Taxonomy of Viruses. *Intervirology, 16*(4), 201-217.

Roux, E., Dumont-Girard, F., Starobinski, M., Siegrist, C. A., Helg, C., Chapuis, B., & Roosnek, E. (2000). Recovery of immune reactivity after T-cell-depleted bone marrow transplantation depends on thymic activity. *Blood, 96*(6), 2299-2303.

Rubin, R. H. (1990). Impact of cytomegalovirus infection on organ transplant recipients. *Rev Infect Dis, 12 Suppl 7*, S754-766.

Ryckman, B. J., Jarvis, M. A., Drummond, D. D., Nelson, J. A., & Johnson, D. C. (2006). Human cytomegalovirus entry into epithelial and endothelial cells depends on genes UL128 to UL150 and occurs by endocytosis and low-pH fusion. *J Virol, 80*(2), 710-722. doi:10.1128/jvi.80.2.710-722.2006

Ryckman, B. J., Rainish, B. L., Chase, M. C., Borton, J. A., Nelson, J. A., Jarvis, M. A., & Johnson, D. C. (2008). Characterization of the human cytomegalovirus gH/gL/UL128-131 complex that mediates entry into epithelial and endothelial cells. *J Virol, 82*(1), 60-70. doi:10.1128/jvi.01910-07

Sallusto, F., & Lanzavecchia, A. (2011). Memory in disguise. *Nat Med, 17*(10), 1182-1183. doi:10.1038/nm.2502

Salvadori, M., Rosso, G., & Bertoni, E. (2015). Update on ischemia-reperfusion injury in kidney transplantation: Pathogenesis and treatment. *World J Transplant, 5*(2), 52-67. doi:10.5500/wjt.v5.i2.52

Scheinberg, P., Melenhorst, J. J., Brenchley, J. M., Hill, B. J., Hensel, N. F., Chattopadhyay, P. K., Roederer, M., Picker, L. J., Price, D. A., Barrett, A. J., & Douek, D. C. (2009). The transfer of adaptive immunity to CMV during hematopoietic stem cell transplantation is dependent on the specificity and phenotype of CMV-specific T cells in the donor. *Blood, 114*(24), 5071-5080. doi:10.1182/blood-2009-04-214684

Schmidt, A. H., Baier, D., Solloch, U. V., Stahr, A., Cereb, N., Wassmuth, R., Ehninger, G., & Rutt, C. (2009). Estimation of high-resolution HLA-A, -B, -C, -DRB1 allele and haplotype frequencies based on 8862 German stem cell donors and implications for strategic donor registry planning. *Hum Immunol, 70*(11), 895-902. doi:10.1016/j.humimm.2009.08.006

Schmitt, A., Tonn, T., Busch, D. H., Grigoleit, G. U., Einsele, H., Odendahl, M., Germeroth, L., Ringhoffer, M., Ringhoffer, S., Wiesneth, M., Greiner, J., Michel, D., Mertens, T., Rojewski, M., Marx, M., von Harsdorf, S., Dohner, H., Seifried, E., Bunjes, D., & Schmitt, M. (2011). Adoptive transfer and selective reconstitution of streptamer-selected

cytomegalovirus-specific CD8+ T cells leads to virus clearance in patients after allogeneic peripheral blood stem cell transplantation. *Transfusion, 51*(3), 591-599. doi:10.1111/j.1537-2995.2010.02940.x

Schoeppler, K. E., Lyu, D. M., Grazia, T. J., Crossno, J. T., Jr., Vandervest, K. M., & Zamora, M. R. (2013). Late-onset cytomegalovirus (CMV) in lung transplant recipients: can CMV serostatus guide the duration of prophylaxis? *Am J Transplant, 13*(2), 376-382. doi:10.1111/j.1600-6143.2012.04339.x

Schrier, R. D., Rice, G. P., & Oldstone, M. B. (1986). Suppression of natural killer cell activity and T cell proliferation by fresh isolates of human cytomegalovirus. *J Infect Dis, 153*(6), 1084-1091.

Schust, D. J., Tortorella, D., Seebach, J., Phan, C., & Ploegh, H. L. (1998). Trophoblast class I major histocompatibility complex (MHC) products are resistant to rapid degradation imposed by the human cytomegalovirus (HCMV) gene products US2 and US11. *J Exp Med, 188*(3), 497-503.

Sester, U., Presser, D., Dirks, J., Gartner, B. C., Kohler, H., & Sester, M. (2008). PD-1 expression and IL-2 loss of cytomegalovirus- specific T cells correlates with viremia and reversible functional anergy. *Am J Transplant, 8*(7), 1486-1497. doi:10.1111/j.1600-6143.2008.02279.x

Shabir, S., Kaul, B., Pachnio, A., Banham, G. D., Smith, H., Chand, S., Jham, S., Harper, L., Ball, S., Rahbar, A., Soderberg-Naucler, C., Moss, P., & Borrows, R. (2013). Impaired direct priming of CD8 T cells by donor-derived cytomegalovirus following kidney transplantation. *J Am Soc Nephrol, 24*(10), 1698-1708. doi:10.1681/asn.2013040340

Shellam, G. R., Allan, J. E., Papadimitriou, J. M., & Bancroft, G. J. (1981). Increased susceptibility to cytomegalovirus infection in beige mutant mice. *Proc Natl Acad Sci U S A, 78*(8), 5104-5108.

Sinzger, C. (2008). Entry route of HCMV into endothelial cells. *J Clin Virol, 41*(3), 174-179. doi:10.1016/j.jcv.2007.12.002

Sinzger, C., Grefte, A., Plachter, B., Gouw, A. S., The, T. H., & Jahn, G. (1995). Fibroblasts, epithelial cells, endothelial cells and smooth muscle cells are major targets of human cytomegalovirus infection in lung and gastrointestinal tissues. *J Gen Virol, 76 (Pt 4)*, 741-750. doi:10.1099/0022-1317-76-4-741

Skerra, A., & Schmidt, T. G. (1999). Applications of a peptide ligand for streptavidin: the Strep-tag. *Biomol Eng, 16*(1-4), 79-86.

Snyder, C. M., Cho, K. S., Bonnett, E. L., van Dommelen, S., Shellam, G. R., & Hill, A. B. (2008). Memory inflation during chronic viral infection is maintained by continuous production of short-lived, functional T cells. *Immunity, 29*(4), 650-659. doi:10.1016/j.immuni.2008.07.017

Soderberg-Naucler, C. (2006). Does cytomegalovirus play a causative role in the development of various inflammatory diseases and cancer? *J Intern Med, 259*(3), 219-246. doi:10.1111/j.1365-2796.2006.01618.x

Sommermeyer, D., Hudecek, M., Kosasih, P. L., Gogishvili, T., Maloney, D. G., Turtle, C. J., & Riddell, S. R. (2016). Chimeric antigen receptor-modified T cells derived from defined CD8+ and CD4+ subsets confer superior antitumor reactivity in vivo. *Leukemia, 30*(2), 492-500. doi:10.1038/leu.2015.247

Stasiak, P. C., & Mocarski, E. S. (1992). Transactivation of the cytomegalovirus ICP36 gene promoter requires the alpha gene product TRS1 in addition to IE1 and IE2. *J Virol, 66*(2), 1050-1058.

Stemberger, C., Dreher, S., Tschulik, C., Piossek, C., Bet, J., Yamamoto, T. N., Schiemann, M., Neuenhahn, M., Martin, K., Schlapschy, M., Skerra, A., Schmidt, T., Edinger, M., Riddell, S. R., Germeroth, L., & Busch, D. H. (2012). Novel serial positive enrichment technology enables clinical multiparameter cell sorting. *PLoS One, 7*(4), e35798. doi:10.1371/journal.pone.0035798

Stemberger, C., Graef, P., Odendahl, M., Albrecht, J., Dossinger, G., Anderl, F., Buchholz, V. R., Gasteiger, G., Schiemann, M., Grigoleit, G. U., Schuster, F. R., Borkhardt, A., Versluys, B., Tonn, T., Seifried, E., Einsele, H., Germeroth, L., Busch, D. H., & Neuenhahn, M. (2014). Lowest numbers of primary CD8(+) T cells can reconstitute protective immunity upon adoptive immunotherapy. *Blood, 124*(4), 628-637. doi:10.1182/blood-2013-12-547349

Stemberger, C., Huster, K. M., Koffler, M., Anderl, F., Schiemann, M., Wagner, H., & Busch, D. H. (2007). A single naive CD8+ T cell precursor can develop into diverse effector and memory subsets. *Immunity, 27*(6), 985-997. doi:10.1016/j.immuni.2007.10.012

Stetson, D. B., Mohrs, M., Reinhardt, R. L., Baron, J. L., Wang, Z. E., Gapin, L., Kronenberg, M., & Locksley, R. M. (2003). Constitutive cytokine mRNAs mark natural killer (NK) and NK T cells poised for rapid effector function. *J Exp Med, 198*(7), 1069-1076. doi:10.1084/jem.20030630

Stinski, M. F. (1978). Sequence of protein synthesis in cells infected by human cytomegalovirus: early and late virus-induced polypeptides. *J Virol, 26*(3), 686-701.

Susal, C., & Opelz, G. (2013). Current role of human leukocyte antigen matching in kidney transplantation. *Curr Opin Organ Transplant, 18*(4), 438-444. doi:10.1097/MOT.0b013e3283636ddf

Szczech, L. A., Berlin, J. A., Aradhye, S., Grossman, R. A., & Feldman, H. I. (1997). Effect of anti-lymphocyte induction therapy on renal allograft survival: a meta-analysis. *J Am Soc Nephrol, 8*(11), 1771-1777.

Szczech, L. A., Berlin, J. A., & Feldman, H. I. (1998). The effect of antilymphocyte induction therapy on renal allograft survival. A meta-analysis of individual patient-level data. Anti-Lymphocyte Antibody Induction Therapy Study Group. *Ann Intern Med, 128*(10), 817-826.

Taylor-Wiedeman, J., Sissons, J. G., Borysiewicz, L. K., & Sinclair, J. H. (1991). Monocytes are a major site of persistence of human cytomegalovirus in peripheral blood mononuclear cells. *J Gen Virol, 72 (Pt 9)*, 2059-2064. doi:10.1099/0022-1317-72-9-2059

Tennankore, K. K., Kim, S. J., Alwayn, I. P. J., & Kiberd, B. A. (2016). Prolonged warm ischemia time is associated with graft failure and mortality after kidney transplantation. *Kidney International, 89*(3), 648-658. doi:http://dx.doi.org/10.1016/j.kint.2015.09.002

Thibaudin, D., Alamartine, E., de Filippis, J. P., Diab, N., Laurent, B., & Berthoux, F. (1998). Advantage of antithymocyte globulin induction in sensitized kidney recipients: a randomized prospective study comparing induction with and without antithymocyte globulin. *Nephrol Dial Transplant, 13*(3), 711-715.

Turtle, C. J., Swanson, H. M., Fujii, N., Estey, E. H., & Riddell, S. R. (2009). A distinct subset of self-renewing human memory CD8+ T cells survives cytotoxic chemotherapy. *Immunity, 31*(5), 834-844. doi:10.1016/j.immuni.2009.09.015

Uhlin, M., Gertow, J., Uzunel, M., Okas, M., Berglund, S., Watz, E., Brune, M., Ljungman, P., Maeurer, M., & Mattsson, J. (2012). Rapid salvage treatment with virus-specific T cells for therapy-resistant disease. *Clin Infect Dis, 55*(8), 1064-1073. doi:10.1093/cid/cis625

US-Renal-Data-System. (2016a). Chapter 1: Incidence, Prevalence, Patient Characteristics, and Treatment Modalities. *American Journal of Kidney Diseases, 67*(3), S139-S158. doi:10.1053/j.ajkd.2016.02.012

US-Renal-Data-System. (2016b). Chapter 7: Transplantation. *American Journal of Kidney Diseases, 67*(3), S227-S238. doi:10.1053/j.ajkd.2016.02.018

van Leeuwen, E. M., de Bree, G. J., ten Berge, I. J., & van Lier, R. A. (2006). Human virus-specific CD8+ T cells: diversity specialists. *Immunol Rev, 211*, 225-235. doi:10.1111/j.0105-2896.2006.00379.x

Vanarsdall, A. L., Ryckman, B. J., Chase, M. C., & Johnson, D. C. (2008). Human cytomegalovirus glycoproteins gB and gH/gL mediate epithelial cell-cell fusion when expressed either in cis or in trans. *J Virol, 82*(23), 11837-11850. doi:10.1128/jvi.01623-08

Varnum, S. M., Streblow, D. N., Monroe, M. E., Smith, P., Auberry, K. J., Pasa-Tolic, L., Wang, D., Camp, D. G., 2nd, Rodland, K., Wiley, S., Britt, W., Shenk, T., Smith, R. D., & Nelson, J. A. (2004). Identification of proteins in human cytomegalovirus (HCMV) particles: the HCMV proteome. *J Virol, 78*(20), 10960-10966. doi:10.1128/jvi.78.20.10960-10966.2004

Visentin, S., Manara, R., Milanese, L., Da Roit, A., Forner, G., Salviato, E., Citton, V., Magno, F. M., Orzan, E., Morando, C., Cusinato, R., Mengoli, C., Palu, G., Ermani, M., Rinaldi, R., Cosmi, E., & Gussetti, N. (2012). Early primary cytomegalovirus infection in pregnancy: maternal hyperimmunoglobulin therapy improves outcomes among infants at 1 year of age. *Clin Infect Dis, 55*(4), 497-503. doi:10.1093/cid/cis423

Wagner, C. S., Ljunggren, H. G., & Achour, A. (2008). Immune modulation by the human cytomegalovirus-encoded molecule UL18, a mystery yet to be solved. *J Immunol, 180*(1), 19-24.

Walker, A., Petheram, S. J., Ballard, L., Murph, J. R., Demmler, G. J., & Bale, J. F., Jr. (2001). Characterization of human cytomegalovirus strains by analysis of short tandem repeat polymorphisms. *J Clin Microbiol, 39*(6), 2219-2226. doi:10.1128/jcm.39.6.2219-2226.2001

Walker, S., Fazou, C., Crough, T., Holdsworth, R., Kiely, P., Veale, M., Bell, S., Gailbraith, A., McNeil, K., Jones, S., & Khanna, R. (2007). Ex vivo monitoring of human cytomegalovirus-specific CD8+ T-cell responses using QuantiFERON-CMV. *Transpl Infect Dis, 9*(2), 165-170. doi:10.1111/j.1399-3062.2006.00199.x

Walter, E. A., Greenberg, P. D., Gilbert, M. J., Finch, R. J., Watanabe, K. S., Thomas, E. D., & Riddell, S. R. (1995). Reconstitution of cellular immunity against cytomegalovirus in recipients of allogeneic bone marrow by transfer of T-cell clones from the donor. *N Engl J Med, 333*(16), 1038-1044. doi:10.1056/nejm199510193331603

Wang, D., & Shenk, T. (2005a). Human cytomegalovirus UL131 open reading frame is required for epithelial cell tropism. *J Virol, 79*(16), 10330-10338. doi:10.1128/jvi.79.16.10330-10338.2005

Wang, D., & Shenk, T. (2005b). Human cytomegalovirus virion protein complex required for epithelial and endothelial cell tropism. *Proc Natl Acad Sci U S A, 102*(50), 18153-18158. doi:10.1073/pnas.0509201102

Wang, X., Popplewell, L. L., Wagner, J. R., Naranjo, A., Blanchard, M. S., Mott, M. R., Norris, A. P., Wong, C. W., Urak, R. Z., Chang, W. C., Khaled, S. K., Siddiqi, T., Budde, L. E., Xu, J., Chang, B., Gidwaney, N., Thomas, S. H., Cooper, L. J., Riddell, S. R., Brown, C. E., Jensen, M. C., & Forman, S. J. (2016). Phase 1 studies of central memory-derived CD19 CAR T-cell therapy following autologous HSCT in patients with B-cell NHL. *Blood, 127*(24), 2980-2990. doi:10.1182/blood-2015-12-686725

Weekes, M. P., Wills, M. R., Sissons, J. G., & Carmichael, A. J. (2004). Long-term stable expanded human CD4+ T cell clones specific for human cytomegalovirus are distributed in both CD45RAhigh and CD45ROhigh populations. *J Immunol, 173*(9), 5843-5851.

Whitelaw, D. M., & Bell, M. (1966). The Intravascular Lifespan of Monocytes. *Blood, 28*(3), 455-464.

Wiertz, E. J., Jones, T. R., Sun, L., Bogyo, M., Geuze, H. J., & Ploegh, H. L. (1996a). The human cytomegalovirus US11 gene product dislocates MHC class I heavy chains from the endoplasmic reticulum to the cytosol. *Cell, 84*(5), 769-779.

Wiertz, E. J., Tortorella, D., Bogyo, M., Yu, J., Mothes, W., Jones, T. R., Rapoport, T. A., & Ploegh, H. L. (1996b). Sec61-mediated transfer of a membrane protein from the endoplasmic reticulum to the proteasome for destruction. *Nature, 384*(6608), 432-438. doi:10.1038/384432a0

Willcox, B. E., Thomas, L. M., & Bjorkman, P. J. (2003). Crystal structure of HLA-A2 bound to LIR-1, a host and viral major histocompatibility complex receptor. *Nat Immunol, 4*(9), 913-919. doi:10.1038/ni961

Willis, M. R., Mason, G. M., & Sissons, G. P. (2013). Adaptive Cellular Immunity to Human Cytomgealovirus. In M. J. Reddehase & N. Lemmermann (Eds.), *Cytomegaloviruses : from molecular pathogenesis to intervention* (Vol. 2, pp. 142-172). Wymondham: Caister Academic Press.

Wills, M. R., Carmichael, A. J., Weekes, M. P., Mynard, K., Okecha, G., Hicks, R., & Sissons, J. G. (1999). Human virus-specific CD8+ CTL clones revert from CD45ROhigh to CD45RAhigh in vivo: CD45RAhighCD8+ T cells comprise both naive and memory cells. *J Immunol, 162*(12), 7080-7087.

Wills, M. R., Okecha, G., Weekes, M. P., Gandhi, M. K., Sissons, P. J., & Carmichael, A. J. (2002). Identification of naive or antigen-experienced human CD8(+) T cells by expression of costimulation and chemokine receptors: analysis of the human cytomegalovirus-specific CD8(+) T cell response. *J Immunol, 168*(11), 5455-5464.

Wolfe, R. A., Ashby, V. B., Milford, E. L., Ojo, A. O., Ettenger, R. E., Agodoa, L. Y., Held, P. J., & Port, F. K. (1999). Comparison of mortality in all patients on dialysis, patients on dialysis awaiting transplantation, and recipients of a first cadaveric transplant. *N Engl J Med, 341*(23), 1725-1730. doi:10.1056/nejm199912023412303

Yang, Z., & Bjorkman, P. J. (2008). Structure of UL18, a peptide-binding viral MHC mimic, bound to a host inhibitory receptor. *Proc Natl Acad Sci U S A, 105*(29), 10095-10100. doi:10.1073/pnas.0804551105

Zeh, H. J., 3rd, Perry-Lalley, D., Dudley, M. E., Rosenberg, S. A., & Yang, J. C. (1999). High avidity CTLs for two self-antigens demonstrate superior in vitro and in vivo antitumor efficacy. *J Immunol, 162*(2), 989-994.

Zhou, W., Longmate, J., Lacey, S. F., Palmer, J. M., Gallez-Hawkins, G., Thao, L., Spielberger, R., Nakamura, R., Forman, S. J., Zaia, J. A., & Diamond, D. J. (2009). Impact of donor CMV status on viral infection and reconstitution of multifunction CMV-specific T cells in CMV-positive transplant recipients. *Blood, 113*(25), 6465-6476. doi:10.1182/blood-2009-02-203307

Zieliński, M., Tarasewicz, A., Zielińska, H., Jankowska, M., Moszkowska, G., Dębska-Ślizień, A., Rutkowski, B., & Trzonkowski, P. (2016). CD28 positive, cytomegalovirus specific cytotoxic T lymphocytes as a novel biomarker associated with cytomegalovirus viremia in kidney allorecipients. *Journal of Clinical Virology, 83*, 17-25. doi:http://dx.doi.org/10.1016/j.jcv.2016.08.290

7. Danksagung

An dieser Stelle möchte ich mich bei allen bedanken, die mich während meine Doktorarbeit begleitet haben und zum Erfolg meiner Promotion beigetragen haben.

Zuerst bedanke ich mich bei meinem Doktorvater Dirk Busch, der mir die Gelegenheit gegeben hat an diesen spannenden Themen zu arbeiten. Dank seiner Unterstützung konnte ich viele praktische Erfahrungen an seinem Institut sammeln, meine Promotion abschließen und mich persönlich weiterentwickeln.

Des Weiteren möchte ich mich auch bei meinem direkten Betreuer und Mentor Michael Neuenhahn bedanken. Danke für die gute Zusammenarbeit, das Vertrauen, die vielen Ratschläge und regen Diskussionen. Ich konnte sehr viel lernen!

Auch möchte ich mich bei meinem Zweitgutachter Volker Hösel für die gute Zusammenarbeit bedanken und seine Unterstützung bei der Suche nach einem geeigneten Nachfolger.

Dank auch an Johannes Müller, der ohne Umschweife die Betreuung meiner Dissertation übernommen hat.

Besondern Dank möchte ich auch allen Mitgliedern der AG Neuenhahn für die gute Zusammenarbeit und das angenehme Arbeitsklima aussprechen. Besonders Julia Albrecht und Isabell Schiedewitz für die immerwährende Hilfestellung, die lustige Zeit in und außerhalb des Labors! Danke auch an Benjamin Faist, Christiane Frömmel, Corinne Angerpointner und Charlotte Lauenstein für die gute Zeit.

Herzlichen Dank auch Stefan Dreher und Christian Stemmberger für die wissenschaftlichen Diskussionen und die große Unterstützung.

Besonders erwähnen möchte ich auch Dominik Steubl für die hervorragende Zusammenarbeit, Diskussionen, Hilfestellung und die Sammlung von Patientenproben. Dies waren wichtige Bausteine meiner Dissertation.

Danke auch all meinen Freunden und meinem Bruder Sebastian für die nicht-wissenschaftlichen Diskussionen, die einem geholfen haben auch mal Abstand von der Dissertation zu bekommen.

Danken möchte ich auch Inge Bartmann für die Hilfestellung und regelmäßige Betreuung von Nero, so dass ich mich auf meine Arbeit konzentrieren konnte. Großen Dank auch an Denise Ketterlein für die viele Unterstützung in den ganzen Jahren.

Großen Dank auch meinen Eltern Amelia und Frank. Danke für die jahrelange Unterstützung! Ohne euch wäre ich nicht so weit gekommen! Danke auch für die herzliche Betreuung von Nero.

Ein ganz besonderer Dank gilt meiner Freundin Juliane Bartmann. In den vielen Jahren in denen wir uns kennen, hast du mich immer bedingungslos unterstütz und angetrieben. Du bist meine Motivation! Danke, dass du immer für mich da bist.